1-1-2013

Capacity Optimization for Radio Resource Allocation in Cognitive Networks

Mohamed Elalem
Ryerson University

CAPACITY OPTIMIZATION FOR RADIO RESOURCE ALLOCATION IN COGNITIVE NETWORKS

by

Mohamed Elalem

Bachelor of Science, Tripoli University, Libya, 1990

Master of Science, Tripoli University, Libya, 2006

A Dissertation

presented to Ryerson University

in partial fulfilment of the

requirements for the degree of

Doctor of Philosophy

in the Program of

Electrical and Computer Engineering

Toronto, Ontario, Canada, 2013

AUTHORS DECLARATION FOR ELECTRONIC SUBMISSION OF A DISSERTATION

I hereby declare that I am the sole author of this dissertation. This is a true copy of the dissertation, including any required final revisions, as accepted by my examiners.

I authorize Ryerson University to lend this dissertation to other institutions or individuals for the purpose of scholarly research.

I further authorize Ryerson University to reproduce this dissertation by photocopying or by other means, in total or in part, at the request of other institutions or individuals for the purpose of scholarly research.

I understand that my dissertation may be made electronically available to the public.

Abstract

Capacity Optimization For Radio Resource Allocation In Cognitive Networks

Doctor of Philosophy

Electrical and Computer Engineering

Ryerson University

With the rapid development of wireless services and applications, the currently radio spectrum is becoming more crowded. How to accommodate more wireless services and applications within the limited radio spectrum becomes a big challenge faced by modern society. Cognitive radio (CR) is proposed as a promising technology to tackle this challenge by introducing secondary users (SUs) to opportunistically or concurrently access the spectrum allocated to primary users (PUs). Currently, there are two prevalent CR models: the spectrum sharing model and the opportunistic spectrum access model. In the spectrum sharing model, the SUs are allowed to coexist with the PUs as long as the interferences from SUs do not degrade the quality of service (QoS) of PUs to an unacceptable level. In the opportunistic spectrum access model, SUs are allowed to access the spectrum only if the PUs are detected to be inactive. These two models known as underlay and overlay schemes, respectively.

This thesis studies a number of topics in CR networks under the framework of these two schemes. First, studied cognitive radio transmissions under QoS delay constraints. Initially, we focused on the concept: *effective capacity* for cognitive radio channels in order to identify the performance in the presence of QoS constraints. Both underlay and overlay schemes are studied taking into consideration the activity of primary users, and assuming the general case of channel fading as Gamma distribution. For this setting, we further proposed a

selection criterion by which the cognitive radio network can choose the adequate mode of operation. Then, we studied the cognitive radio transmissions focusing on Rayleigh fading channel and assumed that no prior channel knowledge is available at the transmitter and the receiver. We investigated the performance of pilot-assisted transmission strategies. In particular, we analyzed the channel estimation using minimum mean-square-error ($MMSE$) estimation, and analyzed efficient resource allocation strategies. In both cases, power allocations and effective capacity optimization were obtained. Effective capacity and interference constraint were analyzed in both single-band and multi-band spectrum sensing settings. Finally, we studied optimal access probabilities for cognitive radio network using Markov model to achieve maximum throughput for both CR schemes.

Acknowledgment

In the name of *ALLAH*, the Beneficent, the Merciful. All praises to Allah who created me and granted me everything and gave me ability to complete this task. Then, this dissertation would not be possible without the help and support of many people. A few words mentioned below cannot adequately express my appreciation.

First, I am most grateful to my research advisor, Professor Lian Zhao. I do believe that she is a real mentor in my research and life. I have benefited a lot from her impressive insights in research. She also helped me improve my academic writing and oral presentation significantly. As a perfect lady, she helped, supported and encouraged me during the course of my Ph.D. I am extraordinarily grateful to Dr. Lian for her criticism, patience, invaluable support and guidance throughout my stay at the Ryerson University. I am also thankful to my committee members, Prof. Jun Cai, Prof. Isaac Woungang, Prof. Xavier Fernando , and Prof. Kaamran Raahemifar, for their valuable comments on my thesis. Their commentaries improved my dissertation.

Finally, I would like to thank my late mother and father, Iftema and Abdorazak, and my wife Naiema for their unconditional love, support, and encouragement. This dissertation is dedicated to them.

Contents

List of Tables

List of Figures

Chapter 1

Introduction

Wireless communication has become an integral part of human life. Recent exponential growth in the use of wireless phones has been attributed to the advances in device technology and applications development in addition to various communication technologies. One of them is the advent of cognitive radio technology.

1.1 Cognitive Radio Models

The term "*cognitive radio*" was first coined by Joseph Mitola in [1], in which the possibility of enhancing the flexibility of personal wireless services through cognitive radio techniques was discussed. Then, the idea of cognitive radio was further expanded and a conceptual overview of cognitive radio was presented in Mitola's PhD dissertation. Cognitive radio is described as a fully reconfigurable wireless device that is sufficiently intelligent about its environment (*e.g.*, radio resources and channel fading states) and is able to automatically change its operating parameters (*e.g.*, transmit power, operating frequency, and modulation strategy) in response to environment changes. Later, Simon Haykin proposed the concept of interference temperature in [2], and characterized this concept as a main constraint in cognitive radio operation. This paves the path for today's spectrum sharing model.

Nowadays, cognitive radio operation models can generally be classified into two categories: opportunistic spectrum access and spectrum sharing. In the opportunistic spectrum access model, cognitive users or better known as secondary users have to sense the surrounding radio environment first, then transmit in vacant or intermittently unused spectrum without causing interference to the spectrum licensees known as primary users. In the spectrum sharing model, secondary user is allowed to transmit concurrently with primary user over the same frequency band provided that the primary user's performance degradation caused by secondary user's transmission is tolerable. This is realized by imposing an interference power constraint on secondary user's transmission, *i.e.*, the interference power received at primary user's receiver must be constrained below a certain prescribed threshold. In the following, brief introductions of these two cognitive radio operation models are presented.

1.1.1 The Opportunistic Spectrum Access Model

In opportunistic spectrum access model, secondary user first does spectrum sensing to detect the ON/OFF status of the primary user. If the primary user is detected to be OFF, then the secondary user can transmit over the spectrum; otherwise, the secondary user has to keep sensing until it finds a vacant spectrum band. A key feature for this model is *listen-before talk* [3]. This model is known as *overlay* scheme. On this basis, spectrum sensing plays a significant role, since the sensing result directly decides whether the target spectrum can be used by the secondary user or not. Two key concepts associated with spectrum sharing are probability of *detection* and probability of *false alarm*. Probability of detection is defined as the probability of correctly detecting the presence of the primary user when it is active; while probability of false alarm is defined as the probability of falsely declaring the presence of the primary user when it is actually inactive.

A lot of effort has been put into the design of sensing schemes. Basically, there are three main types of spectrum sensing schemes: energy detection [4–6], matched filter detection [7],

and cyclostationary feature detection [8]. Energy detection is the most widely used spectrum sensing scheme due to its low computationally complexity. It only needs to measure the power of the received signal, non prior knowledge about the primary user is required (non-coherent detector). Energy detection has a good resistance against the fast time varying radio channels.

In matched filter detection (or coherent detection), prior knowledge of the primary user's signal such as modulation scheme, pulse shape or packet format is required. This knowledge is not always easy to obtain in practice. Coherent detection can achieve maximum signal-to-noise ratio (SNR). The number of samples required for optimal detection is $O(1/SNR)$ [6].

Exploiting the feature that noise has very low correlation, while any man-made signals have some higher degree of correlation, cyclostationary feature detection achieves the best performance even in the worst-case scenario of large power level uncertainty of noise. However, the minimum number of samples required for detection are much more than that for energy detection and matched filter detection. It is reported that the longer the duration of the sensing slot is, the better the sensing result is. However, longer sensing slot leads to shorter transmission time, and thus results in a lower secondary user's throughput. This is known as the sensing throughput tradeoff problem, and this problem was first defined and investigated in [9, 10].

1.1.2 The Spectrum Sharing Model

In spectrum sharing model, the secondary user is allowed to transmit simultaneously with the primary user within the same frequency band on condition that the interference from the former to latter will be kept below a prescribed threshold. This model of operation is know as *underlay* scheme. From this definition, it is easy to see that there are three key features of underlay model. First, no spectrum sensing is needed at the secondary user. This greatly relieves the complexity of the transceiver design. Secondly, the secondary user can start its

transmission at any time without waiting for the spectrum holes. This gives the secondary user the potential to achieve a higher long-term capacity. Thirdly, the interference power from the secondary user to the primary user should be kept below a prescribed threshold. This, as a demerit, will scale down the underlay performance.

1.2 Transmission Power Control

Power control is an essential radio resource management strategy. It aims to control the transmission power levels in such a way that acceptable (QoS) for the users is guaranteed with lowest possible transmission powers. All users benefit from the minimized interference and the preserved signal qualities. Transmission power control is also an efficient technique to mitigate the effect of interference under fading conditions and combat the near-far problem.

Power control which has been employed for improving the link performance in cellular networks can also be applied to CRN. However, power control of cognitive radio networks is more complex, in which it should not only consider the QoS requirements of the secondary users but also protect the primary user communication link who has priority over the secondary user communication. Thus, secondary users should always check the estimated interference at the primary receiver when/after determining their transmission power.

Choosing an appropriate power control algorithm is of prime importance in CRNs, as it should aim at increasing the overall efficiency of the system.

1.3 Pilot-Aided Transmission

Pilot-Aided Transmission (PAT) multiplexes known training signals with the data signals. PAT can be used for channel estimation, receiver adaptation, and optimal decoding. An overview of pilot-aided wireless transmission techniques is presented in [11]. Earlier study has been conducted in [12], where an analytical approach to the design of PATs is presented.

The more pilot symbols are transmitted and the more power is allocated to the pilot symbols, the better estimation quality we have. The price is then the less in transmission efficiency.

1.4 Literature Review

The work related to resource allocation and capacity analysis for CRNs are reviewed in this section.

Since extensive research has been done in these areas, we do not even try to cover all previous research in this field. Instead, we review some of the most relevant work and cite these papers.

Power-control algorithms, as radio resource management, have gained extensive study since the early 1960s. Initially, these studies were proposed for satellite communication systems and later were applied to the cellular systems. Many algorithms with different configurations were proposed for GSM, $CDMA$ and $WCDMA$ systems, where centralized algorithms based on balancing of the received power levels were initially proposed. Since the centralized algorithms were not practically realizable, distributed algorithms, also aiming at balancing the power levels, have been substituted. To match the demanding QoS requirements, many more algorithms were proposed with different criteria, with multiple and fixed step power control.

Recently, the power control approach is also applied for cognitive radio networks to avoid harmful impacts on the primary user's quality of service. Hence, extensive studies have been done to enhance the overall network performance.

In [13], an Orthogonal Frequency Division Multiplexing (OFDM) scheme was considered as a candidate for cognitive radio. The authors proposed two approaches in order to mitigate the mutual interference. The performance of these approaches have been validated by simulation. The study tried to reduce the interference, but the main objective of power

control was not taken into consideration and no clear explanation has been given about how to implement such dynamic system to deactivate the subcarriers.

The power control scheme reported in [14] gave an example of a power control rule which allows secondary users to aggressively increase their transmit powers while still guaranteeing an acceptable level of aggregate interference at the primary receivers. A coherent detection was considered assuming that the licensed transmitter transmits a perfectly known pilot signal or training sequence to aid detection. The algorithm also dealt with the primary user's QoS satisfaction, but not the QoS of the secondary users. We argue that the QoS of the secondary users is also very important to be considered.

A transmission power control using Fuzzy Logic System (FLS) was proposed in [15]. With the built-in fuzzy power controller, the secondary user is able to dynamically adjust its transmission power in response to the changes of the interference level caused by the secondary user to the primary user. The authors modified the reliability of their algorithm by using a preceding knowledge of transmit power control obtained from a group of network experts which was listed in tables. Simulation results showed that using the proposed scheme leads to decreased average transmit power consumption and lower average outage probability compared with the traditional fixed-step power control scheme. The study depends mainly on data obtained from preceding network measurements and it does not give a mathematical model for the proposed algorithm.

In [16, 17], power control for one pair of secondary users coexisting with one pair of primary users has been considered. The use of soft sensing information for optimal power control was explored in [16] to maximize the capacity and SNR of the secondary user under a peak power constraint at the secondary transmitter. In [17], the secondary transmitter adjusts its transmission power to maximize its data rate without increasing the outage probability at the primary receiver. It was assumed in [17] that the channel gain between the primary transmitter and its receiver is known to the secondary user.

In [18], the authors presented power control strategy to protect the primary user's communication from the interference of the cognitive user's transmissions in fading wireless channels and to optimize the achievable rate of cognitive user while guaranteeing the outage probability of the primary user not to be degraded. A protection gap is introduced to enhance the robustness of the algorithm. The paper has studied initially the subject on the fundamental performance limit of a wireless network with cognitive radios from an information theory perspective.

Depending on whether a centralized controller exists, the power control considered in the existing literature for cognitive radio networks can be further divided into two categories: *distributed power control* and *centralized power control*.

The distributed power control is based on the local link gain measurements. Each user measures its local parameters; like gain and SNR to control the power in that link. This type of power control is practically realizable since it does not involve complex signaling and is easier to be implemented.

According to the methods to solve the power control problem in distributed cognitive network, current methods could be classified into two types. The first type is based on parallel and distributed computation. In [19], the authors formulated a power control problem for the cognitive radio network and proposed distributed solutions by using parallel and distributed method and applied it to the cognitive radio ad hoc network. However, no discussion was given about how the proposed distributed power control could be implemented in the cognitive radio ad hoc network.

The second type is based on game theory. In [20], the authors proposed a non-cooperative power control game with exponential pricing by considering the interference to the primary users. But the proposed method could not always ensure that the interference to the primary users was below the interference constraint. And the $SINR$ requirements of cognitive users were ignored.

Although in [21] the authors considered the $SINR$ requirements, they did not discuss the divergence problem of power control. Additionally, the authors proposed a joint power and channel allocation based on game theory with the objective to maximize the capacity, but $SINR$ requirement and protection for primary users were still ignored.

On the other hand, centralized power control is a mechanism with a central controller having the information of all link gains of the system. These link gains are utilized to find the optimal solution to control the power in all the links simultaneously. This type of power control is practically un-realizable, since the equipment is complex and the bandwidth is wasted due to the extreme signaling between base stations and mobile users. Most current studies aiming at centralized power control focus on allocating resources jointly, such as combined allocation of channels and transmitted powers.

The time-varying nature of the channel conditions due to mobility and changing physical environment is one of the key characteristics of wireless communications that greatly impacts system design and performance. A considerable amount of effort has been spent in the study of cases in which the perfect channel state information (CSI) is assumed to be available at either receiver or transmitter or both. With the perfect CSI available at the receiver, the authors in [22, 23] studied the capacity of fading channels.

The effective capacity is firstly defined in [24] as the maximum constant arrival rate that a given time-varying service process can support while meeting the QoS requirements. Effective capacity is realized as a dual concept to effective bandwidth which characterizes the minimum amount of constant transmission rate required to support a time-varying source in the presence of statistical QoS limitations. In [25], a methodology to determine the value of QoS exponent was described. The authors provided numerical and simulation results that demonstrate how the effective capacity formulation can be used to solve a resource allocation problem in audio and video applications to satisfy given QoS requirements.

The application and analysis of effective capacity in various settings have attracted much

interest [25–32], where the authors focused on the problem of resource allocation in the presence of statistical QoS constraints. In [29], energy efficiency was investigated under QoS constraints by analyzing the normalized effective capacity in the low-power and wideband regimes. The authors in [28] studied the effective capacity of a class of multiple-antenna wireless systems subject to Rayleigh flat fading. They suggested that multi-antenna configurations are helpful for delay-sensitive communication over wireless systems.

The paper [30] investigated the case in which the secondary transmitter communicates with its receiver through a relay node under a delay QoS constraint. The authors concluded that secondary users benefit from an intermediate relay node. They extended the study for multiple relay nodes case. They also stated that in systems with loose QoS constraints, the capacity benefits tremendously by increasing the number of relaying terminals.

In [31], tradeoff between average rate and average delay was studied using the notion of effective capacity. The optimal transmit strategy including optimal power allocation was also studied. Illustrations of average queue length compared to average transmission rate were provided to show the impact of the QoS exponent on the system.

The paper [32] analyzed the effective capacity of cognitive radio channels in order to identify the performance levels and to determine the interactions between throughput and channel sensing parameters in the presence of QoS constraints. A state-transition model for cognitive transmission was constructed and an expression for the effective capacity was obtained. The analysis was conducted under the assumption that only the receiver knows the channel realizations and the transmitter, in the absence of such knowledge, transmits the information at two different fixed rate and power levels, chosen according to the presence or absence of the primary users.

The different features of underlay and overlay approaches may have their respective advantages under diverse propagation environment and system parameters. In [33], analytical formulation of Dynamic Spectrum Access (DSA) with imperfect spectrum sensing has been

presented, only the case of the same priority for all the subscribers has been considered. In [34], the authors assumed that primary users and secondary users cannot operate simultaneously on the same spectrum band, then a Continuous Time Markov Chain (CTMC) was proposed to model the interactions between these different users. They analyzed the trade-off between spectrum efficiency and fairness. An optimal access probability with different criteria was given in [35] for pure underlay scheme. The papers [36, 37] introduced a mixed access strategy: when the channel is being used by the primary user, the secondary users access the channel with a probability in underlay manner. When the channel is idle, they choose to access in overlay manner.

1.5 Thesis Contribution

The key contributions of this thesis can be summarized as follows:

- First, we study the effective capacity of cognitive radio channels in order to identify the performance in the presence of statistical QoS constraints. Both underlay and overlay schemes are studied taking into consideration the activity of primary users and assuming the availability of perfect knowledge of channel fading coefficients at the receivers. For both schemes, power allocations and effective capacity optimization are obtained for Gamma fading channel environment. Then we propose a selection criterion that allows us to choose the best mode of operation.

- Thereafter, we extend this approach for the case of imperfect knowledge of channel fading coefficients. Initially, we focus on a time-varying Rayleigh fading channel and assume that no prior channel knowledge is available at the transmitter and the receiver. We investigate the performance of pilot-assisted wireless transmission strategies. We analyze the channel estimation using minimum mean-square-error ($MMSE$) estimation, and analyze efficient resource allocation strategies. We identify a state-transition

model by comparing transmission rates with instantaneous channel capacity values. We determine the effective capacity of cognitive radio transmission by incorporating channel sensing results.

- Later, we analyze the effective capacity and interference constraint in both single-band and multi-band spectrum sensing settings. Cognitive user is assumed to perform sensing in multiple channels and then select a single channel for transmission with rate and power that depend on both sensing outcomes and fading distribution. Interference constraint is statistically analyzed and formulated. Maximum throughput formulas for the cognitive user is obtained. Selection criterion that maximizes the capacity is proposed for arbitrary channel fading. Then we apply it for two different fading distributions. The optimal power allocation strategies are also determined. To the best of our knowledge, effective capacity has not been studied for multichannel spectrum sensing case in CR networks.

- Finally, we propose a mixed overlay and underlay access scheme. The secondary users access the channel with an optimal probability in the underlay scheme when the spectrum is occupied by a primary user. While when the spectrum is idle, the secondary users access the channel in the overlay manner. This approach can maximize the total average throughput for the secondary users and limit the interference to the primary user. The proposed optimized access strategy introduces new optimized parameters to determine the best access probability for each user to achieve the highest throughput. We study the capacity of cognitive users using Markov model and develop new optimal parameters to access the spectrum. By deriving access probabilities for the secondary users, maximum capacity can be achieved for each user for both cognitive radio schemes.

Most of the works reported in this dissertation can be found in peer reviewed research publications [38–47].

1.6 Thesis Organization

The remainder of the thesis is organized as follows:

In Chapter 2, the concept of effective capacity as a measure of the channel throughput is introduced. This concept allows us to take the delay requirement into consideration. System model and general assumptions used through this study are briefly introduced.

In Chapter 3, the effective capacity of the cognitive network is applied instead of ergodic capacity. The general case of *Gamma* distribution is assumed for the channel fading. Both underlay and overlay schemes are studied individually. Optimal power policies and maximum effective capacity formulas are obtained. For the underlay base, the PUs' spectrum-occupancy probability is taken into consideration. Since in the underlay case, the cognitive user does not preform spectrum sensing, it is not possible to differentiate the states of *idle* or *busy*. Hence, we impose the cognitive user to operate in the state that provides higher capacity. For the overlay strategy, we consider the spectrum sensing errors and all possible states are investigated. The transmit power and interference power of both underlay and overlay strategies as a function of primary user activities are investigated. To benefit from underlay and overlay approaches in diverse propagation environment and system parameters, a selection criterion is introduced to make the cognitive network dynamically choose the DSA strategy under different environment. This chapter, as a journal paper, has been submitted to EURASIP Journal on Wireless Communications and Networking for the second round review [39], and, as conference papers, to appear in Proceedings of IEEE ICNC in 2013 [40] and IEEE WCNC in 2013 [41].

In Chapter 4, we study the effective capacity of cognitive radio assuming imperfect and/or

no prior channel knowledge available at the cognitive transceiver. Following channel sensing, the secondary user is assumed to perform channel estimation to learn the channel conditions using $MMSE$ estimator via pilot aided transmission. Then, it transmits the data at two different average power levels depending on the sensing outcomes. Due to interactions and interdependencies between channel sensing and estimation, a challenging scenario may be faced. Hence, not reliable detection of the primary users' activities can lead to degradations in the estimation of the channel conditions, *i.e.*, if the primary users are active but detected as idle, the quality of the channel estimate will deteriorate. After performing the sensing and estimation tasks, the secondary user initiates the data transmission phase. The activity of the primary users is modeled as a two-state Markov process. In this setting, we jointly optimize the training symbol power, data symbol power and transmission rates. This chapter as a journal paper [47] is recently accepted.

In Chapter 5, the effective capacity of cognitive radio channels is studied where the cognitive radio detects the activity of the primary users in a multichannel environment and then performs data transmission in one of the transmission channels. We consider a scenario in which the cognitive system employs multichannel sensing and uses one channel for data transmission thereby decreasing the probability of interference to the primary users. We determine the effective capacity of the cognitive channel under limitations on the average interference power experienced by the primary receiver. Optimal criterion to select the transmission channel out of the available channels is obtained. Optimal power adaptation policies that maximize the effective capacity are derived. We analyze the interactions between the effective capacity, QoS constraints, channel sensing duration, channel detection threshold, detection and false alarm probabilities through numerical techniques. This chapter, as a conference paper, will appear in IEEE WCNC in 2013 [42], and as a journal paper [43] has been accepted for publishing in Journal of Communications and Network.

Chapter 6, proposes an optimized access strategy combining overlay and underlay schemes

for the cognitive radio. We model the service state of the system as a continuous-time Markov model. Based on the service state, the overlay manner or/and the underlay manner can be used by the secondary users. When the primary user is not transmitting and only one secondary user has the requirement to transmit, the secondary system adopts the overlay manner. When the primary user is transmitting and the secondary users want to transmit simultaneously, an underlay scheme with an access probability is adopted. First, the access probability is assumed to be the same for both users. Then the work is extended for the case in which each user has its own probability. We obtain the optimal access probabilities as well as the maximum capacity in closed forms. This chapter, as conference papers, will partly appear in IEEE WCNC in 2013 [44] and partly appeared in IEEE ICUE in 2012 [46], and as a journal paper [45], will be published in Journal of Communications and Network.

Figure 1.1 summerizes the organization of the thesis work. In this thesis, we introduce extensive capacity analysis and resource allocation for different cognitive radio systems and different access schemes that improve the overall system performance.

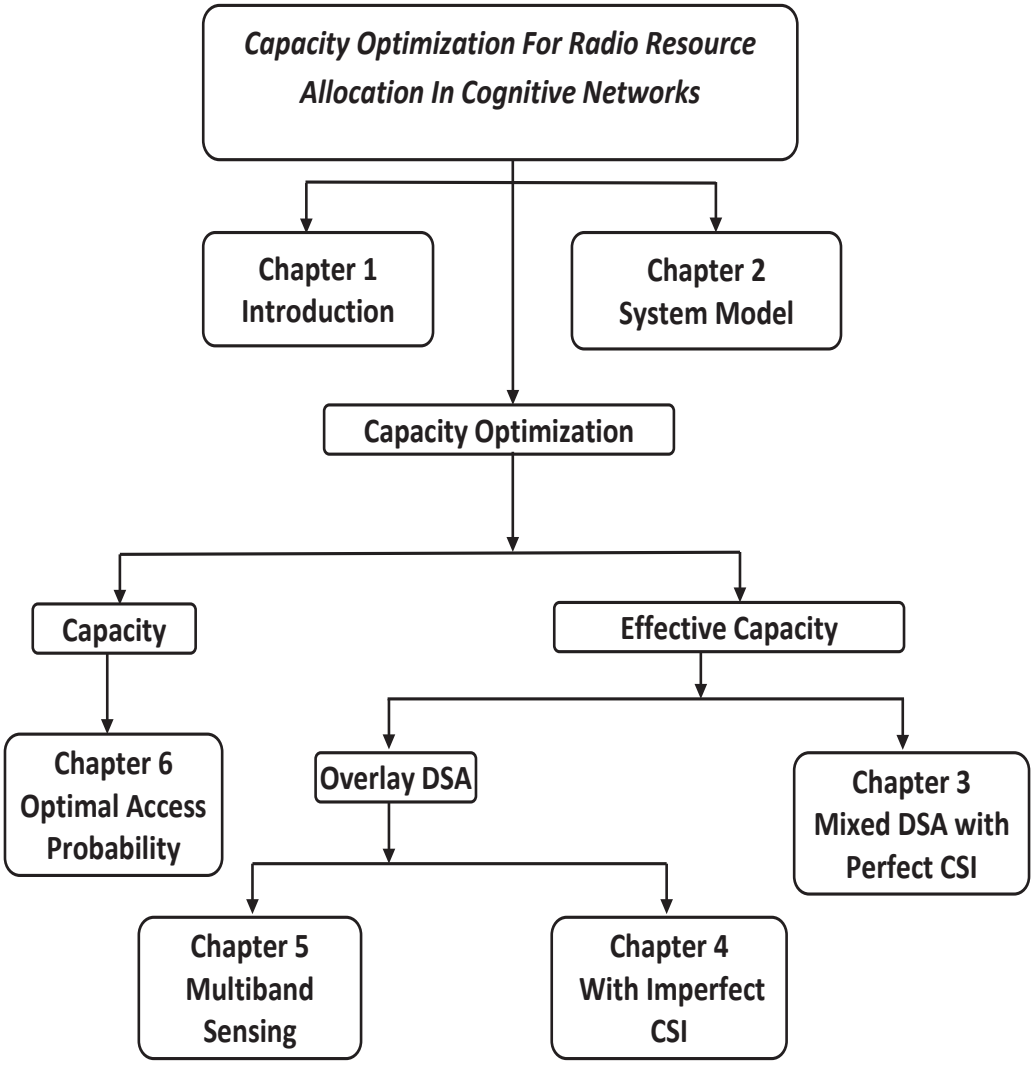

Figure 1.1: Thesis Organization.

Chapter 2

System Model and Assumptions

The maximum throughput achieved in wireless systems operating under statistical QoS constraints can be identified through the concept of *effective capacity*. The effective capacity is defined as the maximum constant arrival rate that a given time-varying service process can support while meeting the QoS requirements [24]. The application and analysis of effective capacity in various settings have attracted much interest [26, 27, 30–32, 48]. In these literatures, we focused on the problem of resource allocation in the presence of statistical QoS constraints.

The rest of this chapter is organized as follows. In Section 2.1, we introduce the effective capacity concept and illustrate its usage in cognitive radio networks. Related details such as the QoS constraint as an important criteria in time varying channels, the difference between effective capacity and Shannon capacity, delay violation, and effective capacity formulation are presented in subsequent subsections. *Gamma* distribution as a general case to model the channel fading is presented in Section 2.2. In Section 2.3, we briefly introduce the system model and general assumptions used through this thesis.

2.1 Effective Capacity

The effective capacity approach is particularly convenient for analyzing the statistical *QoS* performance of wireless transmissions where the service process is driven by the time-varying wireless channel.

2.1.1 Quality of Service Constraints in CRNs

Providing certain *QoS* in many wireless communication systems is crucial in order to provide acceptable performance and quality. However, this is a challenging task in wireless systems due to random variations experienced in channel conditions and random fluctuations in received power levels and supported data rates. Hence, in wireless systems, generally statistical rather than deterministic *QoS* guarantees can be provided.

In CRNs, the situation is further exacerbated in which access to a channel can be intermittent or transmission occurs at lower power levels depending on the activity of the primary users. Furthermore, cognitive radio can suffer from errors in channel sensing in the form of false alarms. Hence, it is more important to analyze the performance of cognitive radio systems in the presence of *QoS* limitations in the form of delay or buffer constraints.

As described before, issues regarding channel sensing, spectrum sharing and throughput in cognitive radio networks have been extensively studied recently. However, critical concerns of providing *QoS* guarantees over cognitive radio channels have not been sufficiently addressed yet.

2.1.2 Effective Capacity vs Shannon Capacity

QoS guarantee in terms of delay constraint plays a critically important role in modern wireless networks. Non-real-time services such as data, aim at maximizing the throughput with a loose delay constraint. While for real-time services, such as multimedia and video

conference, the *QoS* requirement needs a stringent delay-bound to achieve high spectral efficiency. Some other services falling in between such as web browsing and paging system, which are delay-sensitive but the delay *QoS* requirements are not as stringent as those of real-time services. Therefore, the diverse services impose totally different delay *QoS* constraints, which bring great challenges to the design of future wireless networks.

In wireless communications, the most scarce radio resources are power and spectral bandwidth. As a result, extensive research has been devoted to the techniques that can enhance the spectral efficiency of wireless systems. These techniques use the concept of Shannon capacity based on the information theory [49]. Power and rate adaptation has been widely considered as one of the key solutions to improve the spectral efficiency. *Water-filling* algorithm is one of well known schemes that maximizes spectral efficiency [50], in which more power is assigned to a channel which is in good condition and less power when the channel becomes worse. When the channel quality is below a certain threshold, no power is allocated. Additionally, *total channel inversion* algorithm has a different idea of power and rate adaptation [50], in which more power is assigned to a channel that combats with deep fading and less power for the good channel. This is to keep a constant signal-to-noise ratio, such that a constant rate service process can be obtained. Apparently, *water-filling* is better than *total channel inversion* since the former provides higher spectral efficiency [25]. It is important to note that Shannon theory does not place any restrictions on complexity and delay. However, a natural question is whether the former is also better than the latter in terms of *QoS* guarantees. In order to answer the above question, it is necessary to take the *QoS* metrics into account when applying power and rate adaptation.

The dual concepts of effective bandwidth and effective capacity give us a powerful approach to evaluate the statistical *QoS* performance from the networking perspective. The effective-bandwidth theory has been extensively studied in the early 90s with the emphasis on wired asynchronous transfer mode (ATM) networks [51]. This theory enables us to analyze

network statistics such as queue distributions, buffer overflow probabilities, and delay-bound violation probabilities, which are important for statistical QoS guarantees. In [24], the authors proposed an interesting concept, namely *effective capacity*.

By integrating information theory with the effective capacity, we investigate the impact of QoS constraint on the power and rate adaptation over cognitive radio networks. The problem is how to maximize the capacity subject to a given delay QoS constraint. There exists a tradeoff between the capacity and the QoS requirement. The higher capacity gain comes at the price of sacrificing QoS provisioning, and vice versa. When the QoS constraint becomes loose, the optimal power control converges to the water-filling scheme, where Shannon (ergodic) capacity can be achieved. On the other hand, when the QoS constraint becomes stringent, the optimal power-control converges to the total channel inversion such that the system operates at a constant service rate.

2.1.3 Queue Length and Delay Violation

The authors in [24,52] showed that the probability of the queue length of the transmit buffer exceeding a certain threshold q decays exponentially as a function of q. If we define Q as the stationary queue length, then the delay rate of the tail distribution of the queue length Q can be written as

$$\theta = -\lim_{q\to\infty} \frac{\log_e Pr(Q \geq q)}{q}. \tag{2.1}$$

For large threshold (say q^{th}), the following approximation for the buffer violation probability can be made

$$Pr(Q \geq q^{th}) \simeq e^{-\theta\, q^{th}}, \tag{2.2}$$

where $0 < \theta < \infty$ is a constant called QoS exponent, (see [24] for details).

The above equation states that the probability of the queue length exceeding a certain threshold q^{th} decays exponentially fast as the threshold q^{th} increases.

Furthermore, when the focus is on delay-bound violation probability, an expression similar to the above equation can be obtained as [26]

$$Pr(D \geq d^{th}) \simeq e^{-\theta \varepsilon d^{th}}, \tag{2.3}$$

where D and d^{th} denote the delay and delay bound, respectively, and ε is the source arrival rate determined as $\varepsilon = q^{th}/d^{th}$ [28]. The effective bandwidth function intersects with the effective capacity function at the value of ε (see [26] for details).

From Eqs. (2.2) and (2.3), we can see that the parameter θ plays an important role for the statistical QoS guarantees, which indicates the decaying-rate of the QoS violation probability. In practical applications, the value of θ depends on the statistical characterization of the arrival and service processes, bounds on delay or buffer lengths, and target values of the delay or buffer length violation probabilities.

A smaller θ corresponds to a slower decay rate, which implies that the system can only provide a looser QoS guarantee, while a larger θ leads to a faster decay rate, which means that a more stringent QoS requirement can be supported. In particular, when $\theta \to 0$, the system can tolerate an arbitrarily long delay, which corresponds to the scenario studied in information theory. On the other hand, when $\theta \to \infty$, the system cannot tolerate any delay, which corresponds to an extremely stringent delay-bound. Due to its close relationship with statistical QoS demands, θ is called the QoS exponent [24].

2.1.4 Effective Capacity Formulation

Based on the concept of QoS exponent, the effective capacity is defined as the maximum constant arrival rate that a given service process can support for which the QoS exponent θ is fulfilled. Analytically, the effective capacity can be formally expressed as follows.

Let the sequence $\{R[i], i = 1, 2, \cdots\}$ denote a discrete-time stationary and ergodic stochastic service process and $S[t] \triangleq \sum_{i=1}^{t} R[i]$ be the sum of the service process over time

sequence of $i = 1, 2, \cdots, t$. Then, the effective capacity of the service process, denoted by $E_C(\theta)$, where $\theta > 0$, is defined as [24]

$$E_C(\theta) = -\lim_{t\to\infty} \frac{1}{\theta t} \log_e \mathbb{E}[e^{-\theta S[t]}], \tag{2.4}$$

where $\mathbb{E}[\cdot]$ denotes the expectation. When the sequence $\{R[i], i = 1, 2, \cdots\}$ is an uncorrelated process, the effective capacity formula turns to

$$E_C(\theta) = -\frac{1}{\theta} \log_e \mathbb{E}[e^{-\theta R[i]}]. \tag{2.5}$$

Actually, the performance measure of $E_C(\theta)$ is a generalization of the common performance measures: *ergodic capacity*. For $\theta \to 0$, the effective capacity converges to the ergodic capacity. This can be shown using L'Hopital's rule in *calculus*. For $\theta \to 0$, the numerator of the effective capacity formula converges to the ergodic capacity while the denominator converges to one. This case corresponds to less stringent delay-constraints.

On the other hand, for $\theta \to \infty$, the effective capacity in Eq. (2.4) converges to the *delay-limited-capacity* defined in [53]. Therefore, the effective capacity represents an interesting measure which considers non-stringent delay constraints (for finite values of delay exponent θ).

2.2 Gamma Distribution as Channel Fading Model

Among different channel fading models, *Gamma* distribution is found to be an adequate model to characterize wireless channel fading such as slow fading (shadowing) or even fast fading [54, 55]. *Gamma* distribution fits the experimental data [54] and it is considered as a general case of most distributions. The probability density function (*pdf*) of Gamma distribution is given as

$$f_G(x) = \frac{2v x^{2vm-1}}{\phi^m \Gamma(m)} \exp\left[-\left(\frac{x}{\phi}\right)^{2v}\right], \tag{2.6}$$

where m, v, and ϕ are fading parameter, shape parameter, and scaling parameter respectively.

With proper choice of these parameters, m; v; ϕ, we may have:

- *Exponential* distribution ($m = 1$, $v = \frac{1}{2}$)
- *Rayleigh* distribution($m = v = 1$)
- *Weibull* distribution($m = 1$)
- *Log-Normal* distribution($m \to \infty$, $v = 0$)
- *AWGN* distribution($m \to \infty$, $v = 1$)
- *Rice* distribution($m \simeq \frac{(k+1)^2}{2k+1}$, $v = 1$)

Figure 2.1 shows the *pdf* of *Gamma* distribution for different m.

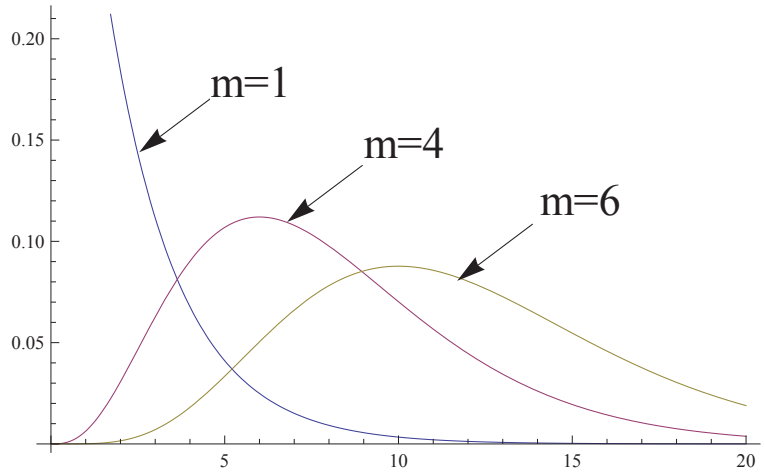

Figure 2.1: Probability density function for Gamma distribution for different fading parameters ($v = \frac{1}{2}$ and $\phi = 2$).

Statistically, if we have two independent Gamma distributions X and Y, then the ratio $Z = \frac{X}{Y}$ will have *Beta prime* distribution [56]. The random variables X and Y should be independent but not necessary to be identically distributed. So the channel coefficients may have different fading and shape parameters.

2.3 System Model and Assumptions

System models adapted in this study have different settings and assumptions. In each chapter, detailed description of the relevant model will be introduced. This section gives the general depiction of the used models and assumptions.

2.3.1 Cognitive radio Network

A typical CRN [36] model is assumed, in which a cognitive wireless network coexists with a primary wireless network by sharing $\mathcal{B}$ Hz spectrum band as shown in Figure 2.2. The cognitive network includes a secondary transmitter T_S and a secondary receiver R_S. The primary network includes a primary transmitter T_P and a primary receiver R_P.

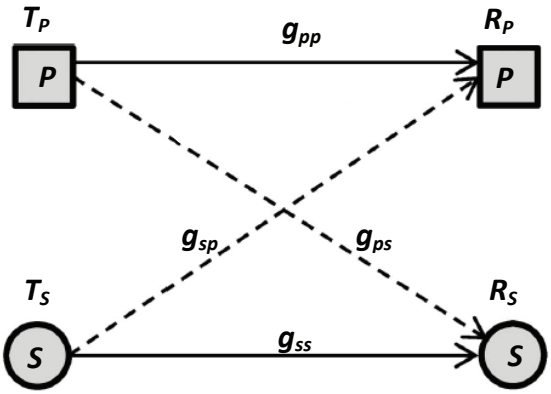

Figure 2.2: The main interference channels for a pair of primary and cognitive links.

The system gain g_{ij} shown in Figure 2.2 represents the channel power gain from the transmitter i to the receiver j, where $i, j \in \{s, p\}$.

The primary transmitter adjusts its transmit power S_p based only on its own transmission requirement. The secondary transmitter transmits with variable power S_s which should not exceed a maximum value of S_s^m.

2.3.2 Underlay Scheme

Even though the concurrent transmission is allowed in underlay cognitive radio system, interference threshold to the primary receiver is highly respected. In this scheme, cognitive users generally transmit at low power. When the cognitive radio applies the underlay scheme, the spectrum sensing is not needed. The secondary user can use the whole frame duration for transmission with adjusted transmit power no matter whether the primary network occupies the spectrum or not.

2.3.3 Overlay Scheme

When applying the overlay scheme, the secondary users need to utilize the spectrum sensing to identify the spectrum occupancy status before accessing the spectrum and can only use the vacant spectrum for transmissions. Therefore, for a frame of T seconds duration, the first τ seconds will be used to sense the channel, and the remaining $(T-\tau)$ seconds will be exploited for data transmission.

The spectrum occupation status can be determined between the following two hypotheses [36]:

$$\begin{aligned} &\text{detected as idle} \quad : \quad y(i) = n(i) \quad i = 1, 2 \cdots \tau\mathcal{B}, \\ &\text{detected as busy} \quad : \quad y(i) = n(i) + n_p(i) \quad i = 1, 2 \cdots \tau\mathcal{B}, \end{aligned} \tag{2.7}$$

where $y(i)$ is the received signal at the detector input of the cognitive transmitter, $n_p(i)$ is the received signal generated by the primary user.

2.3.3.1 Sensing Process

Among different spectrum sensing schemes for reliably identifying the spectrum holes, E*nergy Detection* incurs a very low implementation cost and is hence widely used [4]. It has a good resistance against dynamic radio environment where none a priori knowledge about the

primary user is available (non-coherent detector). In order to identify the presence of primary user with unknown frequency locations, energy detector serves as the optimal sensing scheme since it only needs to measure the power of the received signal. Figure 2.3 is a block diagram of an energy detector, where the bandpass filter is to limit the bandwidth of the input signal, followed by a squaring device to measure the received energy and the integrator determining the observation interval T. After the integrator is a threshold device, which compares the output of the integrator with a predetermined threshold to decide whether the signal is present or not.

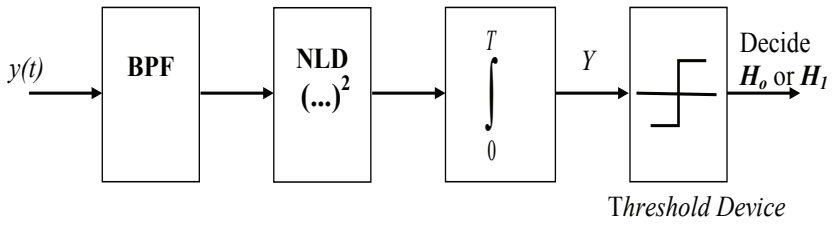

Figure 2.3: Block diagram of a simple energy detector

Two terms associated with spectrum sensing are probability of *detection* and probability of *false alarm* which are previously defined in Subsection 1.1.1.

2.4 General Assumptions

For all system models used through this thesis, the following assumptions are applied. Other assumptions may occur in each individual chapter.

- All channel power gains are assumed to be stationary and ergodic independent random processes.
- Information of interference channel gains can be obtained by direct feedback from the primary receiver or indirect feedback from a third-party such as a band manager

which interposes between the primary and cognitive users [57]. It can also be obtained through periodic sensing of pilot signal from the primary receiver assuming channel reciprocity. The case of imperfect information of channel coefficients will be separately analyzed.

- The background noise at the secondary and primary receivers are modeled as $AWGN$ independent Circularly Symmetric Complex Gaussian ($CSCG$) random variable with zero-mean and variance σ_s^2 and σ_p^2, respectively.

- The maximum interference at the primary receiver I^{th} is assumed to be known to cognitive user.

- Small scale variations are assumed in all settings. Other variations such as distance path loss dependent or shadowing impacts are considered as background noise or/and interference.

- A block-fading channel model is assumed in which the fading coefficients stay constant in the frame, and they may change from one block to another independently. When spectrum sensing is used, the sensing process is assumed to be the same within the frame and it may change between frames.

- The probability of the channel being occupied by the primary users is equal to P_b, it is assumed to be known to the cognitive user. It represents the existence activity of the primary user.

- When using markov model, the state transitions between states are assumed to occur every frame and they may change between frames.

- Single transceiver for each network is assumed. Multiple user case is suggested as a future work.

2.4.1 Symbolism in the Thesis

For the abbreviations used in the thesis, the common subscripts s and p refer to the secondary user and primary user respectively. The superscripts u, o, $\{0, 1\}$ and $*$ refer to the underlay, overlay, state number and optimal value respectively. The upper limit of a quantity is always written with superscripts (*e.g.*, I^{th}, S^m, E_c^{opt}). The power is denoted by capital S, while the channel power gain is given the letter g with two subscribes ij which refer to the channel power gain from the transmitter i to the receiver j.

Chapter 3

Effective Capacity Analysis for CRNs and Selection Criteria

Recently, satisfaction of QoS demands for secondary users has attracted great attention. The secondary user can not only discover the transmission opportunities, but also cognitively adapts the dynamic spectrum access strategies to its own QoS requirement and the environment variations. In this chapter, we study how the delay QoS requirement affects the strategy on network performance. We first treat the delay-QoS in interference constrained CRN by applying the *effective capacity* concept, focusing on the two dominant DSA schemes: *underlay* and *overlay*. We obtain the effective capacity of the secondary network and determine the power allocation policies that maximize the throughput. The underlay and overlay approaches may have their respective advantages under diverse propagation environment and system parameters. If the cognitive network can dynamically choose the DSA strategy under different environment, its performance could be further improved. We propose a selection criterion to determine whether to use underlay or overlay scheme under the given QoS constraint and the primary users' spectrum-occupancy probability. Thus, the throughput of the CRN could be increased.

The functions of cognitive radio networks have been broadened such that the cognitive users can not only detect the transmission opportunities under the specific DSA approach, but also cognitively adapt the dynamic spectrum access strategies to the QoS requirement and the channel variations. In this chapter, we focus on the QoS driven underlay and overlay schemes by introducing the concept of effective capacity proposed in [24]. We present a systematic approach which suggests the best access scheme for a given system requirement. The mixed strategy proposed in this chapter is similar in spirit to the sensing-based spectrum sharing proposed in [36] except that, in our study, the effective capacity is adopted instead of ergodic capacity and the general case of *Gamma* distribution is assumed for the channel fading. Also in [36], just overlay scheme is analyzed. In this study, both DSA schemes are studied. We further introduce a new selection criterion to obtain the best access scheme.

The rest of this chapter is organized as follows. The system model and assumptions are introduced in Section 3.1. In Section 3.2, the effective capacity optimization and optimal resource allocation for the underlay scheme are studied. In Section 3.3, spectrum sensing, effective capacity, and power allocation for the overlay case are studied in three subsequent subsections. Then, we propose an access strategy selection criterion in Section 3.4. Performance analysis and numerical results are presented in Section 3.5. Section 3.6 summarizes this chapter.

3.1 System Model and Assumptions

A typical CRN [36] model is assumed as shown in Figure 2.2. In which a cognitive wireless network coexists with a primary wireless network by sharing $\mathcal{B}$ Hz spectrum band. The cognitive network includes a secondary transmitter T_S and a secondary receiver R_S. The primary network includes a primary transmitter T_P and a primary receiver R_P.

All channel power gains are assumed to be stationary and ergodic independent random

processes. These system gains are grouped in the vector $\mathbf{G} = [g_{ss}, g_{sp}, g_{pp}, g_{ps}]$ for a specific realization as shown in Figure 2.2. All channel power gains are assumed to be independent and identically distributed (*i.i.d.*), and follow *Gamma* distribution since it considered as a general case. It is also assumed that the cognitive transmitter has perfect information of interference channel gains. The case of imperfect information of the channel coefficients will be analyzed in Chapter 4.

The probability density functions (*pdf*)s of $f_{g_{ss}}$, $f_{g_{sp}}$, $f_{g_{pp}}$, and $f_{g_{ps}}$, are given as

$$f_X(x) = \frac{x^{\mu-1}e^{-x/\phi}}{\Gamma(\mu)\phi^{\mu}}; \qquad x \geq 0, \tag{3.1}$$

where $\Gamma(\cdot)$ is the Gamma function which is defined in Appendix A, μ is known as the shape parameter of the distribution, and ϕ is the scale parameter. The average $\mathbb{E}[X] = \mu\phi$, and $\mathbb{V}ar[X] = \mu\phi^2$. Without loss of generality, we assume the parameter $\phi = 1$. The background noise at the secondary and primary receivers are modeled as $AWGN$ independent Circularly Symmetric Complex Gaussian ($CSCG$) random variable with zero-mean and variance σ_s^2 and σ_p^2 respectively.

The maximum interference at the primary receiver should be kept below a threshold value I^{th}. This value is a system parameter which can be specified by the primary network operator or by the spectrum regulator. Small scale variations are assumed in this chapter where other variations such as distance path loss dependent or shadowing impacts are considered as background noise or/and interference.

As mentioned above, in the underlay scheme, the secondary user is required to always satisfy the interference constraint. Therefore, even in circumstances when the primary user is not transmitting, the cognitive user has to adjust its transmission power based on the interference threshold constraint. Consequently, the derived resource allocation schemes should not be only a function of system gain vector $\mathbf{G}$, but also will be varied with different QoS requirement. In order to clearly illustrate our concept, we assume that each frame at the data link layer (DLL) of the cognitive transmitter has the same time duration. The

frames are stored at the transmit buffer and split into bit-streams at the physical layer (PHY). The cognitive transmitter employs adaptive modulation and power control based on the statistical QoS constraint and the system gain vector $\mathbf{G}$.

The factors that impact the resource allocation of the cognitive network include:

1. the average transmit and interference power constraints;
2. the statistical delay QoS requirement;
3. the primary network activities;
4. the DSA strategy used by the cognitive network; and
5. the interference caused by the primary transmitter on the cognitive network.

The existing literatures studied only the underlay strategy, and the primary network activities are ignored. In this chapter, the primary users spectrum-occupancy probability will be taken into consideration even for the underlay strategy. It is assumed that the primary network will choose whether to use the spectrum or not at the beginning of each frame. As the spectrum-occupancy status of the primary network can be viewed as the two hypothesis tests from the cognitive user's perspective, we denote the probability that the primary network does not occupy the spectrum as P_i (idle probability), and the probability that the spectrum is occupied as P_b (busy probability). We assumed that these probabilities will not change during the frame interval.

3.2 Optimal Resource Allocation For Underlay Scheme

In this section, we aim at obtaining the optimal resource allocation which can maximize the throughput of the cognitive network under a given statistical delay QoS guarantee determined by QoS exponent θ.

When the cognitive radio applies the underlay scheme, the spectrum sensing is not needed. The secondary user can use the whole frame duration for transmission with adjusted transmit power no matter whether the primary network occupies the spectrum or not. The cognitive network with the underlay scheme has two system states for each frame, which are listed as follows:

- **State** 0: The channel is idle, *i.e.*, it is not occupied by the primary network, with a probability P_i.
- **State** 1: The channel is busy, *i.e.*, it is currently used by the primary network, with a probability P_b.

We denote the service rates of these two states as $R^{u,i}$ and $R^{u,b}$ at secondary user, respectively. Based on Shannon information theory, the achievable service rates of the two system states can be written as

$$R^{u,i} = T\mathcal{B}P_i \log_2\left(1+\frac{g_{ss}S_s^{u,i}}{\sigma_s^2}\right), \quad \text{and} \qquad R^{u,b} = T\mathcal{B}P_b \log_2\left(1+\frac{g_{ss}S_s^{u,b}}{g_{ps}S_p+\sigma_s^2}\right), \quad (3.2)$$

where $S_s^{u,i}$ and $S_s^{u,b}$ are two transmit power levels of the cognitive transmitter when the spectrum is idle and busy, respectively. The effective capacity formula of the cognitive network for each state mentioned above can be written as

$$E_C^{u,i}(\theta) = -\frac{1}{\theta}\log_e\left(\mathbb{E}_{g_{ss}}[e^{-\theta R^{u,i}}]\right) \quad (3.3)$$

$$E_C^{u,b}(\theta) = -\frac{1}{\theta}\log_e\left(\mathbb{E}_{z}[e^{-\theta R^{u,b}}]\right), \quad (3.4)$$

where $\mathbb{E}_{g_{ss}}$ is the expectation over the random variable g_{ss}, and $\mathbb{E}_z$ is the expectation operator over the ratio of the random variables g_{ss} and g_{ps} which will be discussed shortly.

Since in the underlay case, the cognitive user does not preform spectrum sensing, it is not possible to differentiate state 0 or state 1. Hence, we can impose the cognitive user to operate in the state that provides higher capacity. Therefore, the aim now is to solve Eq. (3.3) and Eq. (3.4) individually, and make the cognitive user to choose a power level that provides better performance.

The effective capacity Eq. (3.3) can be written as

$$\begin{aligned} E_C^{u,i}(\theta) &= -\frac{1}{\theta}\log_e\left(\mathbb{E}_{g_{ss}}\left[e^{-T\mathcal{B}P_i\theta\log_2\left(1+\frac{g_{ss}S_s^{u,i}}{\sigma_s^2}\right)}\right]\right) \\ &= -\frac{1}{\theta}\log_e\left(\mathbb{E}_{g_{ss}}\left[\left(1+\frac{g_{ss}S_s^{u,i}}{\sigma_s^2}\right)^{-\alpha^{u,i}}\right]\right), \end{aligned} \tag{3.5}$$

where the term $\alpha^{u,i} = (T\mathcal{B}P_i\theta/\ln 2)$ can be named as the normalized QoS exponent. It can characterize the statistical delay QoS requirement since it is only a function of θ.

Eq. (3.5) can be evaluated by taking the expectation over the random variable g_{ss} which has the *pdf* given in Eq. (3.1), and by evaluating the integration, the following formula can be obtained (see also the derivation in Appendix B)

$$\begin{aligned} E_C^{u,i} = -\frac{1}{\theta}\log_e\Bigg[\Bigg(&\frac{\Gamma(\alpha^{u,i}-\mu_1)}{\Gamma(\alpha^{u,i})}(\gamma^u)^{\mu}\ {}_1F_1\left(\mu_1;1+\mu_1-\alpha^{u,i};\gamma^u\right) \\ &+\frac{\Gamma(\mu_1-\alpha^{u,i})}{\Gamma(\mu_1)}(\gamma^u)^{\alpha^{u,i}}\ {}_1F_1\left(\alpha^{u,i};1+\alpha^{u,i}-\mu_1;\gamma^u\right)\Bigg)\Bigg], \end{aligned} \tag{3.6}$$

where $\gamma^u = \frac{\sigma_s^2}{S_s^{u,i}}$, $\mu_1 = \mu$, and the function ${}_1F_1$ is called *Confluent Hypergeometric* function of first kind, defined in Appendix A.

To evaluate Eq. (3.4), we refer to the statistical fact that says: *the ratio of two independent Gamma distributed random variables with shape parameters μ_1 and μ_2, respectively is* Beta Prime *distributed random variable with parameters μ_1 and μ_2* [58]. Let us define the random variables X and Y as $X = g_{ss}$, and $Y = (g_{ps}S_p + \sigma_s^2)/S_s^{u,b}$. Since power channel fading is assumed to be Gamma distributed, Y is also Gamma distributed with mean μ_2. The *pdf* of Y can be expressed as

$$f_Y(y) = \frac{y^{\mu_2-1}e^{-y}}{\Gamma(\mu_2)}, \tag{3.7}$$

where $\mu_2 = \frac{(\mu_1 S_p+\sigma_s^2)}{S_s^{u,b}}$. Then, the *pdf* of the ratio random variable $Z = \frac{X}{Y}$ has the following Beta Prime distribution

$$f_Z(z) = \frac{z^{\mu_1-1}(1+z)^{-\mu_1-\mu_2}}{\beta(\mu_1,\mu_2)}. \tag{3.8}$$

Here, $\mu_1 = \mu$ is the expected value of power channel fading. In Eq. (3.8), $\beta(\mu_1,\mu_2)$ is the

Beta function which is related to *Gamma function* as $\beta(\mu_1, \mu_2) = \frac{\Gamma(\mu_1)\Gamma(\mu_2)}{\Gamma(\mu_1+\mu_2)}$. Substituting $R^{u,b}$ defined in Eq. (3.2) into Eq. (3.4), we get

$$\begin{aligned} E_C^{u,b}(\theta) &= -\frac{1}{\theta}\log_e\left(\mathbb{E}_z\left[e^{-T\mathcal{B}P_b\theta\log_2\left(1+\frac{g_{ss}S_s^{u,b}}{g_{ps}S_p+\sigma_s^2}\right)}\right]\right) \\ &= -\frac{1}{\theta}\log_e\left[\mathbb{E}_z\left[(1+z)^{-\alpha^{u,b}}\right]\right], \end{aligned} \tag{3.9}$$

where $\alpha^{u,b} = T\mathcal{B}P_b\theta/\ln 2$.

Eq. (3.9) can be evaluated by taking the expectation over the random variable z which has the *pdf* given in Eq. (3.8). By evaluating the integration using the *symbolic integration* provided by *MapleSoft-12* software, the following formula can be obtained

$$E_C^{u,b} = -\frac{1}{\theta}\log_e\left[\left(\frac{\Gamma(\alpha^{u,b}+\mu_2)\Gamma(\mu_1+\mu_2)}{\Gamma(\alpha^{u,b}+\mu_1+\mu_2)\Gamma(\mu_2)}\right)\right]. \tag{3.10}$$

The effective capacity formula Eq. (3.6) and Eq. (3.10) are derived using the properties of gamma and hypergeometric functions listed in Appendix A.

In Figure 3.1, we plot Eqs. (3.6) and (3.10) as a function of P_i in which we allocate the powers in fixed manner depending on how the channel is busy or idle (*i.e.*, $S_s^{u,i} = P_i S^m$ and $S_s^{u,b} = P_b S^m$). The figure shows that, depending on the probabilities of spectrum activity, the maximum achieved effective capacity may vary from a state to another. As a result of nonexistence of sensing information in underlay base, it is not easy for the cognitive transmitter to know what power should be used to perform transmission. For this reason, the following algorithm is proposed to notify the transmitter which power level has to be used to achieve optimal performance.

Now, the main objective is to find the optimal power allocation for the two power levels $\{S_s^{u,i}, S_s^{u,b}\} = \{\frac{\sigma_s^2}{\gamma^u}, \frac{\mu_1 S_p+\sigma_s^2}{\mu_2}\}$ to maximize the effective capacity of the cognitive network subject to the upper bounded transmit and interference powers. From Eq. (3.6), we can formulate an expression for the optimal effective capacity for the cognitive network channel

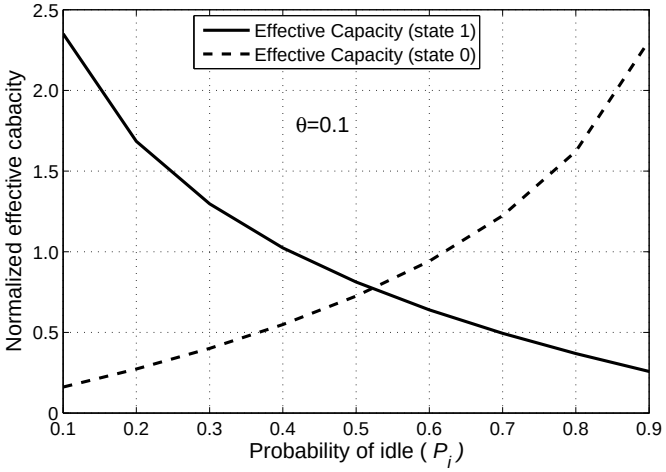

Figure 3.1: Effective capacity versus probability of idle for idle and busy states. $S_p = S^m$=10 dBw, B=1 KHz, T=50 ms, $\sigma^2 = 1$.

in the state 0, and write the optimization problem as follows

$$\begin{aligned} \max_{\gamma^u} -\frac{1}{\theta}\log_e \Bigg[\Bigg(& \frac{\Gamma(\alpha^{u,i}-\mu_1)}{\Gamma(\alpha^{u,i})}(\gamma^u)^{\mu}\ {}_1F_1\left(\mu_1; 1+\mu_1-\alpha^{u,i}; \gamma^u\right) \\ & + \frac{\Gamma(\mu_1-\alpha^{u,i})}{\Gamma(\mu_1)}(\gamma^u)^{\alpha^{u,i}}\ {}_1F_1\left(\alpha^{u,i}; 1+\alpha^{u,i}-\mu_1; \gamma^u\right) \Bigg) \Bigg], \end{aligned} \tag{3.11}$$

$$S.t. \qquad 0 \le S_s^{u,i} \le S_s^m,$$

$$\mathbb{E}[g_{sp} S_s^{u,i}] \le I^{th}.$$

The cognitive transmitter should satisfy transmit power constraint, which appears in the first constraint in Eq. (3.11). At the same time, since the transmissions of the cognitive network will interfere the primary network, in order to protect the QoS of the primary network, the average interference power constraint is imposed in the second constraint of Eq. (3.11).

Using the fact that $\log(\cdot)$ is a monotonically increasing function, the solution to the

maximization problem Eq. (3.11) can be mapped to the following minimization problem

$$\begin{aligned} \min_{\gamma^u} \Bigg(& \frac{\Gamma(\alpha^{u,i}-\mu_1)}{\Gamma(\alpha^{u,i})} (\gamma^u)^{\mu} \ {}_1F_1\left(\mu_1; 1+\mu_1-\alpha^{u,i}; \gamma^u\right) \\ & + \frac{\Gamma(\mu_1-\alpha^{u,i})}{\Gamma(\mu_1)} (\gamma^u)^{\alpha^{u,i}} \ {}_1F_1\left(\alpha^{u,i}; 1+\alpha^{u,i}-\mu_1; \gamma^u\right) \Bigg), \\ S.t. \quad & 0 \le S_s^{u,i} \le S_s^m, \\ & \mathbb{E}[g_{sp} S_s^{u,i}] \le I^{th}. \end{aligned} \tag{3.12}$$

By studying the behavior of the function ${}_1F_1$ through its properties given in Appendix A, it can be shown that the objective function of the above optimization problem is convex function. Also the constraints are linear with respect to the optimized variable $S^{u,i}$. As a result, we can conclude that the problem in Eq. (3.12) has no more than one minimum. This global minimum can be found by taking the first derivative of the above objective function and equating it to zero. So the corresponding optimal power allocation is the solution of the following equation

$$\begin{aligned} & \Bigg[C_1^u \mu_1 (\gamma^{*u})^{\mu_1} \left({}_1F_1(\mu_1; 1+\mu_1-\alpha^{u,i}; \gamma^{*u}) + \frac{\gamma^{*u} \ {}_1F_1(1+\mu_1; 2+\mu_1-\alpha^{u,i}; \gamma^{*u})}{1+\mu_1-\alpha^{u,i}} \right) \\ & + C_2^u \alpha^{u,i} (\gamma^{*u})^{\alpha^{u,i}} \left({}_1F_1(\alpha^{u,i}; 1+\alpha^{u,i}-\mu_1; \gamma^{*u}) + \frac{\gamma^{*u} \ {}_1F_1(1+\alpha^{u,i}; 2+\alpha^{u,i}-\mu_1; \gamma^{*u})}{1+\alpha^{u,i}-\mu_1} \right) \Bigg] = 0, \end{aligned} \tag{3.13}$$

$$\text{where} \quad C_1^u = \Gamma(\alpha^{u,i}-\mu_1)/\Gamma(\alpha^{u,i}), \qquad C_2^u = \Gamma(\mu_1-\alpha^{u,i})/\Gamma(\mu_1).$$

Eq. (3.13) can be solved numerically in the domain $\left[0 \le S_s^{*u,i} \le \min\{\frac{I^{th}}{\mu_1}, S^m\}\right]$, where $S_s^{*u,i} = \frac{\sigma_s^2}{\gamma^{*u}}$.

Similar to the work done in the state 0, the optimization problem to adapt $S_s^{u,b}$ can be formulated to the following minimization problem

$$\begin{aligned} \min_{\mu_2} \quad & \frac{\Gamma(\alpha^{u,b}+\mu_2)\Gamma(\mu_1+\mu_2)}{\Gamma(\alpha^{u,b}+\mu_1+\mu_2)\Gamma(\mu_2)}, \\ S.t. \quad & 0 \le S_s^{u,b} \le S_s^m, \\ & \mathbb{E}[g_{sp} S_s^{u,b}] \le I^{th}, \end{aligned} \tag{3.14}$$

and the corresponding optimal power allocation of the state 1 is the solution of the following equation

$$\Psi\left(\alpha^{u,b}+\mu_2^*\right)+\Psi\left(\mu_1+\mu_2^*\right)-\Psi\left(\alpha^{u,b}+\mu_1+\mu_2^*\right)-\Psi\left(\mu_2^*\right)=0 \tag{3.15}$$

in the domain $\left[0 \leq S_s^{*u,b} \leq \min\{S^m, \frac{I^{th}}{\mu_1}\}\right]$. We use the property of $\Gamma(x) \neq 0, \forall x \in \mathcal{R}$ to simplify Eq. (3.15). Note that the optimal value μ_2^* is the value of μ_2 corresponding to $S_s^{*u,b}$, *i.e.*, $\mu_2^* = (\mu_1 S_p + \sigma_s^2)/S_s^{*u,b}$. The function Ψ in Eq. (3.15) is known as *Polygamma* function defined as [59]

$$\Psi(z)=\int_0^\infty \frac{t^m e^{-zt}}{e^t-1}dt=-\gamma_0+\sum_{k=0}^{\infty}\frac{1}{k+1}-\frac{1}{k+z} \quad z\neq 0,-1,-2,\cdots, \tag{3.16}$$

where $\gamma_0 \simeq 0.57721$ is the Euler-Mascheroni constant.

The cognitive transmitter will be allocated the power that maximizes the effective capacity. The optimal power allocation for the underlay cognitive radio $S_s^{*u} \in \{S_s^{*u,i}, S_s^{*u,b}\}$ which optimizes the effective capacity can be determined by

$$S_s^{*u}=\underset{S_s^{*u,i},S_s^{*u,b}}{\arg\max}\left(E_C^{u,i}\left(S_s^{*u,i}\right),E_C^{u,b}\left(S_s^{*u,b}\right)\right). \tag{3.17}$$

As a result, the optimal effective capacity of the underlay scheme is

$$E_C^{u,opt}(\theta,S_s^{*u})=\max\left(E_C^{u,i}(\theta,S_s^{*u}),E_C^{u,b}(\theta,S_s^{*u})\right). \tag{3.18}$$

3.3 Optimal Resource Allocation For Overlay Scheme

In this section, we aim at deriving optimal resource allocation strategy for the overlay scheme. As discussed previously, while applying the overlay scheme, the secondary users need to utilize the spectrum sensing to identify the spectrum occupancy status before accessing the spectrum and can only use the vacant spectrum for transmissions. Therefore, for a frame of T seconds duration, the first τ seconds will be used to sense the channel, and the remaining $(T-\tau)$ seconds will be exploited for data transmission. The resulting frame structure is shown in Figure 3.2.

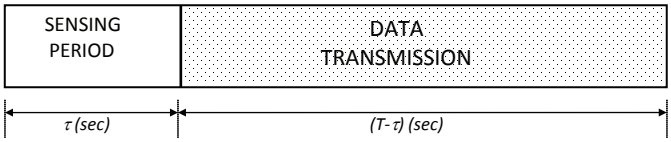

Figure 3.2: The transmission frame structure.

3.3.1 Spectrum Sensing Model

According to [5, 9, 36], the spectrum occupation status can be determined between the following two hypotheses:

$$\begin{aligned} &\text{detected as idle} \quad : \quad y(i) = n(i) \quad i = 1, 2 \cdots \tau\mathcal{B}, \\ &\text{detected as busy} \quad : \quad y(i) = n(i) + n_p(i) \quad i = 1, 2 \cdots \tau\mathcal{B}, \end{aligned} \tag{3.19}$$

where $y(i)$ is the received signal at the detector input of the cognitive transmitter, $n_p(i)$ is the received signal generated by the primary user. Since the bandwidth is $\mathcal{B}$, we assume that the symbol rate is $\mathcal{B}$ complex symbols per second. So we have $\tau\mathcal{B}$ symbols in a duration of τ seconds (for simplicity, we assume that $\tau\mathcal{B}$ is an integer). Assuming that $\{n_p(i)\}$ samples are *i.i.d.* signal and modeled as zero-mean Gaussian distributed with variance of $\sigma_{n_p}^2$. The optimal detector response for this hypothesis problem is given in [60] as

$$\mathcal{Y} = \frac{1}{\tau\mathcal{B}} \sum_{i=1}^{\tau\mathcal{B}} |y_i|^2 \lessgtr_{busy}^{idle} \delta, \tag{3.20}$$

where δ is a pre-designed threshold. The cognitive radio assumes that the primary system is in operation if $\mathcal{Y} \geq \delta$. Otherwise, it is idle. Assuming $\tau\mathcal{B}$ is sufficiently high, $\mathcal{Y}$ can be approximated, using Central Limit Theorem [61], as a Gaussian random variable with mean and variance

$$\mathbb{E}[\mathcal{Y}] = \begin{cases} \sigma_s^2 & \text{if PU is inactive} \\ \sigma_s^2 + \sigma_{n_p}^2 & \text{if PU is active,} \end{cases} \tag{3.21}$$

and

$$\sigma_{\mathcal{Y}}^2 = \begin{cases} \sigma_s^4/(\tau\mathcal{B}) & \text{if PU is inactive} \\ \left(\mathbb{E}[\,|n_p|^4] + \sigma_s^4 + 2\sigma_{n_p}^2\sigma_s^2 - \sigma_{n_p}^2\right)/(\tau\mathcal{B}) & \text{if PU is active,} \end{cases} \tag{3.22}$$

respectively, where $\mathbb{E}[|n_p|^4]$ is the forth moment of the received signal n_p. Note that $\mathbb{E}[|n_s|^4] = 2\sigma_s^2$ for the $CSCG$ assumption [10]. The probability of false alarm of the energy detector is given as follows

$$\mathcal{P}_f = Pr\{\mathcal{Y} > \delta | P_i\} = Q\left(\frac{\delta - \sigma_s^2}{\sqrt{\sigma_s^4/(\tau\mathcal{B})}}\right), \tag{3.23}$$

where $Q(\cdot)$ is the complementary cumulative distribution function of the standard Gaussian. If we assume that the primary signal n_p has complex-valued PSK waveform [10], the probability of detection of the energy detector can be written as

$$\mathcal{P}_d = \quad Pr\{\mathcal{Y} > \delta | P_b\} = Q\left(\frac{\delta - \sigma_{n_p}^2 - \sigma_s^2}{\sigma_s\sqrt{\left(2\sigma_{n_p}^2 + \sigma_s^2\right)/(\tau\mathcal{B})}}\right), \tag{3.24}$$

Due to the unavoidable sensing errors, the cognitive network has four states, which are listed as follows:

1. **State** 0 : Channel is idle, detected as idle, with probability: $(1 - \mathcal{P}_f)P_i$
2. **State** 1 : Channel is busy, detected as idle, with probability: $(1 - \mathcal{P}_d)P_b$
3. **State** 2 : Channel is idle, detected as busy, with probability: $\mathcal{P}_f P_i$
4. **State** 3 : Channel is busy, detected as busy, with probability: $\mathcal{P}_d P_b$

As defined in the overlay strategy, the cognitive network can access the spectrum only when the channel is sensed as idle. Therefore, the service rates of the cognitive network for the first two states, denoted by $R^{o,i}, R^{o,b}$ are

$$\begin{aligned} R^{o,i} = &\quad (T-\tau)\mathcal{B}(1-\mathcal{P}_f)P_i \log_2\left(1 + \frac{g_{ss}S_s^{o,i}}{\sigma_s^2}\right), \\ \text{and,} \quad R^{o,b} = &\quad (T-\tau)\mathcal{B}(1-\mathcal{P}_d)P_b \log_2\left(1 + \frac{g_{ss}S_s^{o,b}}{g_{ps}S_p + \sigma_s^2}\right), \end{aligned} \tag{3.25}$$

where $S_s^{o,i}$ and $S_s^{o,b}$ are two transmit power levels for the state 0 and 1, respectively. While the service rates of the last two states are *zero* because the channel has been detected as busy and no transmission is allowed in this case.

The cognitive user in both states 0 and 1 detects the spectrum as idle, but due to possible sensing errors, the channel is actually idle as in state 0 (correct detection event) and it is

actually busy as in state 1 (false-alarm event). The cognitive user can not differentiate between state 0 and state 1 in each of them the channel is sensed as idle.

The effective capacity of the overlay scheme for states 0 and 1 can be written as

$$\begin{aligned} E_C^{o,i}(\theta) = &\quad -\frac{1}{\theta}\log_e\left(\mathbb{E}[e^{-\theta R^{o,i}}]\right) \\ \text{and,}\quad E_C^{o,b}(\theta) = &\quad -\frac{1}{\theta}\log_e\left(\mathbb{E}[e^{-\theta R^{o,b}}]\right). \end{aligned} \tag{3.26}$$

Using the same idea presented in the underlay case, Eq. (3.26) can be expanded as

$$\begin{aligned} E_C^{o,i}(\theta) &= -\frac{1}{\theta}\log_e\left(\mathbb{E}_{g_{ss}}\left[e^{-(T-\tau)\mathcal{B}(1-\mathcal{P}_f)P_i\theta\log_2\left(1+\frac{g_{ss}S_s^{o,i}}{\sigma_s^2}\right)}\right]\right) \\ \text{and,}\quad E_C^{o,b}(\theta) &= -\frac{1}{\theta}\log_e\left(\mathbb{E}_{w}\left[e^{-(T-\tau)\mathcal{B}(1-\mathcal{P}_d)P_b\theta\log_2\left(1+\frac{g_{ss}S_s^{o,b}}{g_{ps}S_p+\sigma_s^2}\right)}\right]\right), \end{aligned} \tag{3.27}$$

where $\mathbb{E}_w$ is the expectation over the ratio $\frac{g_{ss}S_s^{o,b}}{g_{ps}S_p+\sigma_s^2}$.

Let $\alpha^{o,i} = (T-\tau)\mathcal{B}(1-\mathcal{P}_f)P_i\theta/\ln 2$, and $\alpha^{o,b} = (T-\tau)\mathcal{B}(1-\mathcal{P}_d)P_b\theta/\ln 2$ as the normalized QoS exponent for each state. These parameters can characterize the statistical delay QoS requirement, since at certain sensing time it is only a function of θ. Eqs. (3.27) can be written as

$$\begin{aligned} E_C^{o,i}(\theta) = &\quad -\frac{1}{\theta}\log_e\left(\mathbb{E}_{g_{ss}}\left[\left(1+\frac{g_{ss}S_s^{o,i}}{\sigma_s^2}\right)^{-\alpha^{o,i}}\right]\right) \\ \text{and,}\quad E_C^{o,i}(\theta) = &\quad -\frac{1}{\theta}\log_e\left(\mathbb{E}_{w}\left[(1+w)^{-\alpha^{o,b}}\right]\right). \end{aligned} \tag{3.28}$$

Similar to the work done in Eq. (3.9), Eqs. (3.28) can be evaluated, a solution for each case can be obtained as

$$\begin{aligned} E_C^{o,i} = &-\frac{1}{\theta}\log_e\left(\frac{\Gamma(\alpha^{o,i}-\mu_1)}{\Gamma(\alpha^{o,i})}(\gamma^o)^{\mu}\ {}_1F_1\left(\mu_1;1+\mu_1-\alpha^{o,i};\gamma^o\right)\right. \\ &\left.+\frac{\Gamma(\mu_1-\alpha^{o,i})}{\Gamma(\mu_1)}(\gamma^o)^{\alpha^{o,i}}\ {}_1F_1\left(\alpha^{o,i};1+\alpha^{o,i}-\mu_1;\gamma^o\right)\right), \\ \text{and,}\quad E_C^{o,b} = &-\frac{1}{\theta}\log_e\left(\frac{\Gamma(\alpha^{o,b}+\mu_3)\,\Gamma(\mu_1+\mu_3)}{\Gamma(\alpha^{o,b}+\mu_1+\mu_3)\,\Gamma(\mu_3)}\right), \end{aligned} \tag{3.29}$$

where $\gamma^o = \frac{\sigma_s^2}{S_s^{o,i}}$, and $\mu_3 = \frac{(\mu_1 S_p+\sigma_s^2)}{S_s^{o,b}}$. The derivation is similar to the underlay case of Eq. (3.6) and Eq. (3.10). See Appendix B for details.

Depending on the factors $(1-\mathcal{P}_f)P_i$ and $(1-\mathcal{P}_d)P_b$, the capacity that can be achieved

from each state might vary. Figure 3.3 illustrates the impact of these probabilities on the effective capacity in each state. As it can be seen from Eq. (3.25), even though, the state 0 with power level $S_s^{o,i}$ is most likely to be chosen, but in some cases, transmission using the power level $S_s^{o,b}$ which refers to state 1 may get better, especially for lower probability of idle as depicted in Figure 3.3. Thus, an algorithm which will be able to notify the cognitive user to select one of these states (whether 0 or 1) is needed. The cognitive user will be forced to transmit with a power that attains more capacity while satisfying the power and interference constraints. The cognitive user does not necessarily know what the state is (0 or 1), the algorithm will compromise between two levels of power (referred as $S_s^{o,i}$ and $S_s^{o,b}$).

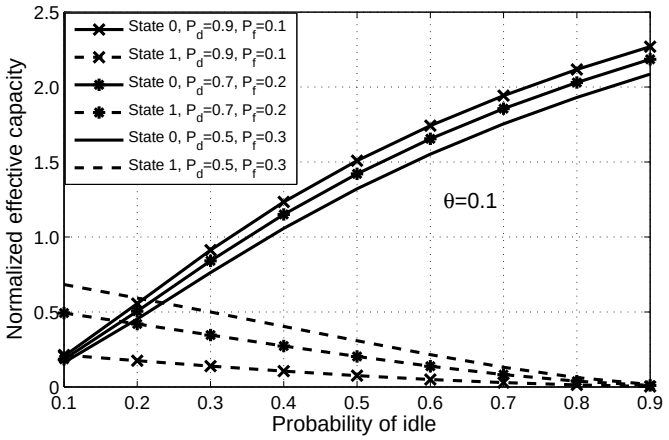

Figure 3.3: The impact of sensing probabilities on effective capacity for states 0 and 1 in overlay scheme.

3.3.2 Optimal Power Allocation for Overlay Scheme

The power allocation of the cognitive radio network, $\{S_s^{o,i}, S_s^{o,b}\}$ should be carefully assigned to optimize the overall capacity of the channel. Furthermore, the sensing period τ, which plays a great role on the system performance, should also be considered in this optimization process.

The cognitive network needs to meet transmit power constraint, this can be expressed as

$$\text{state } 0 \quad : \qquad \tfrac{T-\tau}{T} S_s^{o,i} \leq S_s^m, \tag{3.30}$$

$$\text{state } 1 \quad : \qquad \tfrac{T-\tau}{T} S_s^{o,b} \leq S_s^m. \tag{3.31}$$

Similarly, the interference from the cognitive transmitter to the primary should also meet the following interference constraint

$$\text{state } 0 \quad : \qquad \tfrac{T-\tau}{T} \mathbb{E}[g_{sp} S_s^{o,i}] \leq I^{th}, \tag{3.32}$$

$$\text{state } 1 \quad : \qquad \tfrac{T-\tau}{T} \mathbb{E}[g_{sp} S_s^{o,b}] \leq I^{th}. \tag{3.33}$$

Our objective is to derive the optimal resource allocation $\{S_s^{o,i}, S_s^{o,b}, \tau\}$ to maximize the effective capacity under the transmit and interference power constraints in Eqs. (3.30)-(3.33).

The optimization problem of the state 0 can be formulated as

$$\begin{aligned} \max_{\gamma^o,\, \tau} \; & -\frac{1}{\theta} \log_e \Big[\Big(C_1^o (\gamma^o)^{\mu} \; {}_1F_1\left(\mu_1; 1+\mu_1-\alpha^{o,i}; \gamma^o\right) + C_2^o (\gamma^o)^{\alpha^{o,i}} \; {}_1F_1\left(\alpha^{o,i}; 1+\alpha^{o,i}-\mu_1; \gamma^o\right) \Big) \\ & \textit{S.t.} \qquad \textit{Eq.}\ (3.30) \quad \& \quad \textit{Eq.}\ (3.32) \qquad \text{hold}, \quad \text{and} \;\; 0 < \tau < T/2, \end{aligned} \tag{3.34}$$

With the same manner, the optimization problem of the state 1 can be formulated as

$$\begin{aligned} \max_{\mu_3,\, \tau} \; & \frac{\Gamma(\alpha^{o,b}+\mu_3)\Gamma(\mu_1+\mu_3)}{\Gamma(\alpha^{o,b}+\mu_1+\mu_3)\Gamma(\mu_3)} \Big] \\ & \textit{S.t.} \qquad \textit{Eq.}\ (3.31) \quad \& \quad \textit{Eq.}\ (3.33) \qquad \text{hold}, \quad \text{and} \;\; 0 < \tau < T/2, \end{aligned} \tag{3.35}$$

where C_1^o and C_2^o in (3.34) are defined as $C_1^o = \Gamma(\alpha^{o,i}-\mu_1)/\Gamma(\alpha^{o,i})$, $C_2^o = \Gamma(\mu_1-\alpha^{o,i})/\Gamma(\mu_1)$. The variables γ^o and μ_3 are related to the original optimized variables $S_s^{o,i}$ and $S_s^{o,b}$ as $\gamma^o = \frac{\sigma_s^2}{S_s^{o,i}}$ and $\mu_3 = (\mu_1 S_p + \sigma_s^2)/S_s^{o,b}$ respectively. The optimized sensing period variable τ is embedded in the variables $\alpha^{o,i}$ and $\alpha^{o,b}$. Furthermore, we assume that the sensing time should not last more than half of the frame period T. The authors in [10] conclude that for multi slot spectrum sensing, in all cases, the optimal throughput is obtained when the sensing period is less than $T/8$.

The problems in Eqs. (3.34) and (3.35) can be solved by two steps. In the first step, we try to obtain the optimal power allocation under a given sensing time τ. In the second step,

we can obtain the optimal sensing time by exhaustive search given the power allocation.

Similar to the underlay case, the solution of the above maximization problems can be mapped to the following minimization problems

$$\begin{aligned} \min_{\gamma^o,\,\tau} \quad & \Big[\Big(C_1^o (\gamma^o)^{\mu}\ {}_1F_1\left(\mu_1; 1+\mu_1-\alpha^{o,i}; \gamma^o\right) + C_2^o (\gamma^o)^{\alpha^{o,i}}\ {}_1F_1\left(\alpha^{o,i}; 1+\alpha^{o,i}-\mu_1; \gamma^o\right) \Big) \\ S.t. \quad & 0 \le \frac{T-\tau}{T} S_s^{o,i} \le S_s^m \quad \text{and} \quad \frac{T-\tau}{T}\mu_1 S_s^{o,i} \le I^{th}. \end{aligned} \tag{3.36}$$

$$\begin{aligned} \min_{\mu_3,\,\tau} \quad & \frac{\Gamma\left(\alpha^{o,b}+\mu_3\right)\Gamma\left(\mu_1+\mu_3\right)}{\Gamma\left(\alpha^{o,b}+\mu_1+\mu_3\right)\Gamma\left(\mu_3\right)} \Big] \\ S.t. \quad & 0 \le \frac{T-\tau}{T} S_s^{o,b} \le S_s^m \quad \text{and} \quad \frac{T-\tau}{T}\mu_1 S_s^{o,b} \le I^{th}. \end{aligned} \tag{3.37}$$

The corresponding optimal power allocation in the state 0 for a given τ can be derived by differentiating the objective function in Eq. (3.36) and equating it to zero, beneficial from the convexity of the confluent hypergeometric function ${}_1F_1$. So the following solution can be obtained

$$\begin{aligned} & C_1^o \mu_1 (\gamma^{*o})^{\mu_1} \left({}_1F_1(\mu_1; 1+\mu_1-\alpha^{o,i}; \gamma^{*o}) \quad + \frac{\gamma^{*o}\ {}_1F_1(1+\mu_1; 2+\mu_1-\alpha^{o,i}; \gamma^{*o})}{1+\mu_1-\alpha^{o,i}} \right) \\ & + C_i^o \alpha^{o,i} (\gamma^{*o})^{\alpha^{o,i}} \left({}_1F_1(\alpha^{o,i}; 1+\alpha^{o,i}-\mu_1; \gamma^{*o}) \quad + \frac{\gamma^{*o}\ {}_1F_1(1+\alpha^{o,i}; 2+\alpha^{o,i}-\mu_1; \gamma^{*o})}{1+\alpha^{o,i}-\mu_1} \right) = 0 \end{aligned} \tag{3.38}$$

in the domain $\left[0 \le S_s^{*o,i} \le \min\{\frac{TS^m}{(T-\tau)}, \frac{TI^{th}}{(T-\tau)\mu_1}\}\right]$. Similar to the above, the optimal power allocation in the state 1 for a given τ is the solution of the following equation

$$\left(\Psi(\alpha^{o,b}+\mu_3^*) + \Psi(\mu_1+\mu_3^*) - \Psi(\alpha^{o,b}+\mu_1+\mu_3^*) - \Psi(\mu_3^*) \right) = 0, \tag{3.39}$$

in the domain $\left[0 \le S_s^{*o,b} \le \min\{\frac{TS^m}{(T-\tau)}, \frac{TI^{th}}{(T-\tau)\mu_1}\}\right]$. The term γ^{*o} in Eq. (3.38) is $\gamma^{*o} = \frac{\sigma_s^2}{S_s^{*o,i}}$, and μ_3^* in Eq. (3.39) is the value of μ_3 corresponding to $S_s^{*o,b}$, *i.e.*, $\mu_3^* = (\mu_1 S_p + \sigma_s^2)/S_s^{*o,b}$.

Different sensing time will result in different performance. Thus, determining the optimal sensing time is a critically important task in the resource allocation scheme. Therefore, after deriving the optimal power allocation scheme at any given τ, the optimal sensing time, denoted by τ^*, can be found by *exact line search* method [62].

Among two candidate power levels, the cognitive transmitter will be allocated the power

that maximizes the effective capacity. The optimal power allocation for the overlay scheme $S_s^{*o} \in \{S_s^{*o,i}, S_s^{*o,b}\}$ can be obtained as

$$S_s^{*o} = \underset{S_s^{*o,i}, S_s^{*o,b}}{\arg\max} \left(E_C^{o,i}\left(S_s^{*o,i}\right), E_C^{o,b}\left(S_s^{*o,b}\right)\right). \tag{3.40}$$

As a result, the optimal effective capacity in the overlay strategy is

$$E_C^{o,opt}(\theta) = E_C^{o}(\theta, S_s^{*o,i}, S_s^{*o,b}, \tau^*). \tag{3.41}$$

3.4 Underlay-Overlay Selection Criterion

In the previous sections, we have obtained optimal power allocation for both underlay and overlay schemes. However, underlay and overlay schemes have different features. For example, the underlay strategy does not need to perform spectrum sensing but the interference power constraint should be satisfied all the time. While a portion of time is assigned to sensing process for the overlay case, the cognitive network only needs to meet the interference power requirement when the primary user is detected to be active. Therefore, the underlay and overlay approaches may have their respective advantages under diverse propagation environment and system parameters. If the cognitive network can dynamically choose the DSA strategies, the performance of the whole network could be further improved.

In this section, we aim to develop a *selection criterion* for the cognitive network based on the two most important parameters: the probability of the primary users activity and the QoS requirement. The primary users' traffic load affects the spectrum access activity of the primary network and thus the performance of the cognitive network. The heavier traffic load will cause higher spectrum-occupancy probability and vice versa. Moreover, the QoS guarantee is critically important to the wireless communication system and especially for the cognitive networks. As different applications and services may have diverse QoS requirement, it should also be taken into consideration.

Now, we first take a closer look at the relationship between the QoS requirement and the

QoS exponent. For a given discrete service rate process, the effective capacity E_C can be calculated from Eq. (2.5). The corresponding constraints for queue length-bound violation and delay-bound probabilities are determined from Eq. (2.2) and Eq. (2.3) by

$$Pr\{Q > q^{th}\} \approx e^{-\theta q^{th}} \leq P_Q, \tag{3.42}$$

$$\text{and} \qquad Pr\{D > d^{th}\} \approx e^{-\theta \varepsilon d^{th}} \leq P_D, \tag{3.43}$$

where P_Q and P_D are the maximum queue length-bound violation and delay probabilities that are allowed by the system, respectively.

The QoS requirements depend on the type of service, for example for audio, $d^{th} = 50\ ms$ and the violation probability $P_D = 10^{-2}$, while for video communication $d^{th} = 150\ ms$ and $P_D = 10^{-3}$ [26]. According to these requirements, the limits of the value of θ can be specified. Consequently, the QoS exponent θ should satisfy

$$\theta \geq -\frac{\ln P_Q}{q^{th}}, \quad \text{and} \quad \theta \geq -\frac{\ln P_d}{\varepsilon d^{th}}. \tag{3.44}$$

Note that ε is defined in Subsection 2.1.3.

Substituting the optimal resource allocation schemes $\left\{S_s^{*u,i}, S_s^{*u,b}\right\}$ and $\left\{S_s^{*o,i}, S_s^{*o,b}, \tau^*\right\}$ for the underlay and overlay schemes given in Eqs. (3.18), (3.41), respectively, we can obtain the maximum effective capacity for the DSA schemes.

The methodology of the DSA selection criterion can be summarized by considering a two-dimensional plane, where the x-axis represents the QoS exponent θ and the y-axis denotes the idle probability P_i. Then, we can divide the plane into two regions, denoted by R^u and R^o, respectively. The point $\left(\theta, P_i\right)$ in R^u satisfies $E_C^{u,opt}(\theta) \geq E_C^{o,opt}(\theta)$, and the point (θ, P_i) in R^o satisfies $E_C^{o,opt}(\theta) \geq E_C^{u,opt}(\theta)$. Given the delay bound and its violation probability, the corresponding QoS exponent θ can be calculated. If the point $\left(\theta, P_i\right)$ falls into R^u, the cognitive network should choose the underlay scheme. On the other hand, if $\left(\theta, P_i\right)$ falls into R^o, the cognitive network should select the overlay scheme.

3.5 Numerical Results and Performance Analysis

In this section, numerical results are presented to evaluate the performance of the proposed power allocation strategies for both underlay and overlay schemes. In the calculation, the frame duration is set to $T = 50$ ms, the sampling frequency is 100 K samples/s. Unless otherwise is stated, the probability of the channel to be idle is set to $P_i = 0.4$. Other parameters are listed in the corresponding figures.

Figure 3.4 presents the normalized effective capacity (which is defined as the effective capacity divided by $T\mathcal{B}$ and thus has the unit of "bits/sec/Hz") of both schemes as a function of the QoS exponent θ. In Figure 3.4(a), we can observe that, in underlay scheme, the QoS exponent θ plays a critically important role in the maximum throughput of the cognitive network. When θ is small (*i.e.*, the QoS constraint is loose), the cognitive network can realize higher throughput. On the contrary, when θ is large (*i.e.*, the QoS constraint is stringent), the cognitive network can only support lower arrival rates. Figure 3.4(b) illustrates the normalized effective capacity as a function of delay exponent and the impact of the probability of the channel being idle, P_i for the overlay scheme. We can observe that the effective capacity is a decreasing function of θ and is an increasing function of the probability P_i. In loosely QoS constraint system, the effective capacity variation is insignificant, while for more stringent QoS constraint, the capacity degrade is dramatically.

Higher P_i means the cognitive transmitter assumes that the channel is idle with a higher probability. The secondary user exploits the situation and transmits with a higher power level, which in turn, gains more capacity. While at lower P_i, the cognitive transmitter assumes the channel is busy with a higher probability (since $P_b = 1 - P_i$) and thus, it reduces the transmit power to comply with the interference constraint.

To compare the effective capacities for the proposed adaptive with non adaptive schemes, Figure 3.5 shows the effective capacity as a function of QoS exponent θ for adaptive and non-adaptive schemes. Solid curves show the result for adaptive scheme and dashed curves

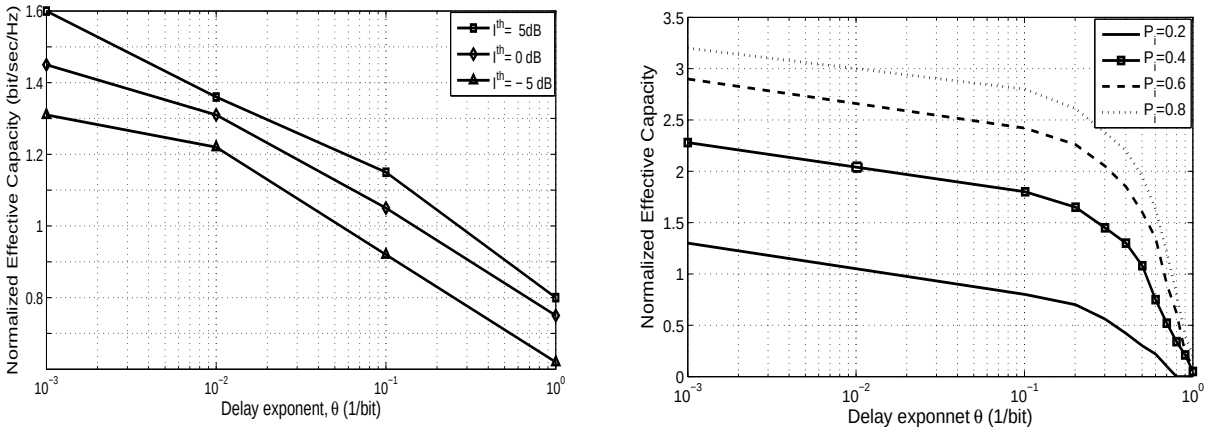

(a) Underlay scheme

(b) Overlay scheme

Figure 3.4: Normalized effective capacity versus exponent delay θ.

for non-adaptive scheme.

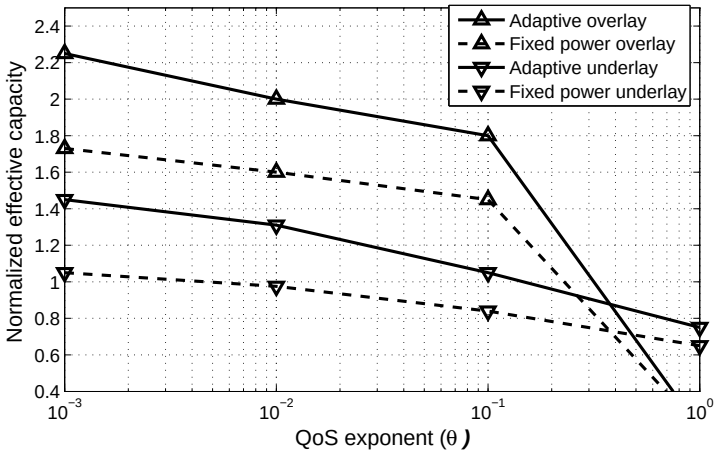

Figure 3.5: Normalized effective capacity versus QoS exponent θ for adaptive and non adaptive power policies.

It is shown that the effective capacities under the adaptive schemes are always higher than the fixed allocated power policies. Moreover, it can be noticed that the rate of performance degradation in the adaptive algorithms is faster than that of the non adaptive algorithm. This means that the adaptive algorithm is more sensitive to the QoS delay exponent variation.

The transmit power of the primary network S_p is another critical parameter that affects

the performance of the cognitive network. Figure 3.6 shows the effective capacity versus S_p for both schemes and for different QoS exponent θ. We can observe that the performance

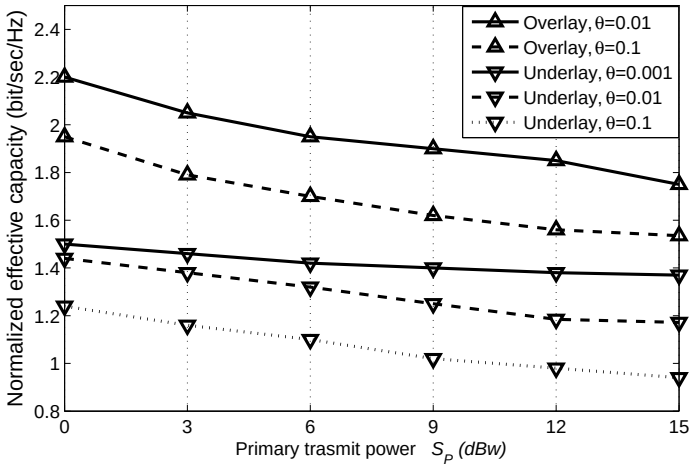

Figure 3.6: Normalized effective capacity versus primary transmit power with different θ, $P_i = 0.4$.

of the cognitive network degrades as S_p increases. This phenomenon can be explained as a larger S_p will cause more severe interference to the cognitive receiver. This causes the cognitive transmitter need more power to overcome the negative impact brought by the interference of the primary sender. However, as shown in Figure 3.6, when the QoS exponent is small (*i.e.*, $\theta = 10^{-3}$), the performance loss of the underlay cognitive network is not obvious. On the contrary, the performance of the cognitive network degrades more obvious when the QoS exponent is large (*i.e.*, $\theta = 0.1$). The reason for this observation is that a small θ denotes loose QoS requirement and the power allocation becomes water-filling as we explained in Subsection 2.1.2, thus the power resource can be more efficiently utilized. However, large θ means stringent QoS requirement, which results the cognitive network transmit with constant rate. Therefore, more power is used to overcome the more serious interference caused by larger S_p and the upper bounded power resource is less efficiently utilized.

Figure 3.7 shows the effective capacity versus sensing time τ for different P_i. We can

observe that the effective capacity is a concave function with respect to τ. In addition, it is also noticed that the optimal sensing time for each curve changes with P_i. The cognitive user needs more sensing time to achieve optimal capacity when P_i is low.

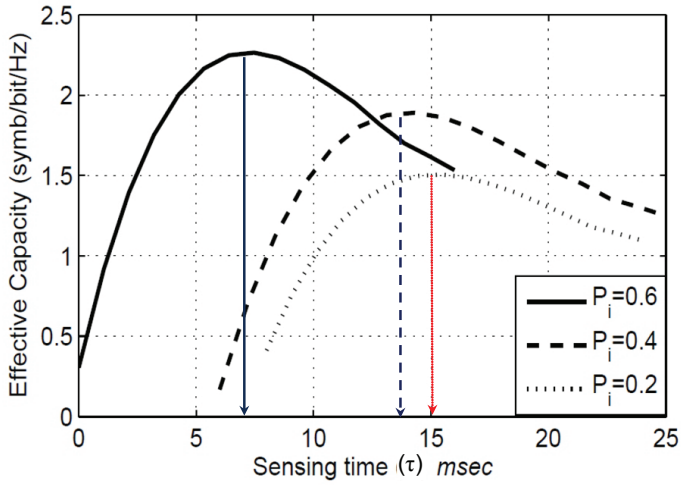

Figure 3.7: Effective capacity of the overlay scheme versus sensing time for different P_i, θ=0.1(1/bit).

In Figure 3.8, each curve divides the plane into two regions. The region below the curve is R^u , where the point (θ, P_i) satisfies $E_C^{u,opt}(\theta) \geq E_C^{o,opt}(\theta)$, and the region above the curve is R^o, where the point (θ, P_i) satisfies $E_C^{o,opt}(\theta) \geq E_C^{u,opt}(\theta)$. Based on the figure, the access strategy selection criterion proposed above can be performed. If the point (θ, P_i) falls below the curved border, the cognitive network should choose the underlay scheme, otherwise, the cognitive network should choose the overlay strategy. If the point falls exactly on the border, which means $E_C^{o,opt} = E_C^{u,opt}$, it gives the same effective capacity for both schemes. Considering the higher implementation complexity of the overlay scheme, the preferred choice is then the underlay scheme.

Furthermore, Figure 3.8 presents the border curves under different interference thresholds. We can observe from the figure that the area of the region R^u increases when the

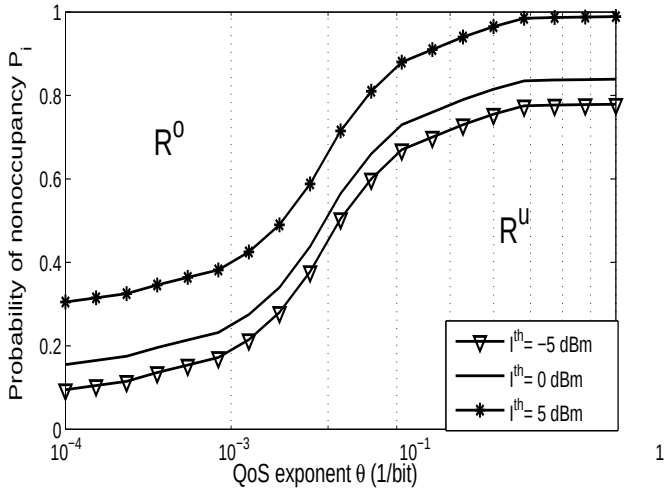

Figure 3.8: Underlay/overlay regions as a function of P_i and θ for different I^{th}.

interference threshold I^{th} becomes larger. Generally, from the analysis and the comparison of the two different DSA schemes, it can be deduced that the selection of the efficient strategy depends on several factors. It is a function of the channel occupancy probability, as well as a function of the interference threshold allowed. The choice of the scheme has also to be compromised between complexity and the achievable performance. By observing the above analysis and results, we can notice that the less busy the primary channel with loose QoS requirement (*i.e.*, high P_i and small θ), it is preferred to use the overlay scheme for higher achievable capacity. On the other side, when the system is more harsh (*i.e.*, low P_i and large θ), underlay scheme is preferred to maintain the achievable capacity performance.

3.6 Chapter Summary

In this chapter, we integrated the concept of effective capacity into information theory and developed the optimal resource allocation for both underlay and overlay DSA schemes. We studied the impact of the delay-QoS constraint on the network performance, and considered the primary users' spectrum-occupancy probability. Analytical results for the effective

capacity for both schemes were derived. Optimal power allocations to achieve maximum effective capacity were also obtained. We propose a selection criterion to determine whether to employ underlay or overlay scheme under the given QoS constraint and the primary users' spectrum-occupancy probability. Thus, the capacity of the CRN might be increased.

Chapter 4

Effective Capacity Based on Pilot Aided Transmissions over Imperfect Channel Information in CRNs

The main challenge for the secondary users is to control their interference levels not to exceed the limit where it may introduce harmful impact to the primary user. For this reason, interference should be carefully controlled under the assumption of imperfect channel estimation and under the probabilities of getting false alarms and/or misdetections in channel sensing process. The secondary user should also guarantee its own QoS requirements by transmitting at certain power for desired rates and by limiting the delay encountered by the transmission in the buffers [29].

Wireless channel conditions vary over time due to changing environment and mobility. The imperfect channel fading coefficients are possibly estimated through training techniques, but this is considered as critical for the successful deployment of cognitive radio systems in practice.

In addition to channel estimation, activities of primary users should be detected through

channel sensing. Hence, more challenging scenario may face the developers. There are certain interdependencies between these tasks of channel estimation and sensing. A mistake in channel sensing may lead to errors in the estimation of the channel coefficients. If the primary users are in the network but not detected, the channel estimate may be worse. Studying the transmission performance of cognitive radio in a practical scenario in which secondary users perform channel sensing, channel estimation, and operate under QoS requirements is the main motivation for recent research.

Some early research in the channel estimation was studied by an analytical approach to the design of pilot-assisted techniques [12]. *Pilot-Assisted Transmission* (PAT), in which a known training symbol is multiplexed with the data symbols, may be used to estimate the channel state and to adapt the receiver parameters accordingly [11, 63].

In this chapter, the transmission performance in cognitive radio networks is studied assuming imperfect channel estimation and by adopting again the concept of effective capacity introduced in Chapter 2.

The cognitive radio initially performs channel sensing, then the channel fading coefficients are estimated in the training phase of the transmission. Finally, data transmission is performed. The activity of the primary user is modeled by a Markov process. In this work, we jointly evaluate and optimize the training symbol and data symbol powers and transmission rates of the secondary users.

The rest of the chapter is organized as follows. In Section 4.1, the cognitive channel model is given and channel sensing expressions are formulated. Section 4.2 discusses the channel training with pilot symbols and derives the $MMSE$ channel estimation technique. In Section 4.3, data transmission phase and its performance is studied. A state transition model for cognitive radio transmission is also analyzed. In Section 4.4, we use the effective capacity concept to formulate the optimum throughput that the secondary user can achieve. We provide numerical results in Section 4.5, and summarize the chapter in Section 4.6.

4.1 Channel Model and Spectrum Sensing

Figure 4.1 depicts the proposed frame model for the cognitive transmission. Initially, the secondary user performs channel sensing which lasts τ seconds of a frame of total duration T seconds. We assume that pilot symbols are employed in the system to facilitate the sensing of channel fading coefficients. This will make the receiver able to track the time-varying channel. Since the $MMSE$ estimate depends only on the training energy and not on the training duration [64], it can be claimed that transmission of a single pilot at every T seconds is enough and optimal [64,65]. Instead of increasing number of pilot symbols, a single symbol with relatively high power is used as a pilot. With this, a decrease in the duration of the data transmission can be avoided. Consequently, it is assumed that the transmission is over flat fading channel in which fading remains constant in each frame. Both powers of pilot

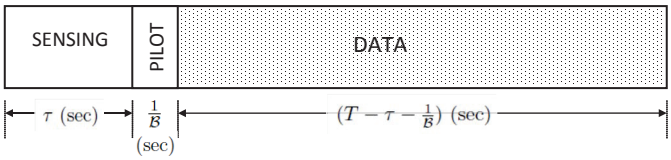

Figure 4.1: Transmission frame model consisting of channel sensing, a single symbol as a pilot, and data transmission.

and data symbols, and transmission rates are related to the channel sensing results. Let S_b and r_b be the average transmission power and rate if the primary user is detected as busy, respectively, while, they are S_d and r_d, if the channel is detected as idle. The input-output relation between the cognitive transmitter and receiver in the i^{th} symbol duration can be expressed as

$$y_i = \begin{cases} h_i x_{1i} + n_i, & \text{if PU is inactive,} \\ h_i x_{2i} + n_i + n_{p_i}, & \text{if PU is active,} \end{cases} \tag{4.1}$$

where x_{1i} and x_{2i} are the secondary transmitted signal when the channel is idle and busy respectively. y_i denotes the channel output signal, h_i represents the fading coefficient between the cognitive transmitter and receiver, modeled as Rayleigh random distribution with rms

value of α. The statistical values of the Rayleigh distribution are [66]:

$$\begin{cases} \mathbb{E}[h] = \alpha\sqrt{\frac{\pi}{2}} \\ \sigma_h^2 = \alpha^2(2 - \frac{\pi}{2}). \end{cases} \tag{4.2}$$

The term $\{n_i\}$ in Eq. (4.1) is zero-mean Gaussian distributed random noise samples at the cognitive receiver with variance σ_n^2 for all i. The term n_{p_i} represents the sum of the active primary users' signals received at the cognitive receiver with a variance of $\sigma_{n_p}^2$.

By performing spectrum sensing for reliably identifying the spectrum holes, and using the E*nergy Detection* described in Chapter 3, Section 3.3.1, the probabilities of detection, false, and miss-detection can be obtained. The decision can be made according to the following two hypotheses:

$$\mathcal{H}_0 : \quad z_i = n_i \qquad i = 1, 2 \cdots \tau\mathcal{B},$$

$$\mathcal{H}_1 : \quad z_i = n_i + n_{p_i} \qquad i = 1, 2 \cdots \tau\mathcal{B}.$$

Since the symbol rate is $\mathcal{B}$, we have $\tau\mathcal{B}$ symbols in a duration of τ seconds.

Regarding the channel sensing result, the cognitive radio network has the following four cases:

1. Correct detection: with two possible cases
   - Channel is busy, detected as busy, (BB).
   - Channel is idle, detected as idle, (DD).
2. Miss-detection: channel is busy, detected as idle(BD).
3. False alarm: Channel is idle, detected as busy (DB).

4.2 Pilot Power Analysis

In Pilot Aided (or Assisted) Transmission (PAT), a known symbol is embedded in the data transmitted stream to facilitate the receiver to estimate the channel fading coefficients [67]. The cognitive transmitter sends one pilot symbol after the processing of channel sensing to make the receiver able to estimate the channel coefficients. Obviously, this estimation will be affected by channel sensing results.

As mentioned in Section 4.1, with the assumption of constant fading within a frame, one pilot symbol is adequate to provide estimations. The first τ seconds of a frame with duration T is reserved for sensing process, while sending a single pilot with relatively high power is optimal [65]. This increases the duration of the data transmission. After channel sensing and pilot symbol transmission phases, the rest $((T-\tau)\mathcal{B}-1)$ symbols are devoted for data transmitting. The average input power in each frame can be written as

$$S_l = \sum_{i=\tau\mathcal{B}+1}^{T\mathcal{B}} \mathbb{E}\left[\, |x_{li}|^2 \right]; \quad i = 0, 1, \cdots, \;\; l = 1, 2. \tag{4.3}$$

where x_{li} is defined in Eq. (4.1). The total power assigned to the pilot and data symbols in a frame is limited by S_b when the channel is sensed as busy, or by S_d when the channel is sensed as idle. For the possible two cases mentioned above in which the channel is busy (*i.e.*, BB and BD), the cognitive transmitter transmits with an average power S_b for the case of BB. While for the case of BD, the cognitive transmitter transmits with an average power S_d, making the active primary user suffer from interference introduced by the secondary user. Depending on the capabilities of the transmitters and the energy resources they are equipped with, there exists peak constraints on both average powers, say: S^m, the following constraint on S_b and S_d must be imposed:

$$\mathcal{P}_d S_b + \mathcal{P}_m S_d \leq S^m, \tag{4.4}$$

where $\mathcal{P}_d$ and $\mathcal{P}_m = (1 - \mathcal{P}_d)$ are the detection and miss-detection probabilities defined in Eqs. (3.23) and (3.24). Additionally, the average interference experienced by the primary user can be expressed as

$$\mathbb{E}\{\mathcal{P}_d S_b |h_{sp}|^2 + \mathcal{P}_m S_d |h_{sp}|^2\} = (\mathcal{P}_d S_b + \mathcal{P}_m S_d)\, \mathbb{E}\{|h_{sp}|^2\} \leq I^{th}, \tag{4.5}$$

where h_{sp} denotes the fading coefficient between the secondary transmitter and primary receiver, and I^{th} is the average interference constraint. Note that h_{sp} is not known at the cognitive transmitter and hence the cognitive transmitter cannot adapt its transmission according to it. However, if the statistics of this coefficient ($\mathbb{E}[|h_{sp}|^2]$) is known, then in

order to satisfy Eq. (4.5), the cognitive transmitter can choose $S^m = \frac{I^{th}}{\mathbb{E}\{|h_{sp}|^2\}}$.

The pilot symbol power is also related to the sensing result. Let the power of the pilot symbol be $S_{pb} = f_b S_b$ if the primary user is detected, while, it is $S_{pd} = f_d S_d$ when primary user is not detected, where f_b and f_d are the fractions of the total power assigned to the pilot symbol and data when channel is detected as busy and idle, respectively. Since we assume that the fading coefficients $\{h_i\}$ be constant within each frame, the index i will be omitted. The received signal in the pilot phase in a certain frame (*i.e.*, y_p), can be written as

$$y_p = \begin{cases} h(S_{pb})^{1/2} + n + n_p & \text{for BB case} \\ h\,(S_{pd})^{1/2} + n & \text{for DD case} \\ h\,(S_{pd})^{1/2} + n + n_p & \text{for BD case} \\ h\,(S_{pb})^{1/2} + n & \text{for DB case.} \end{cases} \tag{4.6}$$

If the receiver employs minimum mean-square error ($MMSE$) estimator to estimate the fading coefficients, then the estimates can be found as [65, 68]

$$\hat{h} = \begin{cases} \frac{\sqrt{S_{pb}}\sigma_h^2}{S_{pb}\sigma_h^2 + \sigma_n^2 + \sigma_{n_p}^2} y_p & \text{for BB and DB cases} \\ \frac{\sqrt{S_{pd}}\sigma_h^2}{S_{pd}\sigma_h^2 + \sigma_n^2} y_p & \text{for BD and DD cases.} \end{cases} \tag{4.7}$$

It is essentially to know that the $MMSE$ estimates given above are related to the channel sensing results. Appendix C provides the derivations of $MMSE$ technique and its relations with the probabilities of the channel occupancy. $\hat{h}$ in Eq. (4.7) is the estimated channel fading, which is a circularly symmetric complex Gaussian random variable with zero mean and variance $\sigma_{\hat{h}}^2$ (*i.e.*, $\hat{h} \sim \mathcal{CN}(0, \sigma_{\hat{h}}^2)$). It can be expressed as $\hat{h} = \sigma_{\hat{h}} w$, where w is a standard complex Gaussian random variable, (*i.e.*, $w \sim \mathcal{CN}(0, 1)$). Thus the fading coefficient can now be expressed as follows [17]

$$\hat{h} = h + \epsilon, \tag{4.8}$$

where ϵ is the estimate error in the fading coefficient h, and $\epsilon \sim \mathcal{CN}(0, \sigma_\epsilon^2)$ [12, 17, 28].

Now, the input-output relationship for data phase in Eq. (4.1) can be rewritten as

$$\hat{y} = \begin{cases} \hat{h}x_1 + n + n_p & \text{if channel is busy,} \\ \hat{h}x_2 + n & \text{if channel is idle,} \end{cases} \tag{4.9}$$

The estimation of the channel variance is [67]

$$\sigma^2_{\hat{h}} = \begin{cases} \frac{S_{pb}\sigma_h^4}{S_{pb}\sigma_h^2+\sigma_n^2+\sigma_{n_p}^2} & \text{for BB case} \\ \frac{S_{pd}\sigma_h^4}{S_{pd}\sigma_h^2+\sigma_n^2} & \text{for DD case} \\ \frac{S_{pd}\sigma_h^4}{(S_{pd}\sigma_h^2+\sigma_n^2)^2}(S_{pd}\sigma_h^2+\sigma_n^2+\sigma_{n_p}^2) & \text{for BD case} \\ \frac{S_{pb}\sigma_h^4}{(S_{pb}\sigma_h^2+\sigma_n^2+\sigma_{n_p}^2)^2}(S_{pb}\sigma_h^2+\sigma_n^2) & \text{for DB case,} \end{cases} \tag{4.10}$$

Using Eq. (4.2) and Eq. (4.8), the variance of the estimation error σ_ϵ^2 can be found as

$$\sigma_\epsilon^2 = \sigma_{\hat{h}}^2 + \alpha^2(1+\frac{\pi}{2}), \tag{4.11}$$

by assuming that there is no correlation between the error and its estimation.

4.3 Data Transmission Phase

Finding the capacity of the channel in Eq. (4.9) is not an easy task. A lower bound capacity is generally obtained by considering the estimate error ϵ as another source of Gaussian noise, *i.e.*, by considering the term $(\epsilon\, x_l + n)$; $l = 1, 2$, in Eq. (4.9) as Gaussian distributed noise uncorrelated with the input [29].

The channel can be modeled as a two Morkov chain states (*i.e.*, ON and OFF), for the state when target transmission rate is greater than or less than the instantaneous rate that the channel can support, respectively. These two states are possible in each of the four cases discussed in Section 4.1 in page (54). Hence, totally there are eight states (2×4).

The lower bound instantaneous channel capacities in a frame for the four scenarios described above can be written as

$$C_k^l = C_o \log_2(1+\eta_k|w|^2), \qquad k = 1, 2, 3, 4 \tag{4.12}$$

where $C_o = \frac{(T-\tau)\mathcal{B}-1}{T}$, and

$$\eta_k = \begin{cases} \frac{S_{db}\sigma^2_{\hat{h}}}{S_{db}\sigma^2_{\epsilon}+\sigma^2_{n}+\sigma^2_{n_p}} & k=1\,;\text{BB case} \\ \frac{S_{dd}\sigma^2_{\hat{h}}}{S_{dd}\sigma^2_{\epsilon}+\sigma^2_{n}} & k=2\,;\text{DD case} \\ \frac{S_{dd}\sigma^2_{\hat{h}}}{S_{dd}\sigma^2_{\epsilon}+\sigma^2_{n}+\sigma^2_{n_p}} & k=3\,;\text{BD case} \\ \frac{S_{db}\sigma^2_{\hat{h}}}{S_{db}\sigma^2_{\epsilon}+\sigma^2_{n}} & k=4\,;\text{DB case,} \end{cases} \tag{4.13}$$

C_k^l is the frame's lower band capacity of each scenario k, which is obtained by assuming the factors $\{\epsilon \cdot x\}$ and $\{n_p\}$ in Eq. (4.9) as worst case noise whereas it is considered as Gaussian distributed [64]. S_{db} is the **d**ata symbol power when the channel is detected as **b**usy, while S_{dd} is the **d**ata symbol power when the channel is detected as i**d**le. These two powers are related to the cognitive average powers, as $S_{db} = S_b(1-f_b)/TC_o = S_b(1-f_b)/((T-\tau)\mathcal{B}-1)$, and $S_{dd} = S_d(1-f_d)/((T-\tau)\mathcal{B}-1)$.

Since $w \sim \mathcal{CN}(0,1)$, the magnitude $|w|$ will have the Rayleigh distribution and the squared magnitude $|w|^2$ will have Exponential distribution [69].

We assume that the transmitter will send its data at fixed rate r_b if the channel is sensed as busy, and at r_d if it is sensed as idle. If these rates are below the instantaneous capacity values, *i.e.*, when $r_b < C_1^l, C_4^l$ or $r_d < C_2^l, C_3^l$, the transmission can be assessed to be in the ON state and, so, the target rates can be achieved. While , if $r_b \geq C_1^l, C_4^l$ or $r_d \geq C_2^l, C_3^l$, the channel is in the OFF state, where reliable communication can not be achieved.

The activity of the primary user between the frames can also be modeled as a two-state Markov model. **B**usy state indicates that the primary user occupied the channel, and i**D**le state indicates the absent of the primary user in the channel, as can be seen in Figure 4.2. Switching from busy state to idle state and from idle state to busy state is with probability b and d, respectively. The state transition is assumed to occur every T seconds. Taking into account the four possible cases related to the channel sensing results jointly with the reliability of the transmissions states, the cognitive radio transmission can be represented by

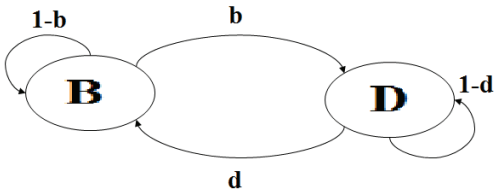

Figure 4.2: Primary user activity between two states: **B**usy and i**D**le

state transition model as $\mathbf{P}(8\times8)$ transition matrix denoted as

$$\mathbf{P} = \begin{bmatrix} p_1 & p_2 & p_3 & p_4 & p_5 & p_6 & p_7 & p_8 \\ p_1 & p_2 & p_3 & p_4 & p_5 & p_6 & p_7 & p_8 \\ \acute{p}_1 & \acute{p}_2 & \acute{p}_3 & \acute{p}_4 & \acute{p}_5 & \acute{p}_6 & \acute{p}_7 & \acute{p}_8 \\ \acute{p}_1 & \acute{p}_2 & \acute{p}_3 & \acute{p}_4 & \acute{p}_5 & \acute{p}_6 & \acute{p}_7 & \acute{p}_8 \\ p_1 & p_2 & p_3 & p_4 & p_5 & p_6 & p_7 & p_8 \\ p_1 & p_2 & p_3 & p_4 & p_5 & p_6 & p_7 & p_8 \\ \acute{p}_1 & \acute{p}_2 & \acute{p}_3 & \acute{p}_4 & \acute{p}_5 & \acute{p}_6 & \acute{p}_7 & \acute{p}_8 \\ \acute{p}_1 & \acute{p}_2 & \acute{p}_3 & \acute{p}_4 & \acute{p}_5 & \acute{p}_6 & \acute{p}_7 & \acute{p}_8 \end{bmatrix} \tag{4.14}$$

The transition probabilities depend on channel coefficients, sensing probabilities, transmission rates, and the two state Markov model in Figure 4.2. Table (4.1) summarizes the entries of the matrix $\mathbf{P}$, where φ_k in the table is defined as:

$$\varphi_k = \begin{cases} \frac{1}{\eta_i}\left(2^{(r_b/C_o)} - 1\right), & k = 1, 4; \\ \frac{1}{\eta_i}\left(2^{(r_d/C_o)} - 1\right), & k = 2, 3. \end{cases} \tag{4.15}$$

The details to calculate these transition probabilities are provided in Appendix D.

Table 4.1: The transition probabilities of Matrix $\mathbf{P}$

$l = 1, 2, 5, 6$		$n = 3, 4, 7, 8$	
$p_{l1} = (1-b)\mathcal{P}_d e^{-\varphi_1}$	$=p_1$	$p_{n1} = d\mathcal{P}_d e^{-\varphi_1}$	$=\acute{p}_1$
$p_{l2} = (1-b)\mathcal{P}_d(1-e^{-\varphi_1})$	$=p_2$	$p_{n2} = d\mathcal{P}_d(1-e^{-\varphi_1})$	$=\acute{p}_2$
$p_{l3} = b(1-\mathcal{P}_f)e^{-\varphi_2}$	$=p_3$	$p_{n3} = (1-d)(1-\mathcal{P}_f)e^{-\varphi_2}$	$=\acute{p}_3$
$p_{l4} = b(1-\mathcal{P}_f)(1-e^{-\varphi_2})$	$=p_4$	$p_{n4} = (1-d)(1-\mathcal{P}_f)(1-e^{-\varphi_2})$	$=\acute{p}_4$
$p_{l5} = (1-b)\mathcal{P}_m e^{-\varphi_3}$	$=p_5$	$p_{n5} = d\mathcal{P}_m e^{-\varphi_3}$	$=\acute{p}_5$
$p_{l6} = (1-b)\mathcal{P}_m(1-e^{-\varphi_3})$	$=p_6$	$p_{n6} = d\mathcal{P}_m(1-e^{-\varphi_3})$	$=\acute{p}_6$
$p_{l7} = b\mathcal{P}_f e^{-\varphi_4}$	$=p_7$	$p_{n7} = (1-d)\mathcal{P}_f e^{-\varphi_4}$	$=\acute{p}_7$
$p_{l8} = b\mathcal{P}_f(1-e^{-\varphi_4})$	$=p_8$	$p_{n8} = (1-d)\mathcal{P}_f(1-e^{-\varphi_4})$	$=\acute{p}_8$

According to the entries of the matrix **P** listed in Table (4.1), the rank of this matrix is 2.

4.4 Effective Capacity Optimization for Cognitive User

The Effective Capacity (E_C) theory introduced in Chapter 2, is a powerful approach to evaluate the capability of a wireless channel to support data transmissions with diverse statistical QoS guarantees.

We aim here, to analyze the maximum capacity that the cognitive radio channel can achieve under the constraints specified by the QoS exponent (*i.e.*, Effective capacity instead of ergodic capcity).

The effective capacity for a given θ is defined in Eq. 2.5 as

$$E_c = -\lim_{t\to\infty} \frac{1}{\theta t} \log \mathbb{E}(\exp(-\theta R(t))), \tag{4.16}$$

where $R(t) = \sum_{i=1}^{t} r(i)$ is the time-accumulated service process. Here we assume that $r(i)$ is discrete time stationary and ergodic stochastic service process. $\mathbb{E}(\cdot)$ is the expectation with respect to r.

It can be noticed that the service rate per frame is $r(i) = r_b T$ if the secondary user is in the state ON_1 or ON_7 at time i (the subscript number under the state refers to the state number). Similarly, the service rate is $r(i) = r_d T$ in the states ON_3 and ON_5. For the remaining states ($OFF_j, j = 2, 4, 6, 8$), the target transmission rate is greater than the instantaneous channel capacities and, so, communication can not be achieved. This leads to vanish all the service rates in these four *even* states.

Eq. (4.16) can be solved using the technique given in [70] as follows

$$E_c = -\frac{1}{\theta} \log \rho(\mathbf{M}) = -\frac{1}{\theta} \log \rho(\mathbf{D} \cdot \mathbf{P}), \tag{4.17}$$

where $\rho(\mathbf{M})$ function is the *spectral radius* of the matrix $\mathbf{M}$, $\mathbf{D} = diag(d_1(\theta), \cdots, d_N(\theta))$ is a diagonal matrix with elements equal to the moment generating functions of the processes in the N states [70] (here, we have 8 states). *Spectral radius of a matrix is the maximum*

of the absolute values of its eigenvalues, i.e., $\rho(A) \stackrel{def}{=} \max_i(|\omega_i|)$, ω_i's are the eigenvalues of the matrix A. $\mathbf{P}$ in Eq. (4.17) is the transition matrix given in Eq. (4.14). Note that in our assumptions, the transmission rates are deterministic and constants in each state, thus, the possible rates are: Tr_b, Tr_d, and 0 for which the moment generating functions are $e^{T\theta r_b}$, $e^{T\theta r_d}$ and 1 respectively. Therefore, $\mathbf{D} = diag(e^{T\theta r_b}, 1, e^{T\theta r_d}, 1, e^{T\theta r_d}, 1, e^{T\theta r_b}, 1)$. As a result, the matrix $\mathbf{M}$ can be filled as

$$\mathbf{M} = (\mathbf{D} \cdot \mathbf{P}) = \begin{bmatrix} m_b p_1 & m_b p_2 & m_b p_3 & m_b p_4 & m_b p_5 & m_b p_6 & m_b p_7 & m_b p_8 \\ p_1 & p_2 & p_3 & p_4 & p_5 & p_6 & p_7 & p_8 \\ m_d \acute{p}_1 & m_d \acute{p}_2 & m_d \acute{p}_3 & m_d \acute{p}_4 & m_d \acute{p}_5 & m_d \acute{p}_6 & m_d \acute{p}_7 & m_d \acute{p}_8 \\ \acute{p}_1 & \acute{p}_2 & \acute{p}_3 & \acute{p}_4 & \acute{p}_5 & \acute{p}_6 & \acute{p}_7 & \acute{p}_8 \\ m_d p_1 & m_d p_2 & m_d p_3 & m_d p_4 & m_d p_5 & m_d p_6 & m_d p_7 & m_d p_8 \\ p_1 & p_2 & p_3 & p_4 & p_5 & p_6 & p_7 & p_8 \\ m_b \acute{p}_1 & m_b \acute{p}_2 & m_b \acute{p}_3 & m_b \acute{p}_4 & m_b \acute{p}_5 & m_b \acute{p}_6 & m_b \acute{p}_7 & m_b \acute{p}_8 \\ \acute{p}_1 & \acute{p}_2 & \acute{p}_3 & \acute{p}_4 & \acute{p}_5 & \acute{p}_6 & \acute{p}_7 & \acute{p}_8 \end{bmatrix}, \quad (4.18)$$

where $m_b = e^{T\theta r_b}$, and $m_d = e^{T\theta r_d}$ are the moment generating functions of the possible rates when the channel is busy and idle respectively.

It is easy to note that the matrix $\mathbf{M}$ has also a rank of 2. The characteristic polynomial of the matrix can be written as (See Appendix E for details.):

$$Q(\omega) = \omega^2 - C_7\omega + C_6, \quad (4.19)$$

where the nonzero-eigenvalues ω can be found by solving the above quadratic equation.

The effective capacity in Eq. (4.16) can be optimized by choosing the maximum values of r_b and r_d. This maximization is done by choosing the maximum value of the eigenvalue of the matrix $(\mathbf{D} \cdot \mathbf{P})$ which maximizes the function $\rho(\mathbf{M})$ in Eq. (4.17).

We formulate a general optimization problem for effective capacity in Eq (4.20).

$$
\begin{aligned}
E_c^{opt} = & \max_{\substack{0<S_b,S_d\leq S^m \\ 0<f_b,f_d\leq 1 \\ r_b,r_d\geq 0}} -\frac{1}{\theta T\mathcal{B}}\log\Bigg\{\frac{1}{2}\Big(m_b(p_1+\acute{p}_7)+m_d(p_5+\acute{p}_3)+p_2+p_6+\acute{p}_4+\acute{p}_8\Big) \\
& +\frac{1}{2}\Bigg(\Big(m_b(p_1+\acute{p}_7)+m_d(p_5+\acute{p}_3)+p_2+p_6+\acute{p}_4+\acute{p}_8\Big)^2 \\
& -4\Bigg(m_b^2(\acute{p}_7\,p_1-\acute{p}_1\,p_7)+m_d^2(p_5\,\acute{p}_3-p_3\,\acute{p}_5)+m_b(\acute{p}_7\,p_2+\acute{p}_7\,p_6-\acute{p}_1\,p_4 \\
& -\acute{p}_2\,p_7-\acute{p}_5\,p_7-\acute{p}_6\,p_7-\acute{p}_1\,p_8+\acute{p}_8\,p_1)+m_d(\acute{p}_3\,p_2-\acute{p}_2\,p_3-p_4\,\acute{p}_5 \\
& +p_5\,\acute{p}_4-p_3\,\acute{p}_6+p_6\,\acute{p}_3-\acute{p}_5\,p_8+\acute{p}_8\,p_5)+m_b m_d(\acute{p}_3\,p_1+\acute{p}_7\,p_5-\acute{p}_1\,p_3) \\
& -\acute{p}_2\,p_4+\acute{p}_4\,p_2+\acute{p}_4\,p_1-p_4\,\acute{p}_6+p_6\,\acute{p}_4-\acute{p}_2\,p_8-\acute{p}_6\,p_8+\acute{p}_8\,p_6+\acute{p}_8\,p_2\Bigg)\Bigg)^{\frac{1}{2}}\Bigg\}
\end{aligned}
\tag{4.20}
$$

$$
S.t. \qquad \mathcal{P}_d S_b + \mathcal{P}_m S_d \leq S^m \quad \text{and} \quad (\mathcal{P}_d S_b + \mathcal{P}_m S_d)\mathbb{E}(|h_{sp}|^2) \leq I^m
$$

The effective capacity expression in Eq. (4.20) is obtained by choosing the largest value of the eigenvalues of the matrix $\mathbf{M}$ for a given sensing duration τ, detection threshold δ, and QoS exponent θ. One can note that if the sensing results are perfect with no errors, *i.e.*, the probability of detection $\mathcal{P}_d = 1$, and so ($\mathcal{P}_m = \mathcal{P}_f = 0$), the transition probabilities in matrix $\mathbf{P}$, $p_5 = p_6 = p_7 = p_8 = \acute{p}_5 = \acute{p}_6 = \acute{p}_7 = \acute{p}_8 = 0$.

An analytical optimized solution for the problem Eq. (4.20) is possible whenever the generating function has an analytical expression [62, 71]. In the following section, we investigate the impact of several parameters on the effective capacity through numerical results.

4.5 Numerical Results

In this section, numerical results are presented to illustrate the impact of the sensing duration τ, detection threshold δ, and other factors on the effective capacity. Without loss of generality, we set all variances to unity ($\sigma_h = \sigma_n = \sigma_{n_p} = 1$). We also assume the symbol rate $\mathcal{B}$=10 K symbol/s, and the frame duration T=0.25 s. This means there are 2500 symbols in

the frame. Unless they are not variable, time allocated for sensing is set to 5 ms, and QoS exponent θ is assumed to be 0.1. The maximum power constraint S^m=20 dBm. The fraction assigned to the pilot symbol is 10% whether the channel is busy or idle (*i.e.*, $f_b = f_d = 0.1$). To simplify the objective function of the effective capacity, we set the transition probabilities of the two-state Markov model in Figure 4.2: b and d, such that $b = 1 - d$.

In Figure 4.3, the normalized effective capacity (which is defined as the effective capacity divided by $T\mathcal{B}$) is plotted versus the delay QoS exponent θ for various interference limit values. We observe that the capacity increases as θ decreases. The figure shows that in the case with loose QoS restrictions (*i.e.*, lower values of θ), the capacity benefits significantly, whereas in the case with higher values of θ (*i.e.*, θ= 10 (1/bit)), about 70 % reduction in the capacity is seen.

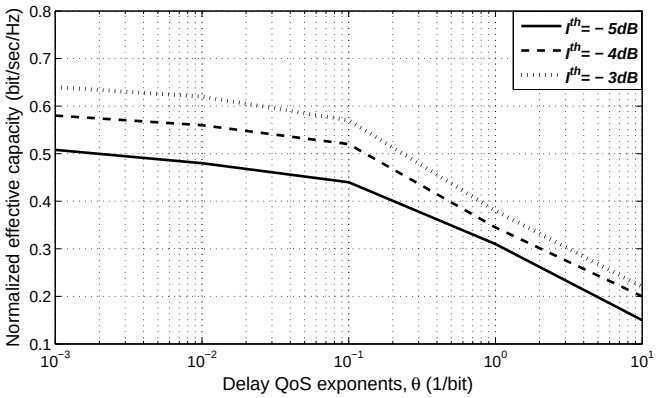

Figure 4.3: Effective capacity versus delay QoS exponents, for various interference-limit.

Figure 4.4 illustrates the effective capacity of the secondary user versus the interference limit I^{th} for various QoS exponent values. This figure reveals that the capacity gain that can be achieved under strict peak interference constraint is much lower than the one under released interference constraint. Also, similar to the conclusion in Figure 4.3, for specific I^{th} value, the capacity increases as θ becomes lower which means loose QoS restrictions.

Figure 4.5 studies the effect of the channel sensing duration τ. It can be seen that for a short time reserved for sensing process, the secondary user is more likely to get a false alarm

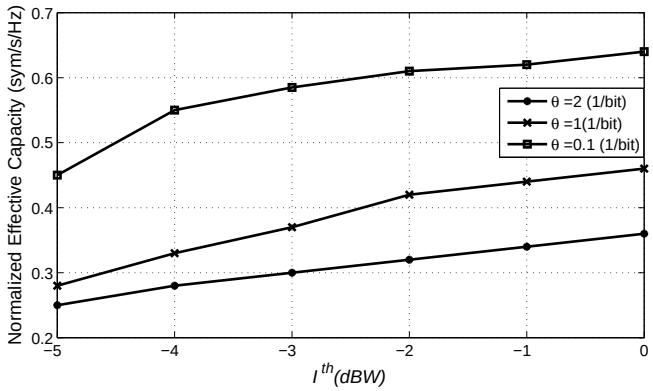

Figure 4.4: Effective capacity versus Interference-limit for various θ.

detecting the primary user, whereas the probability of detection approaches to one for long sensing duration.

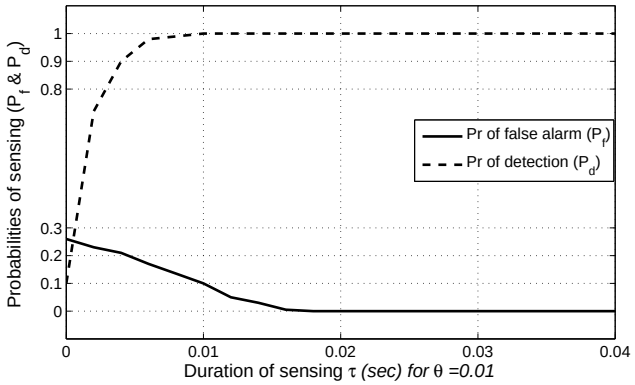

Figure 4.5: Probabilities of sensing ($\mathcal{P}_d$ & $\mathcal{P}_f$) versus channel sensing duration τ.

In Figure 4.6, we display the effective capacity (normalized value) as a function of the probability of detection for different values of S^m. As expected, with increasing S^m, the effective capacity value increases, more power means more relax constraints, which leads to more capacity. The effective capacity increases with probability of detection due to the fact that more reliable detection of the activity primary users leads to fewer miss-detection.

In Figure 4.7, we plot the normalized effective capacity as a function of the ratio of the power allocated to the pilot symbol to the total power when the channel is sensed as busy

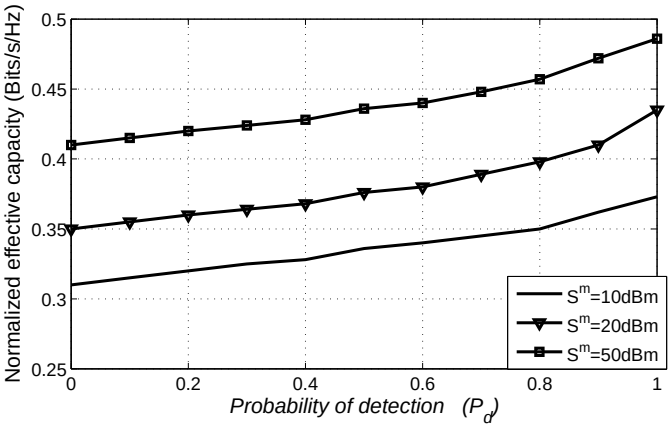

Figure 4.6: Effective capacity versus probability of detection $\mathcal{P}_d$ for different values of S^m.

f_b (here, we assume f_b=f_d). We consider two different interference thresholds. The optimal

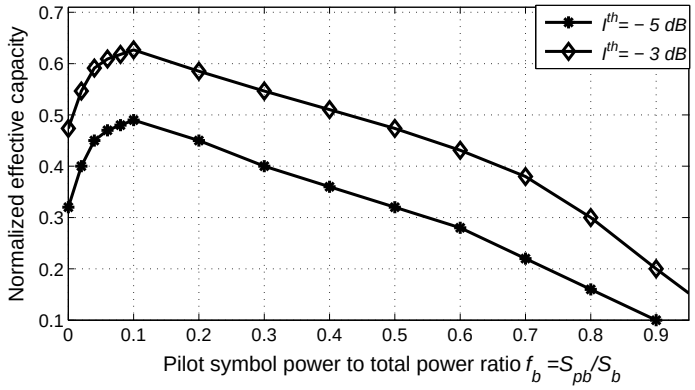

Figure 4.7: Normalized effective capacity versus the ratio of power pilot symbol to the total power allocated for two different values of I^{th}.

ratio occurs at $f_b = f_d \simeq 10\%$. As the interference constraint increases which means more allowance to the secondary user to transmit, the effective capacity increases. This can be intuitively understood. More f_b (or f_d) means more power allocated to the pilot symbol and less power allocated to data transmission, which in turns reduces the capacity.

4.6 Chapter Summary

In this chapter, the effective capacity of cognitive radio channels has been analyzed taking into account QoS constraints, imperfect channel information, and transmission power limitations. First, a system model is introduced in which the cognitive transmitter initially senses the channel in order to detect the activity of the primary user. It then sends a pilot symbol for channel estimation followed by data transmission. The estimation of the channel fading coefficients is performed through pilot transmission in the training phase. The minimum mean square error estimator $MMSE$ is assumed to be employed at the receiver. Through the study, the interrelation between channel sensing and estimation has been investigated. We have observed that degradation in the channel estimation is a result of faulty sensing. The cognitive transmitter is assumed to transmit data at fixed powers and rates according to the channel sensing results. For the secondary user, we have constructed a state-transition model taking into account the reliability of the transmission, channel sensing results, and the primary user activity in the channel. We have formulated the transition probabilities for this model. A closed form for the effective capacity is obtained as a function of exponent delay constraint. Numerical results are provided to examine the impact of delay constraint, interference limit, channel sensing duration, threshold, $\cdots$ *etc*, on the effective capacity. Many insightful observations and investigations are presented.

Chapter 5

Effective Capacity and Interference Analysis in Multichannel Sensing

In this chapter, the performance of multichannel transmission in cognitive radio is studied. Both QoS constraints and interference limitations are considered. The activities of the primary users are initially detected by cognitive user who performs sensing process over multiple channels. The cognitive user transmits in a single channel at variable power and rates depending on the channel sensing decisions and the fading environment. The cognitive operation is modeled as a state transition model in which all possible scenarios are studied. The QoS constraint of the cognitive user is investigated through comprehensive statistical analysis. The effective capacity of the cognitive radio channel is found in a closed form, taking into account the interference caused on the primary users and the required QoS constraints. Optimal power allocation and optimal channel selection criterion are obtained. Impact of several parameters on the transmission performance, as channel sensing parameters, number of available channels, fading and other, are identified through numerical example.

5.1 Introduction

In cognitive radio systems, challenges in providing QoS assurances increase due to the fact that cognitive user should operate under constraints on the interference levels that they produce to primary users. For the secondary user, these interference constraints lead to variations in transmit power levels and channel accesses. This discontinuity in accessing the channels due to the activity of the primary users make it difficult for the cognitive user to satisfy their own QoS requirement. The authors in [72] proposed a QoS constrained power and rate allocation scheme for spectrum sharing systems in which a minimum-rate to the primary user for a certain percentage of time was guaranteed. The same authors, in [73], considered variable-rate variable-power modulation employed under delay QoS constraints over spectrum-sharing channels.

In this chapter, the effective capacity of cognitive radio channels are studied where the cognitive radio detects the activity of the primary users in a multichannel case, and performs data transmission in one of these channels using both rate and power adaptation that depends on the channel conditions and the activity of the primary users. An average interference constraint on the cognitive user is formulated. Maximum throughput formula is obtained through the effective capacity approach. Optimal power allocation is derived and investigated through numerical results.

The rest of the chapter is organized as follows. In Section 5.2, the system model and assumptions are given. Channel capacity and state transition model are formulated and constructed in Section 5.3. Section 5.4 discusses outage constraints and interference limit. In Section 5.5, the effective capacity equation for the cognitive user channel is formulated. Channel selection criterion is proposed in Section 5.6. Numerical results are provided in Section 5.7, and the chapter is summarized in Section 5.8.

5.2 System Model and Assumptions

The considered system model consists of cognitive radio network in which the cognitive user senses L channels with a bandwidth $\mathcal{B}_l$ for each, where $l = 1, 2, \cdots, L$. Among these bands, the cognitive user chooses a channel for data transmission. The channel sensing and data transmission are performed in frames of duration T. It is assumed that τ seconds is allocated for channel sensing while the remaining $(T - \tau)$ seconds are allocated for data transmission. The primary user activity influences the transmission power and rate levels. If all of the channels are detected as busy, the cognitive transmitter selects one channel with a *certain criterion*, and sets the transmission power and rate to $S_{b,l}(i)$ and $r_{b,l}(i)$, respectively, where $i = 1, 2, \cdots$ denotes the time index in the transmission frame. On the contrary, if at least one channel is sensed to be idle, data transmission is sent with power $S_{d,l}(i)$ at rate $r_{d,l}(i)$. In the case of multiple channels are detected as idle, one idle channel can be selected according to a *certain policy* explained later in Section 5.6.

The input-output relation between the cognitive transmitter and receiver in the i^{th} symbol duration in the l^{th} channel can be expressed as

$$y_l(i) = \begin{cases} h_{ss_l}(i)x_l(i) + n_l(i), & \text{if no PU is active,} \\ h_{ss_l}(i)x_l(i) + n_l(i) + n_{p_l}(i), & \text{if at least one PU is active,} \end{cases} \tag{5.1}$$

where $x_l(i)$ and $y_l(i)$ denote the input and output complex-valued channel, respectively. The term, $h_{ss_l}(i)$, is the channel fading coefficient between the cognitive transmitter and receiver with an arbitrary distribution. It is defined $g_{ss_l}(i) = |h_{ss_l}(i)|^2$ as power fading coefficient. A block-fading channel model is assumed in which the fading coefficients stay constant in the frame, and they may change from one block to another independently in each channel. In Eq. (5.1), $n_{p_l}(i)$ denotes the active primary user's signal arriving at the cognitive receiver in the l^{th} channel, and it is assumed to have zero mean and a variance $\sigma^2_{n_{p_l}}$. Finally, $n_l(i)$ in Eq. (5.1) represents the $AWGN$ at the receiver which is modeled as a zero-mean, circularly symmetric, complex Gaussian random variable with variance $\sigma^2_{n_l}$, $\forall l$.

In order to identify the presence of primary user with unknown frequency locations, energy detector serves as the optimal sensing scheme since it only needs to measure the power of the received signal.

The channel sensing can be modeled as a hypothesis test between the noise $n_l(i)$ and the signal $n_{pl}(i)$ in noise. In a duration of τ seconds, there are $\tau\mathcal{B}_l$ complex symbols in each channel with bandwidth $\mathcal{B}_l$, this model can be expressed as

$$\begin{aligned} \mathcal{H}_{d,l}: \quad z_l(i) &= n_l(i), \qquad\qquad i = 1, 2 \cdots \tau\mathcal{B}_l, \\ \mathcal{H}_{b,l}: \quad z_l(i) &= n_l(i) + n_{pl}(i),\ i = 1, 2 \cdots \tau\mathcal{B}_l. \end{aligned} \tag{5.2}$$

By the assumption that $n_{pl}(i)$ signal samples are *i.i.d.*, the optimal detector response for this hypothesis problem is similar to the model given in Eqs. (3.20) - (3.24), and it can be rewritten as

$$\mathcal{Z}_l = \frac{1}{\tau\mathcal{B}_l} \sum_{i=1}^{\tau\mathcal{B}_l} |z_l(i)|^2 \lessgtr_{\mathcal{H}_{b,l}}^{\mathcal{H}_{d,l}} \delta_l, \tag{5.3}$$

where δ_l is a pre-designed threshold. Assuming $(\tau\mathcal{B}_l)$ is sufficiently high, $\mathcal{Z}_l$ can be approximated, using *Central Limit Theorem*, as a Gaussian random variable with mean and variance

$$\mathbb{E}[\mathcal{Z}_l] = \begin{cases} \sigma_{n_l}^2 & \text{if PU is inactive} \\ \sigma_{n_{pl}}^2 + \sigma_{n_l}^2 & \text{if PU is active,} \end{cases} \tag{5.4}$$

$$\sigma_{\mathcal{Z}_l}^2 = \begin{cases} \frac{\sigma_{n_l}^4}{\tau\mathcal{B}_l} & \text{if PU is inactive} \\ \left(\mathbb{E}[\,|n_{p_l}|^4] + \sigma_{n_l}^4 + 2\sigma_{n_{pl}}^2\sigma_{n_l}^2 - \sigma_{n_{pl}}^2\right)/(\tau B_l) & \text{if PU is active,} \end{cases} \tag{5.5}$$

respectively, where $\mathbb{E}[\,|n_{p_l}|^4]$ is the forth moment of the received signal n_{p_l}. Note that $\mathbb{E}[|n|^4] = 2\sigma_n^2$ for the $CSCG$ assumption.

If we assume that the primary signal n_{p_l} has complex-valued PSK waveform, the probabilities of detection and false alarm are given, respectively, as follows [10]

$$\mathcal{P}_{d,l} = Pr\{\mathcal{Y} > \delta | P_b\} = Q\left(\frac{\delta - \sigma_{n_{pl}}^2 - \sigma_{n_l}^2}{\sigma_{n_l}\sqrt{\left(2\sigma_{n_{pl}}^2 + \sigma_{n_l}^2\right)/(\tau B)}}\right), \tag{5.6}$$

$$\mathcal{P}_{f,l} \quad = Pr\{\mathcal{Z}_l > \delta_l | \mathcal{H}_{l,d}\} = Q\left(\frac{\delta_l - \sigma_{n_l}^2}{\sqrt{\sigma_{n_l}^4/(\tau \mathcal{B}_l)}}\right). \tag{5.7}$$

The probability of miss-detection occurs when the primary user is in operation but the cognitive radio fails to detect it, thus $\mathcal{P}_{miss,l} = 1 - \mathcal{P}_{d,l}$.

In Figure 5.1, the probability of detection and the probability of false alarm are illustrated as a function of energy detection threshold δ for different values of channel sensing duration. The bandwidth is set to $\mathcal{B} = 10$ kHz and the frame duration is $T = 100$ ms. We can see that when the detection threshold is low, both $\mathcal{P}_d$ and $\mathcal{P}_f$ tend to be 1, which means that the secondary user, always assuming the existence of an active primary user, transmits with power $S_b(i)$ and rate $r_b(i)$.

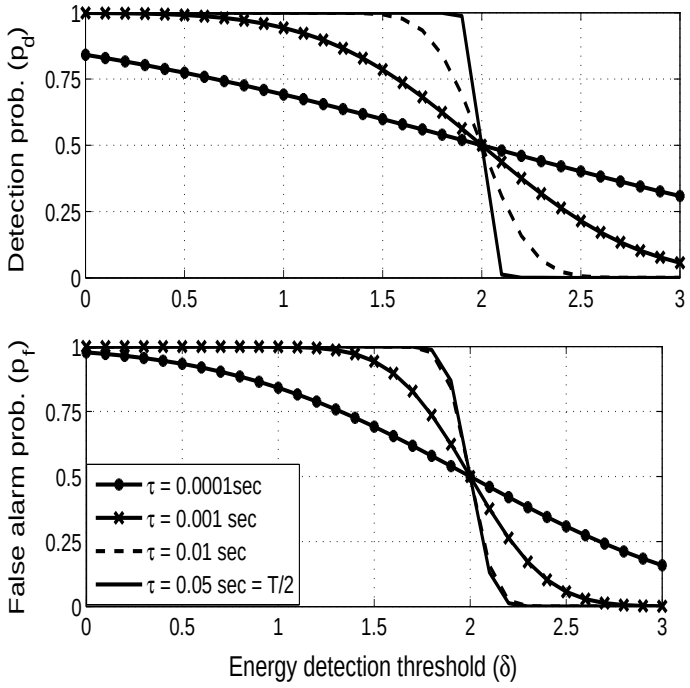

Figure 5.1: Probability of detection $\mathcal{P}_d$ and false alarm $\mathcal{P}_f$ versus detection threshold δ for different sensing times.

On the other hand, when the detection threshold is high, $\mathcal{P}_d$ and $\mathcal{P}_f$ are close to zero, which means that the secondary user, being unable to detect the activity of the primary users,

always transmits with power $S_d(i)$ and rate $r_d(i)$, possibly causing significant interference. The main purpose is to keep $\mathcal{P}_d$ as close to 1 as possible and $\mathcal{P}_f$ as close to 0 as possible. Therefore, we have to keep the detection threshold in a reasonable interval. Note that the duration of sensing τ is also important since increasing the number of channel samples used for sensing improves the quality of channel detection, but on the other hand degrades the transmission time which in turns decreases the throughput.

5.3 Channel Capacity and State Transition Model

Perfect *Channel State Information* (CSI) is assumed at each receiver. It is further assumed that each channel has a bandwidth that is equal to the coherence bandwidth $\mathcal{B}_c$. Coherence bandwidth is a statistical measurement of the range of frequencies over which the channel can be considered to be *flat*. In other words it is the approximate maximum bandwidth over which two frequencies of a signal are likely to experience comparable or correlated amplitude fading. With this assumption, it can be supposed that independent flat fading is experienced in each channel.

In order to further simplify the setting, it is considered a symmetric model in which fading coefficients are identically distributed in different channels. Moreover, the background noise and primary users' signals are also assumed to be identically distributed in different channels and hence their variances σ_n^2 and $\sigma_{n_p}^2$ do not depend on l. So the subscript l in the subsequent expressions will be dropped for the sake of brevity. The probability of each channel being occupied by the primary users is assumed to be the same and equal to P_b. In channel sensing process, the same energy threshold δ is assumed in each channel. Due to possible error in channel sensing, we have the following possible cases

- C_{bb}: All bands are sensed as **b**usy, and the selected channel is actually **b**usy.
- C_{bd}: All bands are sensed as **b**usy, and the selected channel is actually i**d**le.

- C_{db}: At least one band is sensed as i**d**le, and the selected channel is actually **b**usy.
- C_{dd}: At least one band is sensed as i**d**le, and the selected channel is actually i**d**le.

Finding expressions of the probabilities of being in each of these cases is very important for the subsequent analysis. By the assumption that the state transitions occur every frame and they may change between frames, the probability that the channel is detected as busy can be written as

$$\rho \triangleq (P_b\mathcal{P}_d + (1 - P_b)\mathcal{P}_f) \tag{5.8}$$

The probabilities of being in each of the above cases can be formulated as follows:

$$P_{bb} \triangleq \Pr\{\text{being in the case } C_{bb}\} = \rho^{L-1}P_b\mathcal{P}_d, \tag{5.9}$$

$$P_{bd} \triangleq \Pr\{\text{being in the case } C_{bd}\} = \rho^{L-1}(1 - P_b)\mathcal{P}_d, \tag{5.10}$$

$$\begin{aligned} P_{db} &\triangleq \Pr\{\text{being in the case } db\} \\ &= \Pr\{\text{at least one ch is detected as idle}\} \\ &\times \Pr\{\text{the ch chosen is busy} \mid \text{it is detected as idle}\} \\ &= \sum_{l=1}^{L} \binom{L}{l} \rho^{L-l}(1-\rho)^l \times \frac{P_b(1-\mathcal{P}_d)}{1-\rho} = \frac{(1-\rho^L)P_b(1-\mathcal{P}_d)}{1-\rho}. \end{aligned} \tag{5.11}$$

Similarly for the forth case

$$P_{dd} \triangleq \Pr\{\text{being in the case } dd\} = \frac{(1-\rho^L)(1-P_b)(1-\mathcal{P}_f)}{1-\rho}, \tag{5.12}$$

Table 5.1 summarizes these probabilities.

Table 5.1: The Probability of being in each four cases

Case	*Probability being in this case*
Case *bb*	$\rho^{L-1}P_b\mathcal{P}_d$
Case *bd*	$\rho^{L-1}(1-P_b)\mathcal{P}_f$
Case *db*	$\frac{(1-\rho^L)P_b(1-\mathcal{P}_d)}{1-\rho}$
Case *dd*	$\frac{(1-\rho^L)(1-P_b)(1-\mathcal{P}_f)}{1-\rho}$

These probabilities are plotted in Figure 5.2 as a function of the probability of detection for two cases in which the number of channels is $L = 1$ and $L = 5$. As expected, P_{bb} and P_{bd} decrease with increasing the number of channels. It can also be seen that P_{db} and P_{dd} have small values when the probability of detection is high.

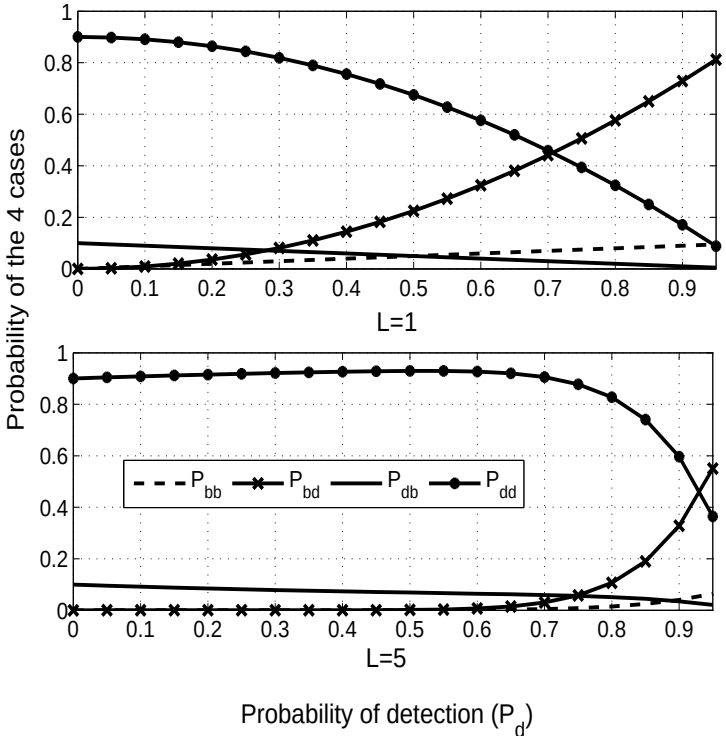

Figure 5.2: Probability of being in each of the four cases vs. probability of detection.

In each of the above cases, we have two states, namely either ON state in which the instantaneous transmission rate exceeds the instantaneous channel capacity, or OFF state if it does not. Assuming the interference caused by the primary users $n_p(i)$ as additional Gaussian noise, the instantaneous channel capacities for the above four cases can be expressed as follows

$$R_l(i) = \mathcal{B}_c \log_2(1 + \gamma_l(i)), \tag{5.13}$$

where $l \in \{bb, bd, db, dd\}$ refers to the possible case and $\gamma_l(i)$ represents the $SINR$ for the

corresponding case in the i^{th} channel which is given by

$$\begin{aligned} \gamma_{bb}(i) &= \frac{S_b(i)g_{ss}(i)}{N_b}, \qquad \gamma_{bd}(i) = \frac{S_b(i)g_{ss}(i)}{N_d} \\ \gamma_{db}(i) &= \frac{S_d(i)g_{ss}(i)}{N_b}, \qquad \gamma_{dd}(i) = \frac{S_d(i)g_{ss}(i)}{N_d}, \end{aligned} \tag{5.14}$$

where $N_b = (\sigma_n^2 + \sigma_{n_p}^2)$ and $N_d = \sigma_n^2$ represent the total noise when a channel is busy and idle respectively.

It can be seen that in the cases C_{bb} and C_{bd}, the cognitive transmitter detects all channels as busy and transmits with rate

$$r_b(i) = \mathcal{B}_c \log_2(1 + \gamma_{bb}(i)). \tag{5.15}$$

While for the cases C_{db} and C_{dd}, at least one channel is sensed as idle and the transmission rate is

$$r_d(i) = \mathcal{B}_c \log_2(1 + \gamma_{dd}(i)), \tag{5.16}$$

since the transmitter assumes the channel as idle, it sets the power level to $S_d(i)$ and expects that no interference from the primary transmissions will be produced as seen by the absence of $\sigma_{n_p}^2$ in the denominator of γ_{dd} in Eq. (5.14).

The transmission rate for the cases C_{bb} and C_{bd} is less than or equal to the instantaneous channel capacity. Hence, reliable transmission at rate $r_b(i)$ is attained and channel is in the ON state. Similarly, the channel is in the ON state in the case C_{dd} in which the transmission rate is $r_d(i)$. While in the case C_{db}, transmission rate exceeds the instantaneous channel capacity (*i.e.*, $r_d(i) > R_{db}(i)$) due to mis-detection. In this case, reliable communication cannot be established, and the channel is assumed to be in the OFF state. The effective transmission rate in this state is zero.

Referring to the above discussion, the cognitive transmission model can be constructed as depicted in Figure 5.3. We have $(L + 1)$ ON states and 1 OFF state. The first ON state is a combined version of the ON states in the cases C_{bb} and C_{bd} in both of which the transmission power and rate are $S_b(i)$ and $r_b(i)$ respectively. All channels are sensed as busy in this first ON state. The remaining ON states labeled 2 through $(L + 1)$ in the

figure can be represented as the expansion of the ON state in the cases C_{dd} in which at least one channel is sensed as idle and the selected channel for transmission is really idle. More specifically, the l^{th} ON state for $l = 2, 3, \cdots, (L+1)$ is the ON state in which $(l-1)$ channels are sensed as idle and the channel selected for transmission is actually idle. The transmission power and rate for these states are $S_d(i)$ and $r_d(i)$ respectively.

The single OFF state labeled $(L+2)$ in the figure represents the case C_{db} in which transmission rate exceeds the instantaneous channel capacity. Reliable communication cannot be established in this state.

To characterize the state transition probabilities, the probability of staying in the first ON state in which all channels are sensed as busy can be easily expressed as

$$p_{11} = (P_b \mathcal{P}_d + (1 - P_b)\mathcal{P}_f)^L = \rho^L \tag{5.17}$$

It is important to note that the transition probability in Eq. (5.17) is obtained under the assumptions that the primary user activity is independent among the channels and also from one frame to another as mentioned above. By this assumption of independence over the frames, the state transition probabilities are independent on the originating state, so the transition probabilities p_{l1}, $l = 1, 2, \cdots, (L+2)$ can be expressed as

$$p_1 \triangleq p_{11} = p_{21} = \cdots = p_{(L+1)1} = p_{(L+2)1} = \rho^L \tag{5.18}$$

For $l = 2, 3, \cdots, L+1$,, we can obtain

$$\begin{aligned}
p_l &\triangleq p_{1l} = p_{2l} = \cdots p_{(L+1)l} = p_{(L+2)l} \\
&= Pr\{(l-1) \text{ out of } L \text{ channels are sensed as idle}\} \\
&\times Pr\{\text{the selected channel is idle} \mid \text{it is sensed as idle}\} \\
&= \begin{pmatrix} L \\ l-1 \end{pmatrix} \rho^{L-l+1}(1-\rho)^{l-1} \times \frac{(1-P_b)(1-\mathcal{P}_f)}{1-\rho} \\
&= C(L, l-1)\rho^{L-l+1}(1-\rho)^{l-2}(1-P_b)(1-\mathcal{P}_f),
\end{aligned}$$

where $C(k,l) = \frac{k!}{l!(k-l)1}$ is the Binomial coefficient.

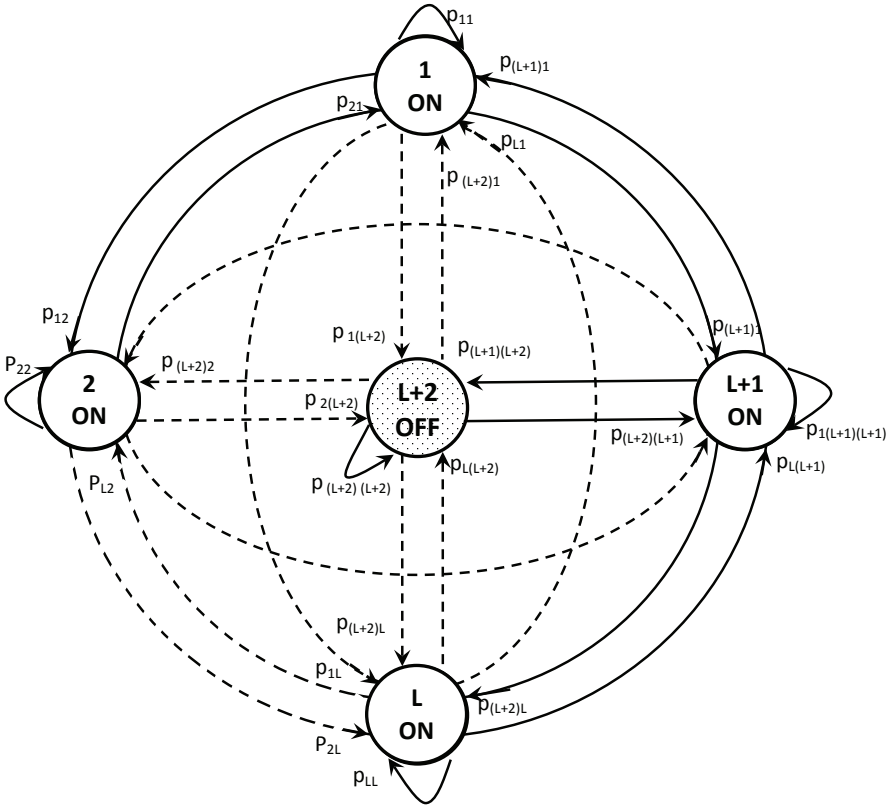

Figure 5.3: $(L+1)$ ON States and one OFF state for the cognitive radio channel and their corresponding state transition probabilities.

The transition probabilities for the OFF state are

$$\begin{aligned} p_{L+2} &\triangleq p_{1(L+2)} = p_{2(L+2)} = \cdots = p_{(L+1)(L+2)} = p_{(L+2)(L+2)} \\ &= 1 - \sum_{l=1}^{L+1} p_{1l} = \sum_{l=1}^{L} C(L,l)\rho^{L-l}(1-\rho)^{l-1} P_b(1-\mathcal{P}_d) = \frac{1-\rho^L}{1-\rho} P_b(1-\mathcal{P}_d). \end{aligned} \tag{5.19}$$

In Eq. (5.11) and Eq. (5.19), we use the series relations in [74, 75] as

$$\sum_{l=1}^{L} \frac{L!}{(L-l)!\,l!} a^{L-l}\,(1-a)^{l-1} = \frac{1-a^L}{1-a}$$

From the above definitions, it can be seen that the state transition probability matrix is $(L+2)\times(L+2)$ with *rank* of 1. Note that in each frame, there are $r_b(l)(T-\tau)$ bits transmitted and received in state 1, and $r_d(l)(T-\tau)$ bits are transmitted and received in states 2 through $(L+1)$, while in state $(L+2)$, the transmitted bits are assumed to be zero.

5.4 Outage Constraints and Interference Limit

To adapt the transmission powers of the cognitive user and ensuring not producing any harmful impact on the primary users, interference power constraints is considered and analyzed in this section.

From the above discussions, it can be concluded that the interference to the primary users is caused only in the cases C_{bb} and C_{db}. In the case C_{bb}, the channel is actually busy, and the cognitive user, detecting the channel as busy, transmits at power level S_b. The instantaneous interference power introduced on the primary user is $(S_b\, g_{sp})$, where g_{sp} is the fading coefficient of the channel between the secondary transmitter and the primary user. While, for the case C_{db}, although the channel is actually busy, the secondary user, detecting the channel as idle, transmits at power S_d . The instantaneous interference power is $(S_d\, g_{sp})$ in this case. Since power adaption is considered, transmission power levels S_b and S_d in general vary with g_{sp} and g_{ss}, which is the power of the fading coefficient between the secondary transmitter and secondary receiver in the chosen transmission channel.

On the other hand, it is important to note that increasing L always brings a benefit to the primary users in the form of decreased probability of interference. In order to quantify this type of gain, we consider below the probability that the channel being selected for transmission is actually busy and hence, the primary user in this channel experiences interference:

$$\begin{aligned} P_I &= Pr\left\{ \begin{pmatrix} \text{ch selected} \\ \text{is actually} \\ \text{busy} \end{pmatrix} AND \begin{pmatrix} \text{all chs are} \\ \text{detected as} \\ \text{busy} \end{pmatrix} \right\} + Pr\left\{ \begin{pmatrix} \text{ch selected} \\ \text{is actually} \\ \text{busy} \end{pmatrix} AND \begin{pmatrix} \text{at least one} \\ \text{is detected} \\ \text{as idle} \end{pmatrix} \right\} \\ &= P_{bb} + P_{db} = P_b \frac{1-\rho^L - \mathcal{P}_d(1-\rho^{L-1})}{1-\rho} \end{aligned} \tag{5.20}$$

Clearly that P_I depends on $\mathcal{P}_d$ and $\mathcal{P}_f$ (through ρ in Eq. (5.8)). It can be seen in Figure 5.4 that this interference probability decreases with increasing the number of channels L.

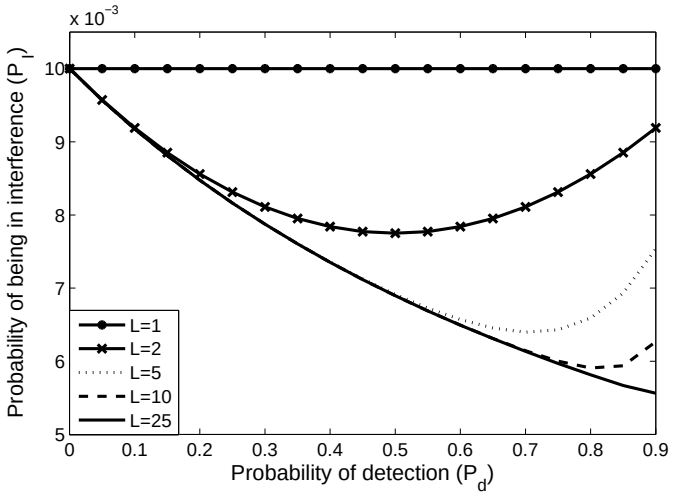

Figure 5.4: Probability of primary user being in interference versus probability of detection for different L, $P_b = 0.2$.

For large L, $\lim_{L\to\infty} P_I = P_b \dfrac{(1-\mathcal{P}_d)}{1-\rho}$. In this asymptotic regime, P_I becomes zero with perfect detection. Note that the cognitive user transmits even when all channels are detected as busy. As L grows up, the probability of such an event vanishes. Having perfect detection makes the cognitive user to avoid the third case C_{db}. Hence, the primary user will be avoided to experience interference.

In the cases: C_{bb} and C_{db} described above, the instantaneous interference power levels depend on both g_{sp} and g_{ss} whose distributions depend on the criterion with which the transmission channel is chosen and the number of available channels from which the selection is performed. For this reason, it is necessary in the case C_{db} to separately consider the individual cases with different number of idle-detected channels. There are L such cases. For instance, in the l^{th} case for $l = 1, 2, \cdots, L$, there are l channels detected as idle and the channel chosen out of these l channels is actually busy.

According to the above considerations, and using Eqs. (5.9), (5.11), the average interfer-

ence has to be constrained to the value I_l^{th}. This can be expressed as

$$\begin{aligned} I_l^{th} > & Pr\{\text{being in } C_{bb}\} \times \text{average interference in } C_{bb} \\ & + Pr\{\text{being in } l^{th} \text{ channel in } C_{db}\} \times \text{average interference in } C_{db}. \end{aligned}$$

This yeilds to: $$I_l^{th} > \left[\rho^{L-1} P_b \mathcal{P}_d \times \mathbb{E}[S_b g_{sp}] + \frac{(1-\rho^L)(1-P_b)(1-p_f)}{1-\rho} \times \mathbb{E}_l[S_d g_{sp}]\right]. \tag{5.21}$$

The expectations should be taken over the distribution g_{sp} and over the probabilities of different cases. The term $\mathbb{E}_l[S_d g_{sp}]$ in Eq. (5.21) depends on the number of idle-detected channels, l.

It can be assumed that the interference constraints of all channels are the same *i.e.*, $I^{th} = I_1^{th} = I_2^{th} = \cdots = I_L^{th}$, regardless of which case is being realized. In general, and for more strict requirements on the interference, the following individual interference constraints can be imposed:

$$\mathbb{E}[S_b g_{sp}] < I^{th}, \quad \text{and} \quad \mathbb{E}_l[S_d g_{sp}] < I_l^{th}. \tag{5.22}$$

As considered in [72], by appropriately choosing the values of I^{th} and I_l^{th} in Eq. (5.22), primary users can be provided a minimum rate guarantee for a certain percentage of the time through the following outage constraints

$$Pr\Big\{ \log_2 \big(1 + \frac{S_p g_{pp}(i)}{S_b(i) g_{sp}(i) + \sigma_n^2}\big) \leq R_{min} \Big\} \leq P_b^{out}, \tag{5.23}$$

$$Pr\Big\{ \log_2 \big(1 + \frac{S_p g_{pp}(i)}{S_d(i) g_{sp}(i) + \sigma_n^2}\big) \leq R_{min} \Big\} \leq P_d^{out}, \tag{5.24}$$

where S_p is the transmission power of the primary user, R_{min} is the required minimum transmission rate to be provided to the primary users with specific outage probabilities. P_b^{out} and $\mathcal{P}_d^{out}$ in Eqs. (5.23), (5.24) are the outage constraints in the cases C_{bb} and C_{db}, respectively. $g_{pp}(i)$ is the power fading of the channel between the primary transmitter and primary receiver and σ_n^2 is the variance the thermal noise at the primary receiver.

In a Rayleigh fading channel between the primary transmitter and receiver, g_{pp} is an

exponential random variable. The outage probability in Eq. (5.23) can be evaluated as

$$Pr\Big\{ \log_2 \big(1 + \frac{S_p g_{pp}(i)}{S_b(i) g_{sp}(i) + \sigma_n^2}\big) \leq R_{min} \Big\} = Pr\Big\{ g_{pp} \leq \frac{2^{R_{min}} - 1}{S_p} \big(S_b(i) g_{sp}(i) + \sigma_n^2\big) \Big\}$$

$$\text{thus} \qquad P_b^{out} \geq \mathbb{E}\big[1 - e^{-\frac{2^{R_{min}}}{S_p}(S_b(i) g_{sp}(i) + \sigma_n^2)}\big] \tag{5.25}$$

where we perform the integration with respect to the probability density function of g_{pp} in the evaluation of the probability expression in Eq. (5.25). The expectation in Eq. (5.25) is with respect to the remaining random g_{sp}. By calling the Jensens inequality [76] and making use of concavity of the function $(1 - e^{-x})$, the right hand side of Eq. (5.25) can be written as

$$\mathbb{E}\big[1 - e^{-\frac{2^{R_{min}}}{S_p}(S_b(i) g_{sp}(i) + \sigma_n^2)}\big] \leq 1 - e^{-\frac{2^{R_{min}}}{S_p} \mathbb{E}[S_b(i) g_{sp}(i)] + \sigma_n^2} \tag{5.26}$$

From this inequality, if the following condition

$$0 \leq \mathbb{E}[S_b g_{sp}] \leq \frac{S_p}{2^{R_{min}} - 1} \big| \log_e(1 - P_b^{out}) \big| - \sigma_n^2 \tag{5.27}$$

is imposed, then the constraint in Eq. (5.23) will be satisfied. A similar analysis can be done for the constraint in Eq. (5.24).

5.5 Effective Capacity for Cognitive User

As a powerful approach to evaluate the capability of a wireless channel to support data transmissions with diverse statistical quality of service QoS guarantees, the Effective Capacity (E_C) term introduced in Section 2.1 of Chapter 2 is again studied here.

It can be noticed that the service rate in our current model is $r(l) = r_b(l)(T - \tau)$ if the cognitive user is in state 1 at the channel l. Similarly, the service rate is $r(l) = r_d(T - \tau)$ in states between 2 and $(L + 1)$. In the remaining state (*i.e.*, OFF state), reliable connection can not be achieved because the instantaneous transmission rate exceeds the instantaneous channel capacities, so the service rates in this state is zero.

The normalized effective capacity defined as the effective capacity divided by $T\mathcal{B}$ (in

$bits/sec/Hz$ or $1/nat$) under the average interference power constraint Eq. (5.21) can be formulated as the following optimization problem

$$\begin{aligned} E_c = \quad & -\frac{1}{\theta T \mathcal{B}_c} \max_{\substack{r_b, r_d > 0 \\ S_b, S_d > 0}} \log_e \Big(p_1 \mathbb{E}[e^{-(T-\tau)\theta r_b}] + \sum_{l=1}^{L} p_{l+1} \mathbb{E}_l[e^{-(T-\tau)\theta r_d}] + p_{L+2} \Big), \\ s.t. \quad & Eq.\ (5.21) \text{ holds}, \end{aligned} \tag{5.28}$$

where p_l for $l = 1, 2, \cdots, L+2$ are the state transition probabilities defined in Section 5.3. The maximization operator should be taken with respect to the power adaptations S_b and S_d.

Note that the expectation $\mathbb{E}[e^{-(T-\tau)\theta r_b}]$ in the objective function and $\mathbb{E}[S_b g_{sp}]$ in the constraint of the above optimization problem are with respect to the joint distribution of (g_{ss}, g_{sp}) of the channel selected for transmission when all channels are sensed busy. The expectations $\mathbb{E}_l[e^{-(T-\tau)\theta r_d}]$ and $\mathbb{E}_l[S_d g_{sp}]$ are with respect to the joint distribution of (g_{ss}, g_{sp}) of the channel selected for transmission when l channels are sensed as idle.

To identify the optimal power allocation that the cognitive user should employ, the problem Eq. (5.28) can be converted to a minimization problem using the fact that logarithmic function is a monotonic function.

$$\begin{aligned} E_c = & \min_{\substack{r_b, r_d > 0 \\ S_b, S_d > 0}} p_1 \mathbb{E}[e^{-(T-\tau)\theta r_b}] + \sum_{l=1}^{L} p_{m+1} \mathbb{E}_l[e^{-(T-\tau)\theta r_d}] + p_{L+2} \\ s.t. \quad & Eq.\ (5.21) \text{ holds} \end{aligned} \tag{5.29}$$

Above, $f(g_{ss}, g_{sp})$ denotes the joint distribution of (g_{ss}, g_{sp}) of the channel selected for transmission when all channels are detected busy. Hence, in this case, the transmission channel is chosen among L channels. Similarly, $f_l(g_{ss}, g_{sp})$ denotes the joint distribution when (l) channels are detected idle, and the transmission channel is selected out of these l channels.

The objective function in Eq. (5.29) is strictly convex and the constraint function in Eq. (5.21) is linear with respect to S_b and S_d. This can be concluded from the fact that strict convexity follows from the strict concavity of r_b and r_d in Eq. (5.15) and Eq. (5.16)

with respect to S_b and S_d respectively, strict convexity of the exponential function, and the fact that the nonnegative weighted sum of strictly convex functions is strictly convex [62,71].

Lagrangian method for solve convex optimization problems is an efficient approach [38, 62]. By inserting Lagrange multiplier (ν), the problem can be converted from a constraint into an unconstrained optimization problem. First, we construct the Lagrange function (or Lagrangian) defined by

$$\begin{aligned}\Lambda(S_b, S_d, \nu) &= p_1\mathbb{E}[e^{-(T-\tau)\theta r_b}] + \sum_{l=1}^{L} p_{m+1}\mathbb{E}_l[e^{-(T-\tau)\theta r_d}] + p_{L+2} \\ &+ \nu\left(\rho^{L-1}P_b\mathcal{P}_d \times \mathbb{E}[S_b g_{sp}] + \frac{(1-\rho^L)(1-P_b)(1-p_f)}{1-\rho} \times \mathbb{E}_l[S_d g_{sp}] - I_l^{th}\right)\end{aligned} \tag{5.30}$$

Taking the partial derivative of the above function for each variable and setting the derivatives of the Lagrangian with respect to S_b and S_d equal to zero, we obtain:

$$\Big[\frac{\nu P_b\mathcal{P}_d g_{sp}}{\rho} - \frac{\alpha g_{ss}}{N_b}\left(1 + \frac{g_{ss}S_b}{(\sigma_n^2 + \sigma_{n_p}^2)}\right)^{-\alpha-1}\Big] \times \rho^L f(g_{ss}, g_{sp}) = 0 \tag{5.31}$$

and

$$\begin{aligned}\Big[\nu P_b(1-\mathcal{P}_d)g_{sp} - \frac{\alpha(1-P_b)(1-\mathcal{P}_f)g_{ss}}{N_d}\left(1 + \frac{g_{ss}S_d}{\sigma_n^2}\right)^{-\alpha-1}\Big] \\ \times \sum_{l=1}^{L}\rho^{L-l}(1-\rho)^{l-1}C(L,l)f_l(g_{ss}, g_{sp}) = 0,\end{aligned} \tag{5.32}$$

The multiplier ν can be found numerically by satisfying the constraint Eq. (5.21) with equality. Algorithm 5.1 presented below illustrates the pseudocode to find the optimal Lagrange multiplier ν.

Solving Eq. (5.31) and Eq. (5.32) for S_b and S_d, we get the optimal power as

$$S_b^* = \begin{cases} \frac{N_b}{g_{ss}}\left(\left(\frac{z}{w_b}\right)^{\frac{1}{\alpha+1}} - 1\right), & \frac{z}{w_b} \geq 1; \\ 0, & \text{otherwise,}\end{cases} \tag{5.33}$$

$$S_d^* = \begin{cases} \frac{N_d}{g_{ss}}\left(\left(\frac{z}{w_d}\right)^{\frac{1}{\alpha+1}} - 1\right), & \frac{z}{w_d} \geq 1; \\ 0, & \text{otherwise,}\end{cases} \tag{5.34}$$

where $z = \frac{g_{ss}}{g_{sp}}$, $\alpha = \frac{\mathcal{B}_c(T-\tau)\theta}{\log 2}$, $w_b = \frac{N_b P_b \mathcal{P}_d}{\alpha\rho}\nu$, and $w_d = \frac{N_d P_b(1-\mathcal{P}_d)}{\alpha(1-P_b)(1-\mathcal{P}_f)}\nu$

Algorithm 5.1 The pseudocode to determine the optimal Lagrange multiplier.

Initialization: ν^i

REPEAT $\cdots$

(1)- Compute: S_b^i and S_d^i by Eq. (5.33) and Eq. (5.34)

(2)- Compute: subgradient of ν^i by substituting S_b^i and S_d^i calculated above in:

$$SG(\nu^i) = \rho^{L-1} P_b \mathcal{P}_d \times \mathbb{E}[S_b^i g_{sp}] + \frac{(1-\rho^L)(1-P_b)(1-p_f)}{1-\rho} \times \mathbb{E}_l[S_d^i g_{sp}] - I_l^{th}.$$

(3)- Update: ν^{i+1} by:

$$\nu^{i+1} = \nu^i + \epsilon \cdot SG(\nu^i)$$

UNTIL ν^i converges.

The parameter ϵ is the stepsize to update the multiplier. It has been chosen to equal to $(1+c)/(a+c)$, where c is some adaptive constant and a is the number of iteration. This variable stepsize is shown to give a fast convergence [38, 71]. See Figure 5.5.

Using these optimal transmission powers, the effective capacity in Eq. (5.29) can be expressed as

$$E_c^{opt} = -\frac{1}{\theta T \mathcal{B}_c} \log_e \Big[p_1 \int_{w_b}^{\infty} \left(\frac{z}{w_b}\right)^{\frac{-\alpha}{\alpha+1}} f(z)dz + \sum_{l=1}^{L} p_{l+1} \int_{w_d}^{\infty} \left(\frac{z}{w_d}\right)^{\frac{-\alpha}{\alpha+1}} f_l(z)dz + p_{L+2} \Big] \quad (5.35)$$

5.6 Channel Selection Criterion

The task in this section is to propose a certain criterion by which the transmission channel is selected from a set of available channels. If a function $g(z)$ is a monotonically decreasing functions of z, then $\big[-\log g(z) \big]$ is an increasing function. Since the terms $(z/w_b)^{\frac{-\alpha}{\alpha+1}}$ and $(z/w_d)^{\frac{-\alpha}{\alpha+1}}$ in Eq. (5.35) are monotonically decreasing functions of z, it can be observed from Eq. (5.35) that the effective capacity depends only on the channel power ratio z, and it is increasing with increasing this power ratio. Therefore, the criterion for choosing the transmission band among multiple busy bands unless there is no idle band detected, or among multiple idle bands if there are idle bands detected should be based on this ratio of the channel gains. Clearly, the policy that maximizes the effective capacity is to choose the channel with the highest ratio of z. This also intuitively leads to a result that as we want to maximize g_{ss} to improve the secondary transmission and at the same time minimize g_{sp} to diminish the interference caused to the primary users. Maximizing z provides us the problem key in the channel selection algorithm.

Let $w = \max\{z_l\}$, $\forall l = 1, \cdots, L$, where $z_l = \frac{g_{ss_l}}{g_{sp_l}}$ is the ratio of the gains in the l^{th} channel. It is assumed here that all these ratios are independent and identical distributed.

By using the statistical fact that states: if $Y = \max(X_1, \cdots, X_L)$, where X_l are independent and identically distributed random variables with probability density function (*pdf*) of $f_x(x)$, then the cumulative density function (*cdf*) and *pdf* of Y are given as [*Theorem* 5.7 in [61]] respectively as

$$F_Y(y) = [F_X(y)]^L \text{ and thus, } \quad f_Y(y) = \frac{dF_Y(y)}{dy} = Lf_X(y)[F_X(y)]^{L-1} \tag{5.36}$$

Using this fact, we can express the *pdf* of w as

$$f(w) = Lf_z(w)\left(F_z(w)\right)^{L-1}, \tag{5.37}$$

where f_z and F_z are the *pdf* and *cdf* of the gain ratio z in one channel, respectively.

Now, the first integral in Eq. (5.35) can be evaluated with respect to this distribution. Similarly, let $w_l = \max\{z_j\}$, $\forall j = 1, \cdots, l$. The *pdf* of w_l can be expressed as follows:

$$f_l(w) = lf_z(w)\left(F_z(w)\right)^{l-1}, l = 1, 2, \cdots, L. \tag{5.38}$$

The second integral of Eq. (5.35) can be evaluated using this distribution, and by using the power series property [74]:

$$\sum_{l=1}^{L} \frac{l\,L!}{(L-l)!}\rho^{L-l}(1-\rho)^{l-1}x^{l-1} = L\left((1-\rho)x+\rho\right)^{L-1}.$$

In the following two subsections we apply this criterion for the case where the channels have *Rayleigh* fading distribution and for the more general case where the channels have *Gamma* fading distribution respectively.

5.6.1 Effective Capacity in Rayleigh Fading Channel

The analysis in the preceding sections apply for arbitrary joint distributions of g_{ss} and g_{sp} under the assumption that they have finite means (*i.e.*, fading has finite average power).

In this subsection, a Rayleigh fading is assumed in which the power gains g_{ss} and g_{sp} are exponentially distributed. We assume that these fading are mutually independent and each has unit-mean. The ratio of two independent exponentially distributed variables has the *pdf*

$$f_z(z) = \frac{1}{(z+1)^2}, z \geq 0 \tag{5.39}$$

(See the proof in Appendix F).

Thus, the *pdf* of w in Eq. (5.37) and Eq. (5.38) can be expressed, respectively, as

$$f(w) = L\frac{1}{(w+1)^2}\left(\frac{w}{w+1}\right)^{L-1} \tag{5.40}$$

$$f_l(w) = l\frac{1}{(w+1)^2}\left(\frac{w}{w+1}\right)^{l-1}. \tag{5.41}$$

Using Eqs. (5.35), (5.18), (5.19) and Eqs. (5.40), (5.41), the effective capacity formula for Rayleigh fading channel can be written as in Eq. (5.42), where $\alpha_1 = \alpha/(\alpha+1)$, $\alpha_2 = (2\alpha+1)/(\alpha+1)$, and the superscript R refers to Rayleigh.

$$\begin{aligned} E_c^R = &- \frac{1}{\theta T \mathcal{B}_c}\log_e\left[L\rho^L w_b^{\alpha_1}\int_{w_b}^{\infty} w^{-\alpha_2+L}\left(\frac{1}{w+1}\right)^{L+1}dw\right. \\ &\left. + (1-P_b)(1-\mathcal{P}_f)w_d^{\alpha_1}\sum_{l=1}^{L} lC(L,l)\rho^{L-l}(1-\rho)^{l-1}\int_{w_d}^{\infty} w^{-\alpha_2+l}\left(\frac{1}{w+1}\right)^{l+1}dw + p_{L+2}\right]. \end{aligned} \tag{5.42}$$

5.6.2 Effective Capacity in Gamma Fading Channel

The Gamma distribution has been considered as an adequate model to characterize wireless channel fading such as slow fading (shadowing) or even fast fading [54, 55]. It has been observed that this distribution fits the experimental data [54].

The *pdf* of Gamma distribution is given in Eq. 3.1 as

$$f_X(x) = \frac{x^{\mu-1}e^{-x/k}}{\Gamma(\mu)k^{\mu}}; \qquad x \geq 0, \tag{5.43}$$

where μ is known as the shape parameter of the distribution, and k is the scale parameter. Note that for a=1, Gamma distribution reduces to exponential distribution. So Gamma

distribution is a general case of exponential distribution, and it closely approximates the log-normal distribution.

As demonstrated in Chapter 2, the ratio of two independent *Gamma* distributed random variables with parameters μ_1 and μ_2 is *Beta Prime* distributed random variable with parameters μ_1 and μ_2 [56, 58].

The *pdf* and *cdf* of the channel power ratio $z = g_{ss}/g_{sp}$ have the following Beta Prime distribution functions

$$f_z(z) = \frac{z^{\mu_1-1}}{\beta(\mu_1,\mu_2)(z+1)^{\mu_1+\mu_2}}, \quad \text{and} \qquad F_z(z) = I_{\frac{z}{z+1}}(\mu_1,\mu_2), \tag{5.44}$$

where $\beta(\mu_1,\mu_2)$ is the Beta function defined in Appendix A, and $I_x(a,b)$ is known as *Regularized Beta* function defined as [77]

$$I_x(a,b) = \frac{\beta(x;a,b)}{\beta(a,b)} = \frac{1}{\beta(a,b)}\int_0^x t^{a-1}(1-t)^{b-1}dt. \tag{5.45}$$

The *cdf* can also be written in terms of Hypergeometric function ${}_2F_1$ [75] as

$$F_z(z) = \frac{z^{\mu_1}\,{}_2F_1(\mu_1,\mu_1+\mu_2,\mu_1+1,-z)}{\beta(\mu_1,\mu_2)}. \tag{5.46}$$

Now, the *pdf* of w in Eqs. (5.37) - (5.38) can be expressed as

$$f(w) = L\frac{w^{\mu_1-1}}{\beta(\mu_1,\mu_2)(w+1)^{\mu_1+\mu_2}}\left[I_{\frac{w}{w+1}}(\mu_1,\mu_2)\right]^{L-1}, \tag{5.47}$$

$$\text{and} \qquad f_l(w) = l\frac{w^{\mu_1-1}}{\beta(\mu_1,\mu_2)(w+1)^{\mu_1+\mu_2}}\left[I_{\frac{w}{w+1}}(\mu_1,\mu_2)\right]^{l-1}, \tag{5.48}$$

Similarly as in Rayleigh, the effective capacity formula for Gamma fading channel can be written as in Eq. (5.49), where the superscript G refers to Gamma.

$$\begin{aligned} E_c^G = -\frac{1}{\theta T\mathcal{B}_c}\log_e\Bigg[&\frac{L\rho^L w_b^{\alpha_1}}{\beta(\mu_1,\mu_2)}\int_{w_b}^{\infty} w^{\alpha_2+\mu_1}\left(\frac{1}{w+1}\right)^{\mu_1+\mu_2}\left(I_{\frac{w}{w+1}}(\mu_1,\mu_2)\right)^{L-1}dw \\ &+\frac{(1-P_b)(1-\mathcal{P}_f)w_d^{\alpha_1}}{\beta(\mu_1,\mu_2)}\sum_{l=1}^{L} lC(L,l)\rho^{L-l}(1-\rho)^{l-1} \\ &\times\int_{w_d}^{\infty} w^{\alpha_2+\mu_1}\left(\frac{1}{w+1}\right)^{\mu_1+\mu_2}\left(I_{\frac{w}{w+1}}(\mu_1,\mu_2)\right)^{l-1}dw + p_{L+2}\Bigg]. \end{aligned} \tag{5.49}$$

The impact of several parameters on the effective capacity is investigated through the

following numerical example.

5.7 Numerical Results

In this section, several numerical analysis for the obtained effective capacity expressions will be investigated. The impact of channel sensing parameters and the average interference constraint are illustrated. Throughout this numerical example, it is assumed that QoS parameter is θ =0.1. The frame duration is T = 100 ms with 10% of this time is conserved for sensing process. The prior probability of the channel being busy is the same for all channels. All variances are set to unity. The channel bandwidth is $\mathcal{B}$=10 KHz.

First, we evaluate the convergency of our algorithm. Figure. 5.5 shows the iterative algorithm for determining the optimal Lagrange multiplier. The maximum secondary transmit power is set to 10 dBw. The interference threshold and the primary transmit power are set to 0 dBw, and S_p=10 dBw, respectively. As shown in Fig. 5.5, the Lagrange multiplier can quickly converge to its optimal value when choosing a dynamic step size stated in Algorithm 5.1.

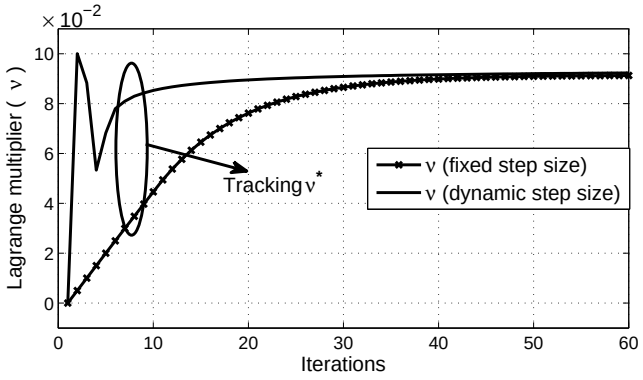

Figure 5.5: Tracking the optimal Lagrange multiplier.

Figure 5.6, shows the effective capacity versus probability of detection for different number of channels when the interference constraint is normalized by the noise power, *i.e.*, $I^{th} = \sigma_n^2$.

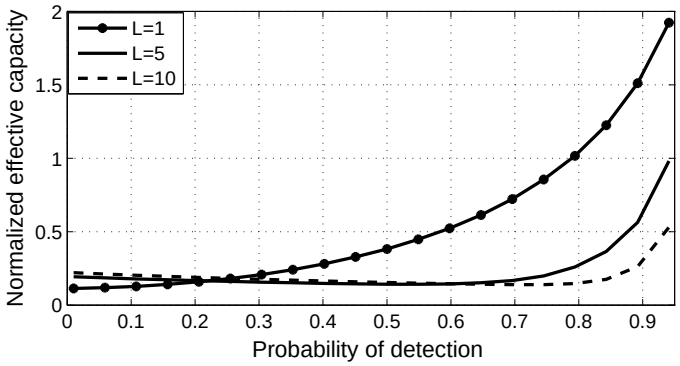

Figure 5.6: Effective capacity vs. probability of detection for different number of channels.

As $\mathcal{P}_d$ increases, the effective capacity increases due to the fact that more reliable detection of the activity of the primary users leads to fewer miss-detection and hence the probability of the case C_{db} effectively diminishes. It can also be seen that the highest effective capacity is attained when $L = 1$. Hence, the cognitive user does not benefit from the availability of multiple channels. This is especially pronounced for high values of $\mathcal{P}_d$. We can further observe that several parameters affect the value of the effective capacity. One explanation for this observation is that the probabilities of the cases C_{bb} and C_{bd}, in which the cognitive user transmits with power S_b, decrease with increasing L; while the probabilities of the cases C_{db} and C_{dd} in which the cognitive user transmits with power S_d, increase as can be seen in Table 5.1. Note that in the case C_{db}, no reliable communication is possible.

In Figure 5.7, the effect of the primary user's occupancy P_b on the effective capacity is investigated for different number of sensed channels. This effect is observable for probability of detection less than 0.8.

Figure 5.8 examines the impact of the QoS exponent values, θ for L=5. This figure confirms that significant capacity gains can be achieved for lossy QoS constraints (*i.e.*, small θ). While the capacity decreases dramatically for highly strength QoS constraints.

In Figure 5.9, the effective capacity is plotted versus the interference threshold I^{th} for different number of channels for the case of Rayleigh fading channel. The probability of

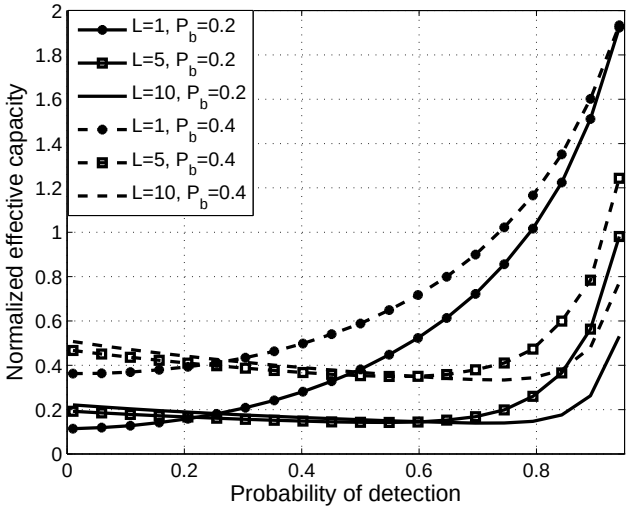

Figure 5.7: Effective capacity vs. probability of detection for different L and different busy probabilities P_b, $\theta = 0.1$. Dashed curves represent the $P_b = 0.4$ case and solid curves represent the $P_b = 0.2$ case for relevant colors.

detection is sit at $\mathcal{P}_d$=0.8. The figure shows that as the interference gets more strict (*i.e.*, I^{th} becomes smaller), a higher number of channels is needed to maximize the effective capacity. As an example, if the interference threshold I^{th} <-15 dB, then five channels are needed to reach maximum capacity; while if the interference threshold $I^{th} < 2$ dB, one channel is enough to get the highest throughput. As it is mentioned before, increasing the number of available channels from which the transmission channel is selected provides no benefit or can even degrade the performance of the cognitive user. On the other hand, it always provides benefits to the primary users in the sense of lowering the probability of interference as it is discussed and drawn in Section 5.4, Eq. (5.20), and in Figure 5.4.

In Figure 5.10, the effective capacity is plotted versus the interference threshold I^{th} for different number of channels for the case of Gamma fading channel. Similar results and conclusions can be observed. Higher capacity is obtained by sensing more than one channel in the presence of strict interference constraints.

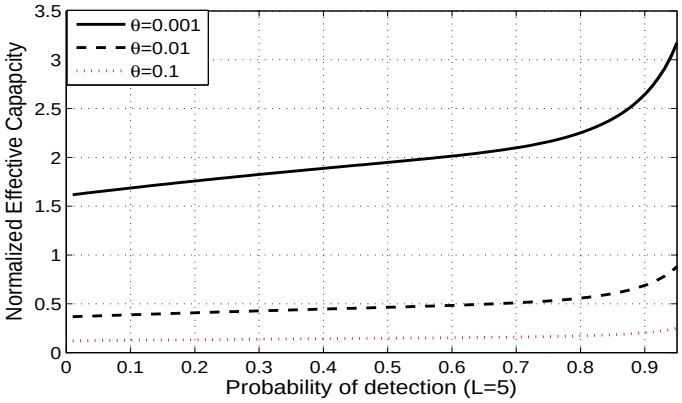

Figure 5.8: Normalized effective capacity vs. probability of detection for different QoS exponent delay θ, $L = 5, P_b = 0.2$.

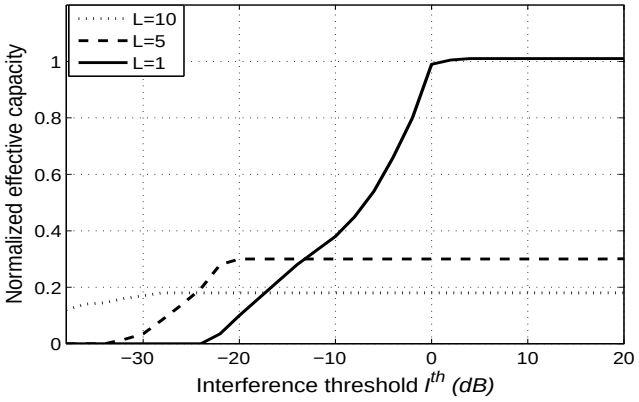

Figure 5.9: Effective capacity vs. I^{th} for different number of channels in the Rayleigh fading channel, $\mathcal{P}_d = 0.8, P_b = 0.2, \theta = 0.1$.

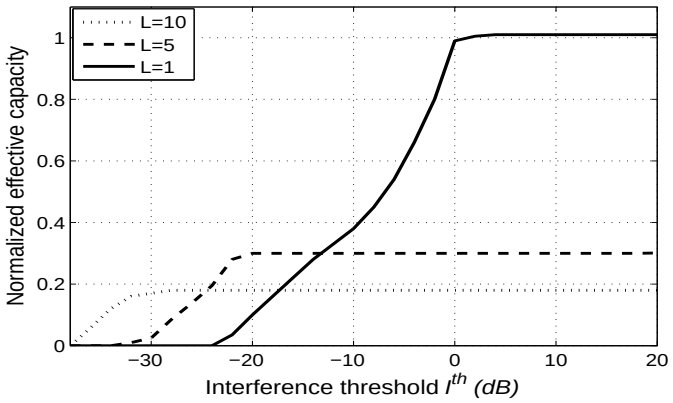

Figure 5.10: Effective capacity vs. I^{th} for different number of channels in the Gamma fading channel, $\mathcal{P}_d = 0.8, P_b = 0.2, \theta = 0.1$.

5.8 Chapter Summary

The performance of cognitive transmission under QoS constraints and interference limitations is studied. Cognitive user is assumed to perform sensing in multiple channels and then select a single channel for transmission with rate and power that depend on both sensing outcomes and fading distribution. A state transition model for this cognitive operation has been constructed . All possible cases and states are considered and analyzed. These states are functions of sensing probabilities, channels being busy or idle, and transmission rates being smaller or greater than the instantaneous channel capacity. Interference constraint is statistically analyzed and formulated. Maximum throughput formulas for the cognitive user is obtained. Selection criterion that maximizes the capacity is proposed for arbitrary channel fading then we apply it for two different fading distributions. The optimal power allocation are also determined.

Increasing the number of available channels from which the transmission channel is selected provides no benefit or can even degrade the performance of the cognitive user. It is found that sensing multiple channels is beneficial only under relatively strict interference constraints. On the other hand, it always provides benefits to the primary users in the sense of decreased probability of interference

Chapter 6

Optimal Access Strategies for Throughput Optimization in CRN

This chapter proposes an optimized access strategy combining overlay and underlay schemes for the cognitive radio. We model the service state of the system as a continuous-time Markov model. Based on the service state, the overlay manner or/and the underlay manner is/are used by the secondary users. When the primary user is not transmitting and only one secondary user has the requirement to transmit, the secondary system adopts the overlay base. When the primary user is transmitting and the secondary users want to transmit simultaneously, an underlay scheme with optimal access probabilities is adopted. We obtain these access probabilities in a closed form which maximizes the overall system throughput.

6.1 Introduction

As it is now well known, that in spectrum sharing systems, the secondary user can adopt two types of access schemes: overlay scheme and underlay scheme. In underlay scheme, the licensed spectrum band can be accessed without considering the primary user's activities, but with strict power constraint. In overlay scheme, the secondary user senses the spectrum

bands and accesses the unused spectrum spots. The secondary users must stop its transmission when the primary user appears in the band and resume when the primary user finishes its service.

The different features of these two schemes enable them to make up with each other. In [36, 37], the papers give a mixed access strategy. When the channel is being used by the primary user, the secondary users access the channel with a probability in underlay manner; when the channel is idle, they choose to access in overlay manner. However, the optimal access probability is not a precise value. An optimal access probability with different criteria is given in [35] for pure underlay scheme. Based on [35], this chapter proposes a mixed overlay and underlay access scheme. The secondary users access the channel with an optimal probability in an underlay scheme when the spectrum is occupied by the primary user. While, when the spectrum is idle, the secondary users access the channel in an overlay manner. This approach can maximize the total average throughput for the secondary users and limit the interference on the primary user.

The optimized access strategy proposed in this chapter shares some similarities to the work done in [35]. We further introduce a new optimized parameter ρ to determine the best access probability to achieve the highest throughput. In this work, closed forms for the achieved capacity are provided as well as the optimized access parameters.

The rest of this chapter is organized as follows. Section 6.2 introduces the system model and assumptions. In Section 6.3, the maximal throughput expressions for the two schemes are given. The optimal access strategy for equiprobability case is introduced in Section 6.4. While Section 6.5 introduces the case of unlike access probability. Performance analysis and simulation results are given in Section 6.6. Finally, the chapter is summarized in Section 6.7.

6.2 System Model And Assumptions

Figure 6.1 illustrates the system model which consists of a primary user (P) and two cognitive users $\{A, B\}$ sharing a $\mathcal{B}$ Hz wireless channel. It is assumed that both cognitive users can sense the primary user perfectly. A cognitive base station is assumed to make the cognitive users exchange their information among them. An example of these information is the real-time service state. The service state indicates a user's requirement for transmitting at specific time. The primary user can employ the channel without considering secondary users' service state.

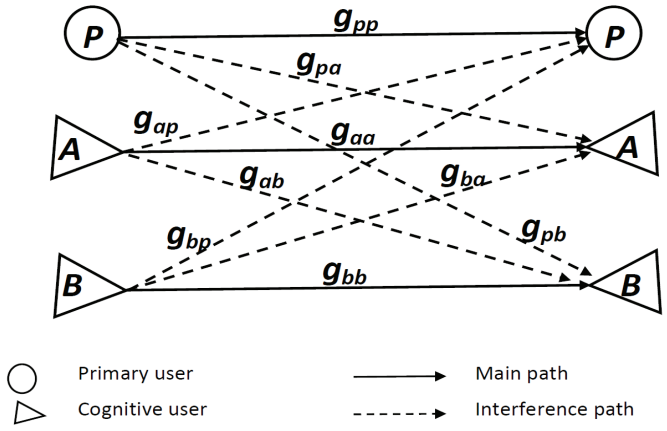

Figure 6.1: The additive interference channel for a pair of primary and cognitive links with channel gain coefficients: $g_{pp}, g_{ss}, g_{ps}, g_{sp}$.

The traffic pattern of the primary and the two secondary users is modeled as independent Poisson processes with arrival rates (in packet/s) λ_P, λ_A and λ_B, respectively. The service times are assumed to be exponentially distributed with rates $1/\mu_P$, $1/\mu_A$ and $1/\mu_B$ in seconds, respectively. The service state of the system is defined as the sum service state of all the users in the system at a moment. Based on the individual's service state, we get the service state set for the system as $\mathcal{S} \in \{0, P, A, B, AB, PA, PB, PAB\}$. State '0' represents there is no user tends to transmit on the channel; State 'P' represents only the primary user is transmitting on the channel; State 'A' represents only user A wants to transmit on

the channel; State 'B' represents only user B wants to transmit on the channel; State 'AB' represents both cognitive users want to transmit on the channel at the same time; State 'PA' represents user A wants to transmit on the channel while the primary is transmitting; State 'PB' represents user B wants to transmit on the channel while the primary user is transmitting; State 'PAB' represents both A and B want to transmit on the channel while the primary user is transmitting.

These states in the cognitive radio system can be modeled as an eight-state continuous time Markov model, as shown in Figure 6.2 [35].

The rate at which transitions take place *out* of state s_i equals to the rate at which transitions take place *into* state s_i. The normalization equations governing this *flow balance* can be written as

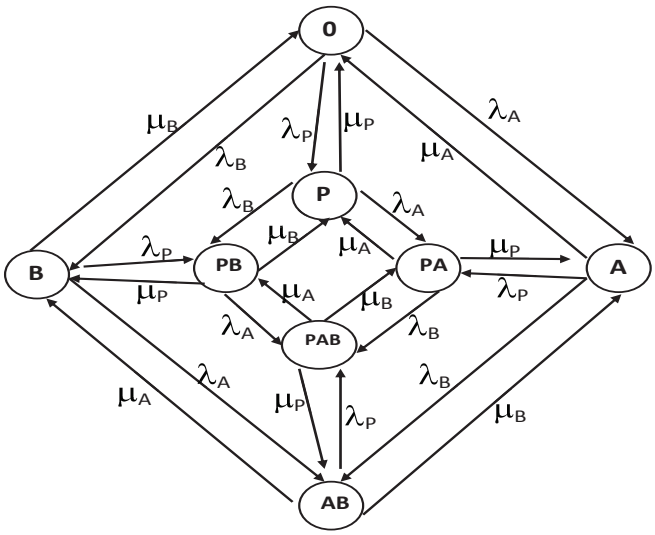

Figure 6.2: The continuous time Markov model of the service state and the flow balance.

$$
\begin{aligned}
\pi_0(\lambda_P+\lambda_A+\lambda_B) &= \pi_P\mu_P+\pi_A\mu_A+\pi_B\mu_B \\
\pi_P(\lambda_A+\lambda_B+\mu_P) &= \pi_0\lambda_P+\pi_{PA}\mu_A+\pi_{PB}\mu_B \\
\pi_A(\lambda_P+\lambda_B+\mu_A) &= \pi_0\lambda_A+\pi_{AB}\mu_B+\pi_{PA}\mu_P \\
\pi_B(\lambda_P+\lambda_A+\mu_B) &= \pi_0\lambda_B+\pi_{AB}\mu_A+\pi_{PB}\mu_P \\
\pi_{AB}(\lambda_P+\mu_A+\mu_B) &= \pi_A\lambda_B+\pi_B\lambda_A+\pi_{PAB}\mu_P \\
\pi_{PA}(\lambda_B+\mu_P+\mu_A) &= \pi_A\lambda_P+\pi_P\lambda_A+\pi_{PAB}\mu_B \\
\pi_{PB}(\lambda_A+\mu_P+\mu_B) &= \pi_B\mu_P+\pi_P\lambda_B+\pi_{PAB}\mu_A \\
\pi_{PAB}(\mu_P+\mu_A+\mu_B) &= \pi_{PA}\lambda_B+\pi_{PB}\lambda_A+\pi_{AB}\lambda_P,
\end{aligned}
\tag{6.1}
$$

where π_{s_i} represents the steady-state probability of being in state s_i and $s_i \in \mathcal{S}$. Also we have

$$
\Sigma_{s_i}\pi_{s_i} = \pi_0+\pi_P+\pi_A+\pi_B+\pi_{AB}+\pi_{PA}+\pi_{PB}+\pi_{PAB}=1. \tag{6.2}
$$

The steady state probabilities for all the states can be found by solving the set of the linear equations Eqs. (6.1) and (6.2).

6.3 Secondary User's Maximal Throughput

6.3.1 Maximal Throughput for Overlay Scheme

In the overlay scheme, the secondary users can only access the spectrum hole which is currently not used by the primary user. They can not co-exist on the same spectrum band. If one secondary user is transmitting, the only interference is the background noise. The user A or B accesses the channel with power S_s^o. Since in the overlay manner, only one user

can transmit, the maximal data rate for each of them individually is

$$\begin{aligned} R_A^o = &\quad \mathcal{B}\log_2\left(1+\frac{g_{aa}S_s^o}{\sigma_s^2}\right) \\ R_B^o = &\quad \mathcal{B}\log_2\left(1+\frac{g_{bb}S_s^o}{\sigma_s^2}\right) \end{aligned} \tag{6.3}$$

where σ_s^2 is noise power. These rates can be achievable with the following corresponding probabilities:

$$P^{o,(A)} = \pi_A \quad \text{and} \quad P^{o,(B)} = \pi_B \quad \text{respectively.}$$

6.3.2 Maximal Throughput for Underlay Scheme

Unlike the overlay scheme, in the underlay system, secondary users are allowed to share the channel simultaneously with the primary user pledging not to violate the limits of interference.

Since the secondary users A and B can get the service state of the system with the help of their base station, A and B make access decision based on the service state of the system. Here, we have two possible service state sets. When the service state is $s_i \in \mathcal{S}_1 = \{A, B\}$, which indicates the primary user P is not transmitting and only one secondary user has the requirement to transmit. The other case is when the service state $s_i \in \mathcal{S}_2 = \{PA, PB, PAB, AB\}$, which indicates that the primary user is transmitting or both secondary users want to transmit at the same time. User A and B have to adopt their powers S_s^u to access the channel with probability $\rho_A = \rho_B = \rho$ in the underlay scheme. In order to protect the primary user and decrease the mutual interference between secondary users, we assume that S_s^u satisfies the minimum $SINR$ requirement.

The probability ρ determines the sum throughput of the secondary users and the interference on the primary user. When ρ is large, the sum throughput may be large and the chance to coexist with primary user is large, too. Our goal is to obtain an optimal access probability ρ to maximize the sum throughput, while limit the interference on the primary

user. The service state set of the system in the underlay manner is $\mathcal{S}_2$. Hence the actual access state set is $\mathcal{S}_3 \in \{A, B, PA, PB, PAB, AB\}$. The users' maximal date rate under each state in the underlay manner is given as

$$\begin{array}{lcllcl} R_A^{u,(PA)} & = & \mathcal{B}\log_2\left(1+\frac{g_{aa}S^u}{S_p g_{pa}+\sigma_s^2}\right); & R_B^{u,(PB)} & = & \mathcal{B}\log_2\left(1+\frac{g_{bb}S^u}{S_p g_{pb}+\sigma_s^2}\right) \\ R_A^{u,(A)} & = & \mathcal{B}\log_2\left(1+\frac{g_{aa}S^u}{\sigma_s^2}\right); & R_B^{u,(A)} & = & \mathcal{B}\log_2\left(1+\frac{g_{bb}S^u}{\sigma_s^2}\right) \\ R_A^{u,(AB)} & = & \mathcal{B}\log_2\left(1+\frac{g_{aa}S^u}{S^u g_{ba}+\sigma_s^2}\right); & R_B^{u,(AB)} & = & \mathcal{B}\log_2\left(1+\frac{g_{bb}S^u}{S^u g_{ab}+\sigma_s^2}\right) \\ R_A^{u,(PAB)} & = & \mathcal{B}\log_2\left(1+\frac{g_{aa}S^u}{S_p g_{pa}+S^u g_{ba}+\sigma_s^2}\right); & R_B^{u,(PAB)} & = & \mathcal{B}\log_2\left(1+\frac{g_{bb}S^u}{S_p g_{pb}+S^u g_{ab}+\sigma_s^2}\right), \end{array} \tag{6.4}$$

where $R_i^{u,(s)}, i \in \{A, B\}, s \in \mathcal{S}_3$ denotes the i's maximal data rate for the underlay case. The term $g_{ij}, i, j \in \{p, a, b\}$ is the channel power gain between the transmitter of the user i and the receiver j as shown in Figure 6.1. S_p is the transmit power of the primary user. The corresponding probabilities of these rates are:

$$P^{u,(PA)} = \rho\pi_{PA} + \rho(1-\rho)\pi_{PAB} \tag{6.5.a}$$

$$P^{u,(PB)} = \rho\pi_{PB} + \rho(1-\rho)\pi_{PAB} \tag{6.5.b}$$

$$P^{u,(A)} = \rho(1-\rho)\pi_{AB} \tag{6.5.c}$$

$$P^{u,(B)} = \rho(1-\rho)\pi_{AB} \tag{6.5.d}$$

$$P^{u,(AB)} = \rho^2\pi_{AB} \tag{6.5.e}$$

$$P^{u,(PAB)} = \rho^2\pi_{PAB} \tag{6.5.f}$$

6.4 Equiprobability Optimal Access Strategy

In this section we introduce an optimal access strategy which makes the cognitive network to operate in both schemes. During primary user's idle periods, the network employs the overlay scheme; while in primary user's busy periods, the network permits the secondary users to use the channel with probability ρ subject to satisfying the interference threshold constraint. The parameter ρ is a secondary service parameter which has to be adjusted based on the spectrum status to achieve maximum throughput.

Based on Eq. (6.3) to Eq. (6.4), we can get the average throughput for the secondary users as

$$\begin{aligned} R_A &= R_A^o P^{o,(A)} + R_A^{u,(PA)} P^{u,(PA)} + R_A^{u,(A)} P^{u,(A)} + R_A^{u,(AB)} P^{u,(AB)} + R_A^{u,(PAB)} P^{u,(PAB)} \\ R_B &= R_B^o P^{o,(B)} + R_B^{u,(PB)} P^{u,(PB)} + R_B^{u,(B)} P^{u,(B)} + R_B^{u,(AB)} P^{u,(AB)} + R_B^{u,(PAB)} P^{u,(PAB)} \end{aligned} \tag{6.6}$$

The total throughput of the cognitive network is

$$R_s = R_A + R_B \tag{6.7}$$

Using Eqs. (6.5) - (6.6), R_s can be written in the quadrature form as

$$R_s(\rho) = \beta_1 \rho^2 + \beta_2 \rho + \beta_3, \tag{6.8}$$

where β_1, β_2 and β_3 are given as follows

$$\begin{aligned} \beta_1 = \;& \pi_{AB} \left(R_A^{u,(AB)} + R_B^{u,(AB)} - \left(R_A^{u,(A)} + R_B^{u,(B)} \right) \right) \\ & + \pi_{PAB} \left(R_A^{u,(PAB)} + R_B^{u,(PAB)} - \left(R_A^{u,(PA)} + R_B^{u,(PB)} \right) \right), \\ \beta_2 = \;& \pi_{AB} \left((R_A^{u,(A)} + R_B^{u,(B)}) \right) + \pi_{PAB} \left(R_A^{u,(PA)} + R_B^{u,(PB)} \right) \\ & + \pi_{PA} R_A^{u,(PA)} + \pi_{PB} R_B^{u,(PB)}, \\ \beta_3 = \;& \pi_A R_A^o + \pi_B R_B^o \end{aligned} \tag{6.9}$$

To maximize the throughput of the secondary users, we take the first derivative of R_s with respect to ρ and equate it to zero. Solving for ρ leads to the optimal access probability,

$$\frac{\partial R_s(\rho)}{\partial \rho} = 2\beta_1 \rho + \beta_2 = 0 \quad \Rightarrow \quad \rho^{opt} = -\frac{\beta_2}{2\beta_1} \tag{6.10}$$

An expression for ρ^{opt} can be written as

$$\begin{aligned} \rho^{opt} &= -\beta_2 / 2\beta_1 \\ &= \frac{\pi_{AB} \left((R_A^{u,(A)} + R_B^{u,(B)}) \right) + \pi_{PAB} \left(R_A^{u,(PA)} + R_B^{u,(PB)} \right) + \pi_{PA} R_A^{u,(PA)} + \pi_{PB} R_B^{u,(PB)}}{2 \left[\pi_{AB} \left(R_A^{u,(A)} + R_B^{u,(B)} - \left(R_A^{u,(AB)} + R_B^{u,(AB)} \right) \right) + \pi_{PAB} \left(R_A^{u,(PA)} + R_B^{u,(PB)} - \left(R_A^{u,(PAB)} + R_B^{u,(PAB)} \right) \right) \right]} \end{aligned} \tag{6.11}$$

We can note from Eq. (6.9) that β_2 is always positive. Since ρ is a probability value (*i.e.*, $\rho^{opt} \in$

$[0,1]$), the value of β_1 is always negative. The throughput function of the secondary network in Eq. (6.8) is concave down. Thus it must have a unique maximum value, it can be expressed as

$$R_s^{opt} = \beta_3 + \frac{\beta_2^2}{4|\beta_1|}, \tag{6.12}$$

where $|\cdot|$ denotes the absolute value.

6.5 Diverse Access Probabilities Strategy

In this section, a similar approach will be followed as in the previous section except that it is assumed that each user A and B has its own access probability (ρ_A and ρ_B) respectively. The goal here is to optimize these parameters. So the best access probability for each secondary user is found to achieve the highest possible throughput.

User A and B have to adopt their powers S_s^u to access the channel with probabilities ρ_A, and ρ_B, respectively in the underlay scheme. In order to protect the primary user and decrease the mutual interference between secondary users, we assume again that S_s^u satisfies the minimum $SINR$ requirement.

These probabilities ρ_A and ρ_B determine the sum throughput of the secondary users and the interference on the primary user. When ρ_A and/or ρ_B are large, the sum throughput may be large and the chance to coexist with primary user is large, too. Our goal is to obtain optimal access probabilities to maximize the total secondary throughput, while limit the interference on the primary user.

Same service state set $\mathcal{S}_3 \in \{A, B, PA, PB, PAB, AB\}$ exists. The users' maximal date rate under each state in the underlay manner is given in Eq. (6.4). The corresponding probabilities of

these rates given in Eq. (6.5) can be written now as

$$P^{u,(PA)} = \rho_A \pi_{PA} + \rho_A(1-\rho_B)\pi_{PAB} \tag{6.13.a}$$

$$P^{u,(PB)} = \rho_B \pi_{PB} + (1-\rho_A)\rho_B \pi_{PAB} \tag{6.13.b}$$

$$P^{u,(A)} = \rho_A(1-\rho_B)\pi_{AB} \tag{6.13.c}$$

$$P^{u,(B)} = (1-\rho_A)\rho_B \pi_{AB} \tag{6.13.d}$$

$$P^{u,(AB)} = \rho_A \rho_B \pi_{AB} \tag{6.13.e}$$

$$P^{u,(PAB)} = \rho_A \rho_B \pi_{PAB} \tag{6.13.f}$$

Using Eqs. (6.6) and (6.13)), R_s can be written in a nonlinear equation form as

$$R_s(\rho_A, \rho_B) = \acute{\beta}_1 \rho_A \rho_B + \acute{\beta}_2 \rho_A + \acute{\beta}_3 \rho_A + \acute{\beta}_4, \tag{6.14}$$

where $\acute{\beta}_i$, $i = 1, \cdots, 4$ is given as follows

$$\begin{aligned}
\acute{\beta}_1 =& -\Big[\pi_{AB}\left(R_A^{u,(A)} + R_B^{u,(B)} - \left(R_A^{u,(AB)} + R_B^{u,(AB)}\right)\right) \\
&+\pi_{PAB}\left(R_A^{u,(PA)} + R_B^{u,(PB)} - \left(R_A^{u,(PAB)} + R_B^{u,(PAB)}\right)\right)\Big] \\
\acute{\beta}_2 =& \left(\pi_{PA} + \pi_{PAB}\right) R_A^{u,(PA)} + \pi_{AB} R_A^{u,(A)}, \\
\acute{\beta}_3 =& \left(\pi_{PB} + \pi_{PAB}\right) R_B^{u,(PB)} + \pi_{AB} R_B^{u,(B)}, \\
\acute{\beta}_4 =& \pi_A R_A^o + \pi_B R_B^o
\end{aligned} \tag{6.15}$$

To find an optimization solution for Eq. (6.14), we bring up the following theorem [75].

Theorem 1 *Let f be a function with two variables with continuous second order partial derivatives f_{xx}, f_{yy} and f_{xy} at a critical point (a, b). Let D is the determinant of the* Hessian *matrix of the*

function f, i.e., $D = f_{xx}(a,b)f_{yy}(a,b) - f_{xy}^2(a,b)$, thus

$$\begin{cases} \text{If } D > 0 \text{ and } f_{xx}(a,b) > 0, & \textit{then } f(a,b) \textit{ is a relative minimum ;} \\ \text{If } D > 0 \text{ and } f_{xx}(a,b) < 0, & \textit{then } f(a,b) \textit{ is a relative maximum ;} \\ \text{If } D < 0, & \textit{then } f(a,b) \textit{ is a saddle value;} \\ \text{If } D = 0, & \textit{then no conclusion can be drawn.} \end{cases} \tag{6.16}$$

Using **Theorem** 1, it is forward to conclude that the possible maximum of the utility function R_s (*i.e.*, Eq. (6.14)) occurs at the saddle point of this function which appears at $(\rho_A^*, \rho_B^*) = (-\frac{\beta_3}{\beta_1}, -\frac{\beta_2}{\beta_1})$. Then the maximum throughput of the secondary users can be found by substituting this point into Eq. (6.14), this yields

$$R_s^{opt} = \acute{\beta}_4 + \frac{\acute{\beta}_2\acute{\beta}_3}{|\acute{\beta}_1|}, \tag{6.17}$$

6.6 Simulation Results

In this section, we will carry a simulation example to illustrate the proposed algorithm. The following powers are set: S_s^o=5 mw and $S_p = S_s^u$=10 mw. The arrival rates are set as λ_P=80 packets/ms, λ_A=110 packets/ms and $100 \leq \lambda_B \leq 120$ with equal average times $1/\mu_\gamma$=10 s, $\gamma \in \{A, B, P\}$. The wireless channel bandwidth $\mathcal{B}$=100 KHz. It is assumed that the loss of power in propagation follows the exponential propagation law with exponent loss 3.5. The position of the primary user's transmitter and receiver are $(300, 0)$ and $(0, 0)$ respectively. The user A's transmitter and receiver locations are at $(600, 0)$ and $(700, 0)$. User B's transmitter and receiver are located at $(450, 0)$ and $(500, 0)$.

In Figure 6.3, the normalized throughput (which is defined as the throughput divided by $\mathcal{B}$) for user A , B are shown. Clearly, user B's throughput is larger than that of A. This is because B's transmitter and receiver are located closer than those of A. As the arrival rate of B increases, the throughput of B gets better, which can be understood intuitively. The throughput of A decreases because the user B transmitting creates more interference to it.

In Figure 6.4, the performance of the optimized access strategy, the pure overlay strategy,

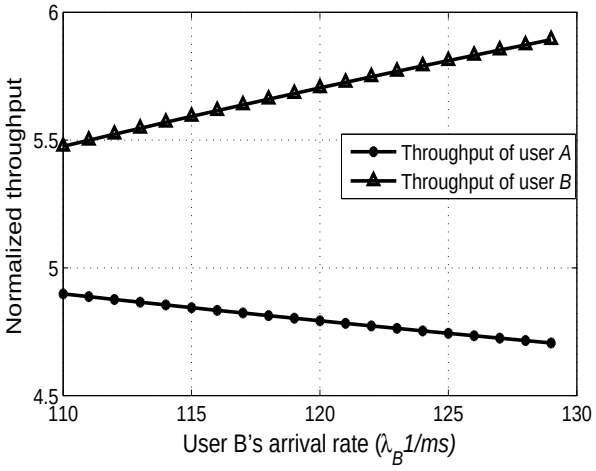

Figure 6.3: Normalized throughput of the secondary system users, A and B.

the pure underlay strategy and the overall throughput of the secondary network are compared. Note that the underlay strategy can obtain more throughput than the overlay strategy because we

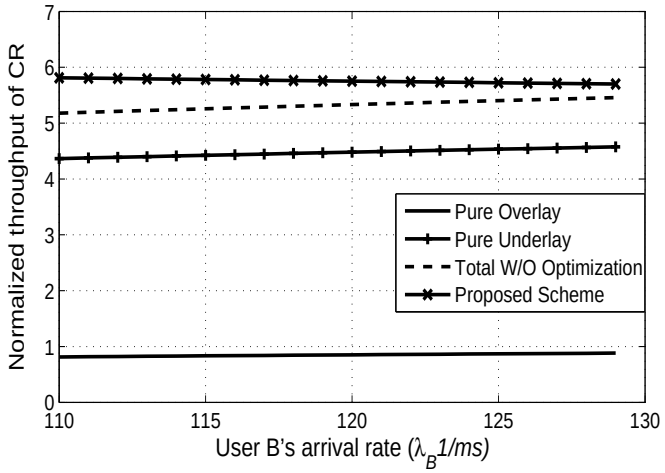

Figure 6.4: Throughput of the secondary system comparison with different access schemes.

assigned more power for S_s^u. It should be remembered that the overlay strategy avoids the coexisting time with the primary user, which has the least influence on the primary user. Our optimized access strategy maximizes the total throughput and has limited interference on the primary user.

In Figure 6.5, the normalized throughput for the pure underlay and the proposed underlay

strategies versus the access probability is shown. The value of the arrival rate of the user B is fixed at $115/ms$. As mentioned in Section 6.4, there is an unique optimal access probability that maximize the throughput.

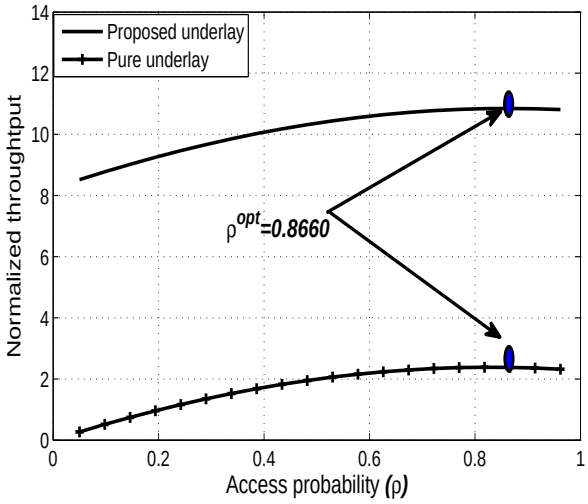

Figure 6.5: Normalized throughput of the secondary system versus the access probability ρ.

In Figure 6.6, the throughput is plotted versus the two access probabilities. When $\rho_A = \rho_B = 0$, the throughput is at the worst case which equivalent to the overlay throughput.

Accessibility of user A enhances the throughput more than that of user B. This is because user A creates less interference on the primary user. The small circle on the graph shows the optimized value of $R_s = 9.78$, note that $(\rho_A > \rho_B)$.

To study the effect of changing the arrival rate of the far user A, λ_B is fixed at 110 packets/ms while λ_A is varied in Figure 6.7. Because of the shorter distance of user B where the probability to introduce interference on the primary is hight, ρ_B is always less than ρ_A. As λ_A increases, both access probabilities decrease to mitigate the interference on the primary user. This degradation is more for the closed user B.

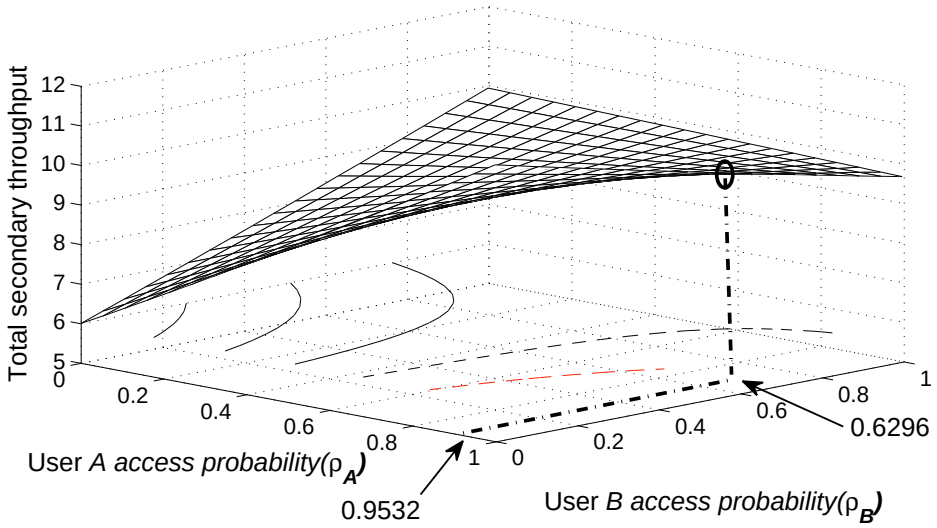

Figure 6.6: Throughput of the secondary system versus the access probabilities ρ_A, ρ_B

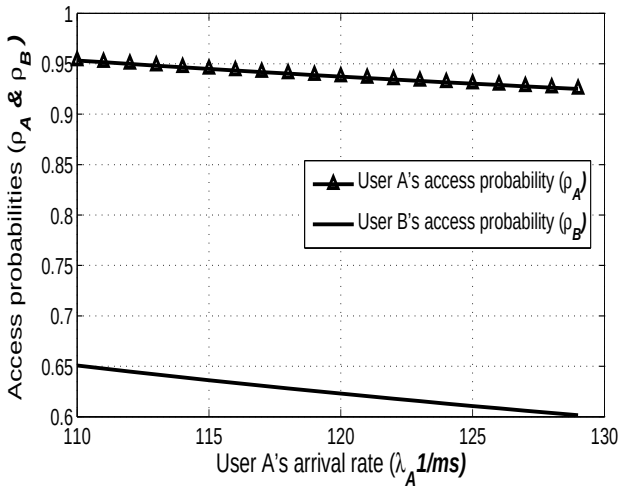

Figure 6.7: The influence of far user's arrival rate on the access probabilities

6.7 Chapter Summary

The two dominant access schemes in the cognitive radio architecture, underlay and overlay, are studied. It is found by some literatures that these two schemes can make up with each other to enhance the system performance. This chapter proposes a mixed access strategy combining these two schemes. It is assumed that the secondary users access the spectrum with a certain access probability. The focus is on the service state of the two schemes. The service state of the system is modeled as a continuous-time Markov chain. Finally, optimal access probabilities for this mixed strategy are obtained in closed forms which maximize the overall throughput of the network. The simulation results show that the proposed underlay can achieve much better performance for the secondary uses, compared with the overlay cognitive radio system.

Chapter 7

Conclusions and Future work

This dissertation is mainly focused on power control and capacity issues in cognitive radio networks. The main contributions and proposed future work of this study are summarized in this chapter.

7.1 Conclusion

The concept of effective capacity as a metric of QoS delay satisfaction, rather than Shannon channel capacity, was applied. We developed optimal resource allocations for both underlay and overlay DSA schemes. Modeling the channels as general Gamma distribution, assuming hybrid DSA schemes, and proposing selection criterion to dynamically choose the best access scheme, were the main contributions compared to the existing literatures. The underlay and overlay approaches may have their respective advantages under diverse propagation environment and system parameters. If the cognitive network can dynamically choose the DSA strategy under different environment, its performance could be further improved. The impacts of different network performance, such as primary users activity, power and interference constraints, required sensing time, delay restrictions, *etc*, were analyzed and investigated.

Then, the study was extended to estimate the channel information via $MMSE$ technique for the case of imperfect information of the channel coefficients. In which, the cognitive radio initially performs channel sensing, then the channel fading coefficients are estimated in the training

phase using Pilot Aided Transmission technique followed by data transmission. The activity of the primary user was considered and modeled in each case. We jointly evaluated and optimized the training symbol and data symbol powers and transmission rates of the cognitive user.

We further studied the case where the cognitive user is assumed to perform sensing in multiple frequency channels and then a single channel was selected for transmission. The applied rate and power depend on both sensing outcomes and fading distribution. A state transition model for this cognitive operation was constructed. All possible cases and states were considered through extensive statistical analysis. These states are functions of sensing probabilities, channels being busy or idle, and transmission rates being smaller or greater than the instantaneous channel capacity. Interference constraint was statistically analyzed and formulated. Maximum throughput formulas for the cognitive users were obtained. Selection criterion that maximizes the capacity was proposed for arbitrary channel fading then we applied it for two different fading distributions. Optimal power allocations were also determined. We concluded that increasing the number of available channels from which the transmission channel is selected provides no benefit or can even degrade the performance of the cognitive users. It was found that sensing multiple channels is beneficial only under relatively strict interference constraints. On the other hand, it always provides benefits to the primary users in the sense of decreased probability of interference.

Finally, we proposed a mixed access strategy combining the two dominate DSA schemes to maximize the overall throughput of the cognitive network. It was assumed that the secondary users can use the spectrum with certain access probabilities. Then we optimized these probability values by modeling the service state of the system as a continuous-time Markov chain. Closed forms for these probabilities, which significantly improve the throughput of channel, were analytically derived.

Extensive numerical and simulation results were provided to examine the proposed algorithms. Many insightful observations and investigations were presented.

7.2 Future Work

As future studies, a number of research topics to be explored in the field of cognitive radio resource management are listed here

- In most of the chapters in this thesis, we analyzed the environment with single-user and single-network assumptions. When multiple users and/or network coexist(s) in a cellular network, resource management and capacity analysis become more critical but complicated. Studying these imperative cases is very important to get a global view of the system requirements.

- The objective functions studied in this thesis examine only secondary user transmit power based on given transmission rate requirement for traffic. Extension to objective functions is possible by considering more network figures, like supporting variable rate traffic, providing the users with a certain requirements like fairness, considering user mobility, *etc.*

- Although this study considers the case of multichannel sensing in Chapter 5 in which the user senses more than one channel at a time and selects the more suitable one, the scheme might be extended toward more recent effective sensing techniques. As an example, cooperative spectrum sensing is a good candidate to reduce the probability of false alarm and miss detection.

- QoS delay satisfaction based on effective capacity concept is considered in this work as an important metric in time variant wireless network. The work does not consider other QoS factors such as throughput, FER, which depends mainly on the modulation schemes. Extending the study jointly with all these QoS requirements might be a good motivation as a future work.

Appendix A

Gamma & Hypergeometric functions

In this Appendix, we illustrate some mathematical definitions and properties of Gamma and Hypergeometric functions [59, 74, 77, 78] which we used to simplify the expected values of the service rates.

A.1 Gamma Function

In mathematics, Gamma function is an extension of the factorial function, with its argument shifted down by 1

$$\Gamma(z) = \begin{cases} (z-1)! = \prod_{i=1}^{z-1} i, & \text{if } z \text{ is positive integer;} \\ \int_0^\infty e^{-t} t^{z-1} dt, & \text{if } z \text{ is real or complex.} \end{cases}, \tag{A.1}$$

The function $\Gamma(z)$ is undefined for negative integers where the function has poles. Using integration by parts in the relation (A.1), Gamma function satisfies the functional equation

$$\Gamma(z+1) = z\Gamma(z). \tag{A.2}$$

Other important functional equation for Gamma function is

$$\Gamma(z)\Gamma(1-z) = \frac{\pi}{\sin \pi z}. \tag{A.3}$$

Sitting $z = 0.5$ in (A.3), we get the best-known value of Gamma function $\Gamma(\frac{1}{2}) = \sqrt{\pi}$.

The derivative of Gamma function can be expressed in terms of Polygamma function as:

$$\frac{\partial}{\partial z}\Gamma(z) = \Gamma(z)\Psi(z), \tag{A.4}$$

where, we previously defined $\Psi(z)$ in (3.16).

Another important special case of Gamma function is that of *Beta function*

$$\beta(x,y) = \beta(y,x) = \int_0^1 (1-t)^{y-1}t^{x-1}dt = \frac{\Gamma(x)\Gamma(y)}{\Gamma(x+y)} \tag{A.5}$$

The derivative of Beta function can be expressed in terms of Beta and Polygamma functions as:

$$\frac{\partial}{\partial x}(\beta(x,y)) = \beta(x,y)(\Psi(x) - \Psi(x+y)) \tag{A.6}$$

A.2 Hypergeometric Function

The general Hypergeometric function ${}_pF_q$ is defined as

$${}_pF_q(a_1,\cdots,a_p;b_1,\cdots,b_q;z) = \sum_{n=0}^{\infty} \frac{(a_1)_n,\cdots,(a_p)_n}{(b_1)_n,\cdots,(b_q)_n}\frac{z^n}{n!}; \tag{A.7}$$

where $(\upsilon)_n$ is known as rising factorial, defined as

$$(\upsilon)_n = \begin{cases} \upsilon(\upsilon+1)(\upsilon+2)\cdots(\upsilon+n-1), & \text{n} \neq 0; \\ 1, & \text{n} = 0. \end{cases} \tag{A.8}$$

A confluent hypergeometric function ${}_1F_1(a,b,z)$ is the first kind of ${}_pF_q$:

$$ {}_1F_1(a,b,z) \;=\; \sum_{n=0}^{\infty} \frac{(a)_n}{(b)_n}\frac{z^n}{n!}; \tag{A.9} $$

and its a solution of a confluent hypergeometric differential equation

$$ z\frac{d^2x}{dz^2} + (b-z)\frac{dx}{dz} - ax = 0. \tag{A.10} $$

There are several common standard forms of confluent hypergeometric functions, *Kummer* function $M(a;b;z)$ is the common form.

The n^{th} derivative of the general hypergeometric function (A.7) is given by [74, 79]

$$ \begin{aligned} \frac{\partial^n}{\partial z^n} \;\; {}_pF_q \;\; & (a_1,\cdots,a_p;b_1,\cdots,b_q;z) \\ = \;\; & \frac{(a_1)_n,\cdots,(a_p)_n}{(b_1)_n,\cdots,(b_q)_n} \times \; {}_pF_q(a_1+n,\cdots,a_p+n;b_1+n,\cdots,b_q+n;z). \end{aligned} \tag{A.11} $$

Hypergeometric function ${}_1F_1$ is related to MapleSoft *Laguerre* function as

$$ L_b^a(z) = \frac{\Gamma(a+b+1)}{\Gamma(a+1)\Gamma(b+1)} \; {}_1F_1(-a;b+1;z) \tag{A.12} $$

There are very useful relations especially, when deriving the expected value of (3.9), these relations are needed to simplify the integration.

Some important properties of ${}_1F_1$

- It converges for any z, it is defined for any a and b, $(b \neq 0)$.
- $M(a;b;0) = 1$ for any a and b, $(b \neq 0)$.
- $M(a;a;z) = e^z$.
- $M(a;b;z) = e^z M(a-b;b;z)$.
- $M(\frac{1}{2};\frac{3}{2};-z^2) = \frac{\pi}{2z} erf(z)$.

♠

Appendix B

Proof of Eq. (3.5) Solution

In Underlay case, for the state 0, to evaluate the expectation term in Eq. (3.5) using the distribution Eq. (3.1), we get

$$\mathcal{I} = \frac{1}{\Gamma(\mu)} \int_0^\infty (1+cz)^{-\alpha} \cdot z^{\mu-1}\, e^z dz \tag{B.1}$$

Using the change of variable, let $u = \frac{1}{1+cz}$, then $du = \frac{-c}{(1+cz)^2} = -cu^2$, and $zu = (1-u)/c$. The integration can be simplified as

$$\mathcal{I} = \frac{c^{-\mu}}{\Gamma(\mu)} \int_0^1 u^{\alpha-\mu-1}(1-u)^{\mu-1} e^{-\frac{(1-u)}{cu}} du \tag{B.2}$$

By using the integration by part and making use of the following definition of ${}_1F_1$

$${}_1F_1(a,b;z) = \frac{\Gamma(b)}{\Gamma(a)\Gamma(b-a)} \int_0^1 e^{zu} u^{a-1}(1-u)^{b-a-1} du, \tag{B.3}$$

and the definition of Gamma function $\Gamma(z) = \int_0^\infty e^{-t} t^{z-1} dt = \Gamma(1+z)/z$, the formula in Eq. (3.6) can be obtained. The proof for the state 0 term in Eq. (3.29) is similar to the above.

While for the state 1 in both schemes, we use *Wolfram Mathematica* services which are the extensive mathematics resources in the Web [75] and by properties of the power series functions illustrated in [59, 77, 78].

The integrations are also verified using two different *symbolic integration softwares* (*MapleSoft-12* and *MatLab R2012a*), similar results are obtained. ♠

Appendix C

$MMSE$ Derivation and Relations

The signal received by the cognitive receiver in the training phase is

$$y = \begin{cases} \sqrt{S_{pt}}h + n & \text{if PUs are inactive(channel is idle)} \\ \sqrt{S_{pt}}h + n + n_p & \text{if PUs are active(channel is busy)} \end{cases} \tag{C.1}$$

S_{pt} represents the pilot's power, which is equal to S_{pb} if sensing result is busy and equal to S_{pd} if sensing result is idle. It is assumed that n and n_p are zero mean independent Gaussian random variables with variances σ_n^2 and $\sigma_{n_p}^2$, respectively. Hence, the overall variance of the noise is σ_n^2 or $\sigma_n^2 + \sigma_{n_p}^2$ depending the sensing results. Noticing that the cognitive receiver does not have exact information about the occupancy status of the PU, but it has predictions via sensing probabilities, the inclusive noise variance, σ^2, is randomly taking these two values.

The Minimum Mean-Squared Error ($MMSE$) estimator of a parameter is defined as the conditional expected value of the parameter given the observations [60, 80]. The $MMSE$ to estimate

h in (C.1) can be expressed as follows:

$$\begin{aligned}
\hat{h} = \mathbb{E}[h|y] &= Pr(\sigma^2 = \sigma_n^2 + \sigma_{n_p}^2|y)\mathbb{E}[h|y, \sigma^2 = \sigma_n^2 + \sigma_{n_p}^2] \\
&+ Pr(\sigma^2 = \sigma_n^2|y)\mathbb{E}[h|y, \sigma^2 = \sigma_n^2] \qquad \text{(C.2)} \\
&= Pr(\sigma^2 = \sigma_n^2 + \sigma_{n_p}^2|y)\frac{\sqrt{S_{pt}}\sigma_h^2}{S_{pt}\sigma_h^2 + \sigma_n^2 + \sigma_{n_p}^2}y \\
&+ Pr(\sigma^2 = \sigma_n|y)\frac{\sqrt{S_{pt}}\sigma_h^2}{S_{pt}\sigma_h^2 + \sigma_n^2}y \qquad \text{(C.3)}
\end{aligned}$$

Here, we use the property of conditional expectation [76] $\mathbb{E}[A|B] = \mathbb{E}[\mathbb{E}[A|B, C]|B]$, where the outer expectation on the right-hand side is with respect to the conditional distribution of C given B. In our setting, C is the noise variance. Hence, the above formulation indicates that we can find the $MMSE$ estimate by evaluating the average of the $MMSE$ estimates with fixed noise variances with respect to the conditional distribution of the noise variance given the observation. This is indeed what is done in (C.2). (C.3) is obtained by noting that the noise variance is fixed.

Using Bayes' rule the conditional probabilities expressions are as follow

$$\begin{aligned}
Pr(\sigma^2 = \sigma_n^2 + \sigma_{n_p}^2|y) &= \frac{Pr(\sigma^2 = \sigma_n^2 + \sigma_{n_p}^2)f(y|\sigma^2 = \sigma_n^2 + \sigma_{n_p}^2)}{f(y)} \qquad \text{(C.4)} \\
Pr(\sigma^2 = \sigma_n^2|y) &= \frac{Pr(\sigma^2 = \sigma_n^2)f(y|\sigma^2 = \sigma_n^2)}{f(y)}
\end{aligned}$$

y is conditionally Gaussian distributed with zero mean and variance σ^2 as the relations (C.4) points. The conditional distribution function of y, *i.e.*, $f(y)$ is defined as [23]

$$\begin{aligned}
f(y|\sigma^2 = \sigma_n^2) &= \frac{1}{\pi(S_{pt}\sigma_h^2 + \sigma_n^2)}e^{-\frac{|y|^2}{S_{pt}\sigma_h^2 + \sigma_n^2}} \qquad \text{(C.5)} \\
f(y|\sigma^2 = \sigma_n^2 + \sigma_{n_p}^2) &= \frac{1}{\pi(S_{pt}\sigma_h^2 + \sigma_n^2 + \sigma_{n_p}^2)}e^{-\frac{|y|^2}{S_{pt}\sigma_h^2 + \sigma_n^2 + \sigma_{n_p}^2}}. \qquad \text{(C.6)}
\end{aligned}$$

The noise variance is related to the channel sensing result. Let us assume that the channel is sensed as busy, so, $Pr(\sigma^2 = \sigma_n^2)$ means that there is no PU in the channel and hence channel is idle. Since our assumption, channel is sensed as busy. Therefore, $Pr(\sigma^2 = \sigma_n^2)$ is equal to the conditional

probability $Pr\binom{\text{Ch is}}{\text{idle}}|\binom{\text{Ch is}}{\text{sensed busy}}$. See the derivations from (C.7) to (C.9).

$$
\begin{aligned}
Pr(\sigma^2=\sigma_n^2) &= Pr\binom{\text{ch is}}{\text{idle}}|\binom{\text{ch is}}{\text{sensed busy}} = \frac{Pr\binom{\text{ch is}}{\text{idle}}\,Pr\left(\binom{\text{ch is}}{\text{sensed busy}}|\binom{\text{ch is}}{\text{idle}}\right)}{Pr\binom{\text{ch is}}{\text{sensed busy}}} \\
&= \frac{Pr\binom{\text{ch is}}{\text{idle}}\overbrace{Pr\left(\binom{\text{ch is}}{\text{sensed busy}}|\binom{\text{ch is}}{\text{idle}}\right)}^{\text{false detection}}}{Pr\binom{\text{ch is}}{\text{idle}}\underbrace{Pr\left(\left(\binom{\text{ch is}}{\text{sensed busy}}|\binom{\text{ch is}}{\text{idle}}\right)\right)}_{\text{false detection}}+Pr\binom{\text{ch is}}{\text{busy}}\underbrace{Pr\left(\left(\binom{\text{ch is}}{\text{sensed busy}}|\binom{\text{ch is}}{\text{busy}}\right)\right)}_{\text{correct detection}}} \\
&= \frac{\frac{b}{b+d}\mathcal{P}_f}{\frac{b}{b+d}\mathcal{P}_f+\frac{d}{b+d}\mathcal{P}_d} = \frac{b\mathcal{P}_f}{b\mathcal{P}_f+d\mathcal{P}_d} \qquad \text{Channel is sensed busy} \qquad \text{(C.7)}
\end{aligned}
$$

Using a similar approach, we can obtain the other cases:

$$
\begin{aligned}
Pr(\sigma^2=\sigma_n^2) &= \frac{b(1-\mathcal{P}_f)}{b(1-\mathcal{P}_f)+d\mathcal{P}_m} \qquad \text{Channel is sensed idle} \\
Pr(\sigma^2=\sigma_n^2+\sigma_{n_p}^2) &= \frac{d\mathcal{P}_d}{b\mathcal{P}_f+d\mathcal{P}_d} \qquad \text{Channel is sensed busy} \qquad \text{(C.8)} \\
Pr(\sigma^2=\sigma_n^2+\sigma_{n_p}^2) &= \frac{d\mathcal{P}_m}{b(1-\mathcal{P}_f)+d\mathcal{P}_m} \qquad \text{Channel is sensed idle}
\end{aligned}
$$

Note that the probability of the channel state can be derived easily from the transition matrix of the two-state Markov chain of Figure 4.2.

$$
P_r(\text{channel in state } i) = \begin{cases} \frac{d}{b+d}, & i \text{ is busy} \\ \frac{b}{b+d}, & i \text{ is idle} \end{cases} \qquad \text{(C.9)}
$$

♠

Appendix D

Transition Probabilities

Let $p_1 = \Pr\{$the channel is being busy and it is detected as busy and $r_b < C_1^l(k)$ in the k^{th} frame given that the channel is being busy and it is detected as busy and $r_b < C_1^l(k-1)$ in the $(k-1)^{th}$ frame$\}$

The chain rule in probability theorem states that if there are four events: A_1, A_2, A_3 and A_4, then

$$\begin{aligned} Pr(A_1, A_2, A_3|A_4) &= Pr(A_1 \cap A_2 \cap A_3|A_4) \\ &= Pr(A_1|A_4) \cdot Pr(A_2|A_1 \cap A_4) \cdot Pr(A_3|A_1 \cap A_2 \cap A_4) \end{aligned} \tag{D.1}$$

Thus

$$\begin{aligned} p_{11} &= Pr\{\text{ch is busy in } i^{th} \text{ frame } \big|\text{ch is busy in } (i-1)^{th}\} \\ &\cdot \quad Pr\{\text{ch is busy in } i^{th} \text{ frame } \big|\text{ ch is busy in } (i)^{th}\} \cdot Pr\{r_b < C_1^l(i)|r_b < C_1^l(i-1)\} \\ &= (1-b)\mathcal{P}_d Pr\{r_b < C_1^l(i)|r_b < C_{i-1}^l(i-1)\} \\ &= (1-b)\mathcal{P}_d Pr\{z_i > \varphi_1|z_{i-1} > \varphi_1\} \\ &= (1-b)\mathcal{P}_d Pr\{z_i > \varphi_1\} = (1-b)\mathcal{P}_d Pr\{z > \varphi_1\} = p_1 \end{aligned} \tag{D.2}$$

We omitted the index i in z_i due to the fact that z_i and z_{i-1} are independent due to the block fading assumption.

By the same manner , the transition probabilities from any state to state 1 can be expressed as

$$\begin{aligned} p_{l1} = p_{11} = p_{21} = p_{31} = p_{41} =& (1-b)\mathcal{P}_d Pr\{z > \varphi_1\} &=& (1-b)\mathcal{P}_d e^{-\varphi_1} &=& p_1 \\ p_{n1} = p_{51} = p_{61} = p_{71} = p_{81} =& d\mathcal{P}_d Pr\{z > \varphi_1\} &=& d\mathcal{P}_d e^{-\varphi_1} &=& \acute{p}_1 \end{aligned} \tag{D.3}$$

Using the same modality, the full transition probabilities can be obtained as listed in Table 4.1. ♠

Appendix E

Eigenvalue Maximization

Let A be an $n \times n$ matrix, the eigenvalues (ω)s of the matrix A are the zeroes of its characteristic polynomial, $\det(\omega I - A)$, which can be written as

$$Q(\omega) = \omega^n - C_{n-1}\omega^{n-1} + C_{n-2}\omega^{n-2} - \cdots (-1)^n C_0 \tag{E.1}$$

It is well known that the coefficients C_{n-1} and C_0 are, respectively, the *trace*(A) (the sum of its diagonal entries) and the *det*(A). All other coefficients $C_{n-k}, k = 1, 2, \cdots$, can be expressed by the sum of the $k-$*rowed principle minors* of A. A k-rowed principal minor of an $n \times n$ matrix A is the determinant of a $k \times k$ submatrix of A whose entries, a_{ij}, have indices i and j that are the elements of the same $k-$element subset of $1, 2, \cdots, n$.

With *rank* (the dimension of the largest square submatrix of A with nonzero determinant) r, where, $r < n$. All nonzero eigenvalues of A are among the zeros of the polynomial [81]

$$Q(\omega) = \omega^r - C_{n-1}\omega^{r-1} + \cdots (-1)^r C_{n-r} \tag{E.2}$$

$$\begin{aligned}
\omega^2 \quad & -\big(+ \acute{p}_8 + \tau_b \acute{p}_7 + p_6 + \tau_d p_5 + \acute{p}_4 + \tau_d \acute{p}_3 + p_2 + \tau_b p_1\big)\omega \\
+ \quad & \big(\tau_d \acute{p}_3 p_2 + \tau_b \tau_d \acute{p}_3 p_1 + \tau_b \acute{p}_7 p_2 + \tau_b \acute{p}_7 p_6 + \tau_b \tau_d \acute{p}_7 p_5 - \tau_b \acute{p}_1 p_4 - \tau_b \tau_d \acute{p}_1 p_3 \tau_d \acute{p}_2 - p_3 + \tau_b^2 \acute{p}_7 p_1 \\
- \quad & \acute{p}_2 p_4 + \acute{p}_4 p_2 \acute{p}_4 p_1 - \tau_d^2 p_3 \acute{p}_5 - \tau_d p_4 \acute{p}_5 + \tau_d p_5 \acute{p}_4 + \tau_d^2 p_5 \acute{p}_3 - \tau_d p_3 \acute{p}_6 - p_4 \acute{p}_6 + p_6 \acute{p}_4 + \tau_d p_6 \acute{p}_3 \\
- \quad & \tau_b^2 \acute{p}_1 p_7 - \tau_b \acute{p}_2 p_7 - \tau_b \acute{p}_5 p_7 - \tau_b \acute{p}_6 p_7 - \tau_b \acute{p}_1 p_8 - \acute{p}_2 p_8 - \tau_d \acute{p}_5 p_8 - \acute{p}_6 p_8 + \acute{p}_8 p_6 + \tau_d \acute{p}_8 p_5 + \acute{p}_8 p_2 \\
+ \quad & \tau_b \acute{p}_8 p_1\big) = 0
\end{aligned} \tag{E.3}$$

The solution for the maximum eigenvalue of (E.3) is

$$\begin{aligned}
\omega \quad &= \frac{1}{2}\big(\acute{p}_8 + \tau_b\acute{p}_7 + p_6 + \tau_d p_5 + \acute{p}_4 + \tau_d\acute{p}_3 + p_2 + \tau_b p_1\big) + \frac{1}{2}\Bigg[\big(\acute{p}_8 + \tau_b\acute{p}_7 + p_6 + \tau_d p_5 + \acute{p}_4 + \tau_d\acute{p}_3 \\
+ \quad & p_2 + \tau_b p_1\big)^2 - 4\Bigg(\tau_d\acute{p}_3\, p_2 + \tau_b\tau_d\acute{p}_3\, p_1 + \tau_b\acute{p}_7\, p_2 + \tau_b\acute{p}_7\, p_6 + \tau_b\tau_d\acute{p}_7\, p_5 - \tau_b\acute{p}_1\, p_4 - \tau_b\tau_d\acute{p}_1\, p_3 \\
- \quad & \tau_d\acute{p}_2\, p_3 + \tau_b^2\acute{p}_7\, p_1 - \acute{p}_2\, p_4 + \acute{p}_4\, p_2 + \acute{p}_4\, p_1 - \tau_d^2 p_3\,\acute{p}_5 - \tau_d p_4\,\acute{p}_5 + \tau_d p_5\,\acute{p}_4 + \tau_d^2 p_5\,\acute{p}_3 - \tau_d p_3\,\acute{p}_6 \\
- \quad & p_4\,\acute{p}_6 + p_6\,\acute{p}_4 + \tau_d p_6\,\acute{p}_3 - \tau_b^2\acute{p}_1\, p_7 - \tau_b\acute{p}_2\, p_7 - \tau_b\acute{p}_5\, p_7 - \tau_b\acute{p}_6\, p_7 - \tau_b\acute{p}_1\, p_8 - \acute{p}_2\, p_8 - \tau_d\acute{p}_5\, p_8 \\
- \quad & \acute{p}_6\, p_8 + \acute{p}_8\, p_6 + \tau_d\acute{p}_8\, p_5 + \acute{p}_8\, p_2 + \tau_b\acute{p}_8\, p_1\Bigg)\Bigg]^{\frac{1}{2}}
\end{aligned} \tag{E.4}$$

♠

Appendix F

Ratio of Exponential distributions

The random variable X is exponentially distributed with rate α if and only if $Pr(X \geq x) = e^{-\alpha x}$ for every $x \geq 0$. Similarly, the random variable Y is exponentially distributed with rate β if and only if $Pr(Y \geq y) = e^{-\beta y}$ for every $y \geq 0$. Let $Z = X/Y$ and $t \geq 0$. Conditioning on X and applying our characterization to $y = X/t$, one gets

$$Pr(Z \leq t) = Pr(Y \leq X/t) = \mathbb{E}[e^{-\beta x/t},]$$

hence for every $\gamma \geq 0$,

$$\mathbb{E}[e^{-\gamma X}] = \int_0^\infty \alpha e^{-(\alpha+\gamma)x} dx = \frac{\alpha}{\alpha+\gamma}\left[e^{-(\alpha+\gamma)}\right]_0^\infty = \frac{\alpha}{\alpha+\gamma}$$

Substituting $\gamma = \beta/t$, we have

$$F_Z(t) = \frac{\alpha}{\beta/t + \alpha}$$

and hence the (*pdf*) of Z is

$$f_Z(t) = \frac{dF_Z(t)}{dt} = \frac{\alpha\beta}{(\alpha t + \beta)^2}$$

For unity mean of the both random variable (*i.e.*, $\alpha = \beta = 1$), the above *pdf* eliminates to (5.39).

♠

Bibliography

[1] J. Mitola, "Cognitive radio: Making software radios more personal," *IEEE Personal Communication*, vol. 6, pp. 13–18, Aug. 1999.

[2] S. Haykin, "Cognitive radio: Brain-empowered wireless communications," *IEEE Trans. on Selected areas in Comm.*, vol. 23, pp. 201–220, Feb 2005.

[3] Y. Liang, A. Hoang, and H. Chen, "Cognitive radio on TV bands: A new approach to provide wireless connectivity for rural areas," *IEEE Wireless Comm.*, vol. 5, no. 3, pp. 16–22, 2008.

[4] F. Digham, M. Alouini, and M. K. Simon, "On the energy detection of unknown signals over fading channels," *IEEE Trans on Comm.*, vol. 55, pp. 21–24, Jan 2007.

[5] W. Zhang, R. Mallik, and K. Letaief, "Optimization of cooperative spectrum sensing with energy detection in cognitive radio networks," *IEEE Trans. on Wireless Comm.*, vol. 8, pp. 5761–5766, Dec 2009.

[6] D. Bhargavi and C. Murthy, "Performance comparison of energy, matched-filter and cyclostationarity-based spectrum sensing," *Signal Processing Advances in Wireless Communications IEEE (SPAWC), Marrakech, Morocco*, Jun 2010.

[7] D. Cabric, A. Tkachenko, and R. Brodersen, "Spectrum sensing measurements of pilot, energy, and collaborative detection," *in Proc. Military Comm. Conf. (MILCOM), Washington, DC, USA*, Oct 2006.

[8] A. Fehske, J. Gaeddert, and J. Reed, "A new approach to signal classification using spectral correlation and neural networks," *in Proc. Int. Symp. on Dynamic Spec. Access Networks (DySPAN), Baltimore, MD, USA*, Nov 2005.

[9] S. Stotas and A. Nallanathan, "Optimal sensing time and power allocation in multiband cognitive radio networks," *IEEE Trans. on Comm.*, vol. 59, pp. 226–235, Jan 2011.

[10] Y. Liang, Y. Zeng, E. Peh, and A. Hong, "Sensing-throughput tradeoff for cognitive radio networks," *IEEE Trans. on Wireless Comm.*, vol. 7, pp. 1326–1337, Apr 2008.

[11] B. Sadler, L. Tong, and M. Dong, "Pilot-assisted wireless transmissions," *IEEE Signal Processing Magazine*, vol. 21, pp. 12–25, Nov 2004.

[12] J. Cavers, "An analysis of pilot symbol assisted modulation for rayleigh fading channels," *IEEE Trans. on Vehicular Tech.*, vol. 40, pp. 686–693, Nov 1991.

[13] T. Hillenbrand, A. Krohn, and F. Jondral, "Mutual interference in OFDM-based spectrum pooling systems," *In Proc. IEEE Vehicular Tech. Conf. (VTC), Milan, Italy*, vol. 44, pp. 1873–1877, May 2004.

[14] N. Hoven and A. Sahai, "Power scaling for cognitive radio," *In Proc. IEEE Wireless Comm. and Networking Conf.(WCNC), Maui, HI, USA*, vol. 1, pp. 250–255, Jun 2005.

[15] T. Le and Q. Liang, "An efficient power control scheme for cognitive radios," *In Proc. IEEE Wireless Comm. and Networking Conf. (WCNC), Hong Kong, China*, pp. 2561–2565, Mar 2007.

[16] S. Srinivasa and S. Jafar, "Soft sensing and optimal power control for cognitive radio," *In Proc. IEEE Global Telecomm. Conf.(GLOBECOM), Washington, DC, USA*, Nov 2007.

[17] Y. Chen and G. Yu, "On cognitive radio networks with opportunistic power control strategies in fading channels," *IEEE Trans. on Wireless Comm.*, vol. 7, pp. 2752–2761, Jul 2008.

[18] Y. Chen, G. Yu, Z. Zhang, H. Chen, and P. Qiu, "On cognitive radio networks with opportunistic power control strategies in fading channels," *IEEE Trans. on Wireless Comm.*, vol. 7, pp. 2752–2761, Jul 2008.

[19] L. Qian, J. Attia, A. Jarosch, and C. Monney, "Power control for cognitive radio ad hoc networks," *Local and Metropolitan Area Networks, 15th IEEE Workshop, New York, NY, USA*, pp. 7–12, Jun 2007.

[20] W. Wang, Y. Cui, and T. Peng, "Noncooperative power control game with exponential pricing for cognitive radio network," *In Proc. IEEE Vehicular Tech. Conf. (VTC), Dublin, Ireland*, pp. 3125–3129, Apr 2007.

[21] S. Cheng and Z. Yang, "Energy-efficient power control game for cognitive radio systems," *in proc. Software Engineering Artificial Intelligence, Networking, and Parallel/Distributed Computing, Qingdao, China*, pp. 526–530, Jul 2007.

[22] W. Lee, "Estimate of channel capacity in rayleigh fading environment," *IEEE Trans. on Vehicular Tech.*, vol. 39, pp. 187–189, Aug 1990.

[23] M. Gursoy, H. Poor, and S. Verd, "The noncoherent Rician fading channel part I: Structure of the capacity-achieving input," *IEEE Trans. on Wireless Comm.*, vol. 4, pp. 2139–2206, Sep 2005.

[24] D. Wu and R. Negi, "Effective capacity: A wireless link model for support of quality of service," *IEEE Trans. on Wireless Comm.*, vol. 2, pp. 630–643, Jul 2003.

[25] J. Tang and X. Zhang, "Quality-of-service driven power and rate adaptation over wireless links," *IEEE Trans. on Wireless Comm*, vol. 6, pp. 3058–3068, Aug 2007.

[26] J. Tang and X. Zhang, "Cross-layer-model based adaptive resource allocation for statistical *QoS* guarantees in mobile wireless networks," *IEEE Trans. on Wireless Comm.*, vol. 7, pp. 2318–2328, Jun 2008.

[27] Q. Du and X. Zhang, "Effective capacity optimization with layered transmission for multicast in wireless networks," *Wireless Communications and Mobile Computing Conference IWCMC, Crete Island, Greece*, pp. 267–272, Aug 2008.

[28] L. Liu and J. Chamberland, "On the effective capacities of multiple-antenna gaussian channels," *Proc. of IEEE int. symposium on information theory (ISIT), Toronto, Canada*, pp. 2583–2587, Jul 2008.

[29] D. Qiao, M. Gursoy, and S. Velipasalar, "Energy efficiency of fixed-rate wireless transmissions under queueing constraints and channel uncertainty," *In Proc. IEEE Global Telecomm. Conf.(GLOBECOM), Honolulu, HI, USA*, pp. 24–29, Nov 2009.

[30] L. Musavian, S. Assa, and S. Lambotharan, "Effective capacity for interference and delay constrained cognitive radio relay channels," *IEEE Trans. on Wireless Comm.*, vol. 9, pp. 1698–1707, May 2010.

[31] E. Jorswieck, R. Mochaourab, and M. Mittelbach, "Effective capacity maximization in multi-antenna channels with covariance feedback," *IEEE Trans. on Wireless Comm.*, vol. 9, pp. 2988–2993, Oct 2010.

[32] S. Akin and M. Gursoy, "Effective capacity analysis of cognitive radio channels for quality of service provisioning," *IEEE Trans. Wireless Comm.*, vol. 9, pp. 3354–3364, Nov 2010.

[33] D. Wong, A. Hoang, and F. Chin, "Dynamic spectrum access with imperfect sensing in open spectrum wireless networks," *In Proc. IEEE Wireless Comm. and Networking Conf. (WCNC), Las Vegas, USA*, pp. 2765–2770, Mar. Apr. 2008.

[34] B. Wang, Z. Ji, K. Liu, and T. Clancy, "Primary-prioritized markov approach for dynamic spectrum allocation," *IEEE Trans. on Wireless Comm.*, vol. 8, pp. 1854–1865, Apr. 2009.

[35] H. Hu and Q. Zhu, "Dynamic spectrum access in underlay cognitive radio system with $SINR$ constraints," *Proc. of the 5th Int. Conf. on Wireless Comm., Networking and Mobile Computing (WiCOM), Beijing, China*, Sep 2009.

[36] X. Kang, Y. Liang, H. Garg, and L. Zhang, "Sensing-based spectrum sharing in cognitive radio networks," *IEEE Trans. on Vehicular Tech.*, vol. 58, pp. 4649–4654, Oct 2009.

[37] M. Khoshkholgh, K. Navaie, and H. Yanikomeroglu, "Access strategies for spectrum sharing in fading environment: overlay, underlay, and mixed," *IEEE Trans. on Mobile Computing*, vol. 9, pp. 1780–1793, Dec 2010.

[38] M. Elalem and L. Zhao, "Novel power control algorithm by decomposed geometric programming method for cdma cognitive radio networks," *In Proc. IEEE Int. Conf. Comm. (ICC), Ottawa, Canada*, Jun 2012.

[39] M. Elalem and L. Zhao, "Effective capacity analysis for cognitive networks under *QoS* satisfaction," *Submitted to EURASIP Journal on Wireless Communications and Networking*, Dec 2012.

[40] M. Elalem and L. Zhao, "Effective capacity optimization for cognitive radio network based on underlay scheme in gamma fading channels," *In Proc. IEEE Int. Conf. on Computing, Networking and Communications (ICNC), San Diego, NV, USA*, Jan 2013.

[41] M. Elalem and L. Zhao, "Effective capacity optimization based on overlay cognitive radio network in gamma fading environment," *In Proc. IEEE Wireless Comm. and Networking Conf.(WCNC), Shanghai, China*, Apr 2013.

[42] M. Elalem and L. Zhao, "Effective capacity and interference constraints in multichannel cognitive radio network," *In Proc. IEEE Wireless Comm. and Networking Conf.(WCNC), Shanghai, China*, Apr 2013.

[43] M. Elalem and L. Zhao, "Effective capacity and interference analysis in multiband dynamic spectrum sensing," *Journal of Communication and Network (CN), to appear*, Feb 2013.

[44] M. Elalem and L. Zhao, "Optimal access strategy for capacity optimization in cognitive radio system," *In Proc. IEEE Wireless Comm. and Networking Conf.(WCNC), Shanghai, China*, Apr 2013.

[45] M. Elalem and L. Zhao, "Throughput maximization based on optimal access probabilities in cognitive radio system," *Journal of Communication and Network (CN), to appear*, Feb 2013.

[46] M. Elalem and L. Zhao, "Optimal access probabilities to maximize capacity in cognitive radio system," *In Proc. 11^{th} International Conference for Upcoming Engineers (ICUE), Toronto, Canada*, Aug 2012.

[47] M. Elalem and L. Zhao, "Channel estimation and effective capacity over imperfect rayleigh channel environment in cognitive radio," *Journal of Communication and Computer(JCC) to appear*, Feb 2013.

[48] J. Tang and X. Zhang, "*QoS*-driven adaptive power and rate allocation for multichannel communications in mobile wireless networks," *IEEE Trans. on Wireless Comm.*, vol. 6, pp. 4349–4360, Jul 2007.

[49] T. Cover and J. Thomas, *Elements of Information Theory.* John Wiley & Sons, 2^{nd} ed., pp. 183- 220, 2006. ISBN: 978-0471241959.

[50] A. Goldsmith and S. Chua, "Variable-rate variable-power MQAM for fading channels," *IEEE Trans. on Information Theory*, vol. 43, pp. 1986–1992, Nov 1997.

[51] G. Kesidis, J. Walrand, and C. Chang, "Effective bandwidths for multiclass markov fluids and other ATM sources," *IEEE/ACM Trans. on Networking*, vol. 1, pp. 424–428, Aug 1993.

[52] C. Chang, "Stability, queue length, and delay of deterministic and stochastic queueing neyworks," *IEEE Trans. on Automatic Control*, vol. 39, pp. 913–931, May 1994.

[53] E. Biglieri, J. Proakis, and S. Shamai, "Fading channels: informationtheoretic and communications aspects," *IEEE Trans. on Information Theory*, vol. 44, pp. 2619–2692, Oct 1998.

[54] F. Ramos, V. Kontorovitch, and M. Lara, "High order fading distributions in nakagami wireless channels," *in Proc. IEEE Vehicular Tech. Conf.(VTC), Dublin, Ireland*, pp. 564–568, Apr 2007.

[55] S. Al-Ahmadi and H. Yanikomeroglu, "On the approximation of the generalized-K distribution by a gamma distribution for modeling composite fading channels," *IEEE Tran. on Wireless Comm.*, vol. 9, pp. 706–713, Feb 2010.

[56] S. Kotz, N. Jonhnson, and N. Balakrishnan, *Continuous Univariate Distributions: Models and applications*, vol. 2. John Wiley and Sons, 2^{nd} ed., pp. 337-386, 2000. ISBN: 978-0471183877.

[57] Q. Zhao, S. Geirhofer, L. Tong, and B. Sadler, "Opportunistic spectrum access via periodic channel sensing," *IEEE Trans. on Signal process.*, vol. 56, pp. 785–796, Feb 2008.

[58] R. Kwan and C. Leung, "Gamma variate ratio distribution with application to cdma performance analysis," *IEEE-Sarnoff Symposium on Advances in Wired and Wireless Communication, Princeton, NJ, USA*, pp. 188–191, Apr 2005.

[59] F. Olver, D. Lozier, R. Boisvert, and C. Clark, *NIST Handbook of Mathematical Functions.* Cambridge University Press, pp. 144-145, 2010. ISBN: 978-0521140638.

[60] H. Poor, *An Introduction to Signal Detection and Estimation.* Springer, New York, 2^{nd} ed., pp 84-88, 1994. ISBN: 978-0387941738.

[61] R. Yates and D. Goodman, *Probability and Stochastic Processes: A Friendly Introduction for Electrical and Computer Engineers.* John Wiley & Sons, 2^{nd} ed., pp. 257-264, 2005. ISBN: 978-0470592519.

[62] S. Boyd and L. Vandenberghe, *Convex Optimization.* UK: Cambridge University Press, 7^{th} ed., pp. 464, 2009. Electronice version.

[63] S. Akin and M. Gursoy, "Ergodic capacity analysis in cognitive radio systems under channel uncertainty," *In Proc. IEEE Information Sciences and Systems Conf.(CISS), Princeton, NJ, USA*, Mar 2010.

[64] B. Hassibi and B. Hochwald, "How much training is needed in multiple-antenna wireless links," *IEEE Trans. Inform. Theory*, vol. 49, pp. 951–963, Apr 2003.

[65] M. Gursoy, "An energy efficiency perspective on training for fading channels," *In Proc. IEEE Int. Symposium on Information Theory (ISIT), Nice, France*, pp. 24–29, Jun 2007.

[66] T. Rappaport, *Wireless Communication; Principles and Practice.* Prentice Hall, 2^{nd} ed., pp. 210-212, 2002. ISBN: 978-0130422323.

[67] S. Akin and M. Gursoy, "Performance analysis of cognitive radio systems under *QoS* constraints and channel uncertainty," *In Proc. IEEE Global Telecomm. Conf.(GLOBECOM), Miami, FL, USA*, Dec 2010.

[68] M. Sencan and M. Gursoy, "Achievable rates for pilot-assisted transmission over rayleigh fading channels," *In Proc. IEEE Information Sciences and Systems Conf., Princeton, NJ, USA*, Mar 2006.

[69] W. Feller, *An Introduction to Probability Theory and Its Applications*, vol. II. Wiley, 2^{th} ed., Ch. 1, 1971. ISBN: 978-0471257097.

[70] C. Chang, *Performance Guarantees in Commucation Networks.* Springer, London, pp. 244-245, 2000. ISBN: 978-1852332266.

[71] D. Bertsekas, *Convex Analysis and Optimization.* Belmont, MA: Athena Scientific, Ch 1,2,4, and 5, 2003. ISBN: 978-1886529458.

[72] L. Musavian and S. Aissa, "Quality-of-service based power allocation in spectrum-sharing channels," *In Proc. IEEE Global Telecomm. Conf.(GLOBECOM), New Orleans, LA, USA*, Dec 2008.

[73] L. Musavian and S. Aissa, "Adaptive modulation in spectrum-sharing systems with delay constraints," *In Proc. IEEE Int. Conf. Commun. (ICC), Dresden, Germany*, Jun 2009.

[74] W. Magnus, F. Oberhettinger, and F. Tricomi, *Higher Transcendental Functions*, vol. 1,2. McGraw Hill, Ch 1,2,4 and 6, 1982. Electronic version.

[75] Wolfram Mathematica; the web's most extensive mathimatics resourses, *Avialable Online at http://mathworld.wolfram.com.*

[76] B. Fristedt and G. Lawrence, *A Modern Approach to Probability Theory.* Birkhäuser, Boston, USA, 1996.

[77] I. Gradshteyn and I. Ryzhik, *Table of Integrals, Series, and Products.* Elsevier Inc., 7^{th} ed., pp. 910, 2007. ISBN: 978-0123736376.

[78] M. Abramowitz and I. Stegun, *Handbook of Mathematical Functions With Formulas, Graphs, and Mathematical Tables.* Dover, New York, 10^{th} ed., pp. 503-566, 1972. ISBN: 978-0318117300.

[79] J. Pearson, "Computation of hypergeometric functions," master of science in mathematical modelling and scientifc computing, University of Oxford, Sep 2009.

[80] S. kay, *Fundamentals of Statistical Signal Processing: Estimation Theory.* Prentice Hall, 2^{nd} ed., pp 344-350, 1993. ISBN: 0-13-042268-1.

[81] S. Venit and R. Katz, "Eigenvalues of matrices of low rank," *The College Mathematics Journal*, vol. 31, pp. 208–210, May 2000.